PHS 6317 Nanoengineering of thin films

Course schedule – Winter 2024

12 January	Introduction – Scientific and technological challenges
19	Fabrication methods – Vacuum physics and vapor-phase techniques
26*	Fabrication methods – Plasma processes and process optimization
2 February	Fabrication methods - Plasma-surface interactions and diagnostics
9**	Fabrication methods – Thermal/Plasma spray technologies
16*	Optics of thin films 1, optical characterization, *Miniquiz1 (5%)*
23*	Optics of thin films 2, design of optical filters
1*** March	*Presentations – Emerging fabrication techniques (30%)*
	March 4-8 - Winter/Spring break
15**	Tribomechanical properties of films and coatings
22**	Electrochemical properties – corrosion and tribo-corrosion*(filter-20%)*
5 April	Passive functional films and coatings, *Miniquiz 2 (5%)*
12	Active functional films and coatings
16	Life cycle analysis and environmental impact
19***	*Presentations – Emerging applications of nanostructured films (40%)*

Deadlines:

Project #1 – Fabrication technique:

Choice of the subject: **26 January**

Abstract and references: **9 February**

Report and presentation: **1st March**

Projet #2 – Design of an optical filter:

Choice of the subject: **23 February**

Report: **22 March**

Projet #3 – Application of nanostructured thin films:

Choice of the subject: **16 February**

Abstract and references: **15 March**

Report and presentation: **19 April**

Project #1: Techniques for the fabrication of nanostructured films and coatings

Mohamed Ammari – HiPIMS (High Power Impulse Magnetron Sputtering)
Veronika Cervenkova - Atomic layer deposition (ALD)
Emilien Martel – HVOF
Alexandre Lussier – DIBS
Gabriel Juteau - Organo-metallic MBE
Thomas Lapointe – Supersonic MBE
Luc Montpetit - Plasma-MBE
Alexandre Fall - Hollow cathode discharge for ALD
Arghavan Yazdanpanah Ardakani - PECVD
Alexandre Pinel – Reactive sputtering (pulsed DC, RF, HiPIMS)
Izacard Bastien – Cold spray
Christelle Abou Zeidan - Ultra-High Vacuum Chemical Vapor Deposition (UHVCVD)
Mathieu Bruzzese - Ion-beam assisted CVD

Etienne Tremblay-Nathan Sasseville – PIII
Alexandre Gamache-Thomas Sicotte – PLD
Alexandre Carrière-Yusef Ben Mami – Langmuir-Blodgett

Plasma system and process control

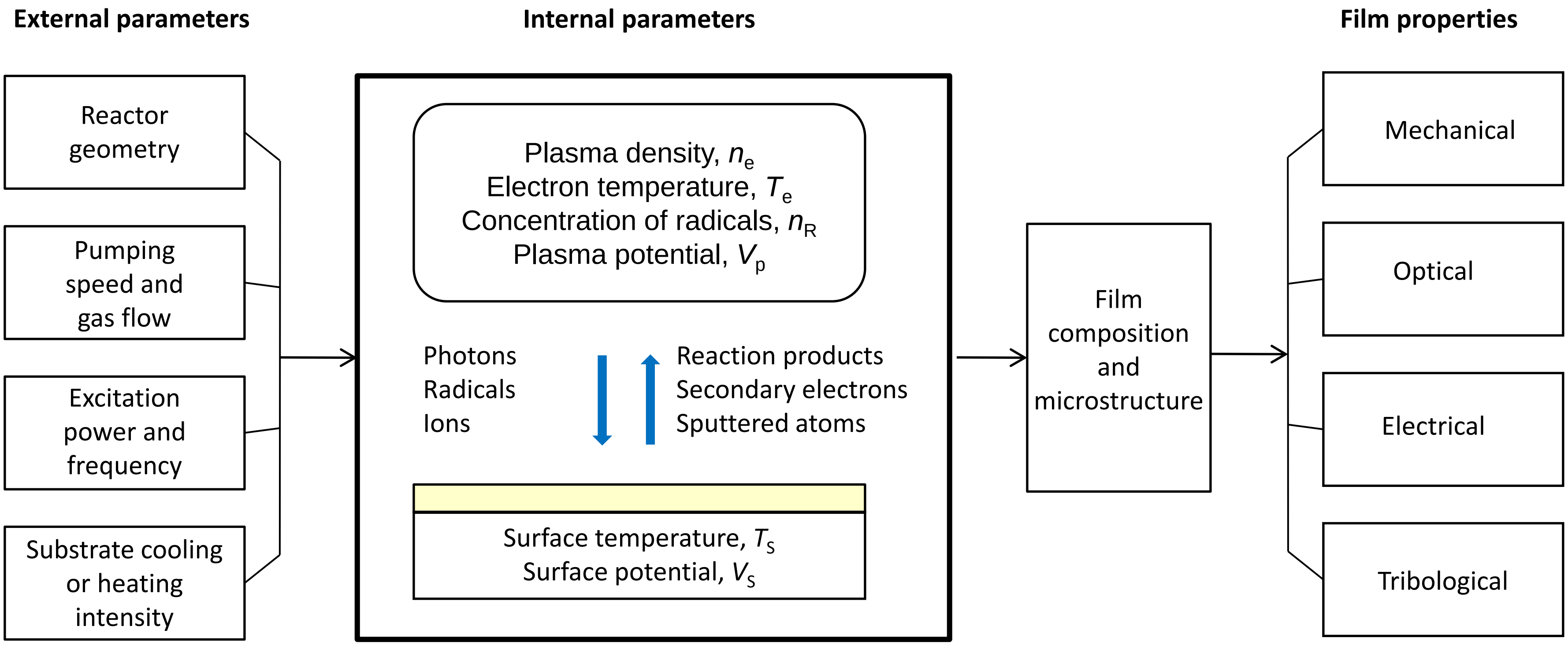

External parameters

Internal parameters

Film properties

Reactor geometry

Pumping speed and gas flow

Excitation power and frequency

Substrate cooling or heating intensity

Plasma density, n_e
Electron temperature, T_e
Concentration of radicals, n_R
Plasma potential, V_p

Photons
Radicals
Ions

Reaction products
Secondary electrons
Sputtered atoms

Surface temperature, T_S
Surface potential, V_S

Film composition and microstructure

Mechanical

Optical

Electrical

Tribological

Today:

Reactive sputtering
Microstructural evolution during the film growth – Structure zone model
Plasma diagnostics

L. Martinu et al., Chapter 9 in “*Handbook of Thin Film Process Technology*”, P.M. Martin, ed., Elsevier, 2010.

Plasma-surface interactions : Ions

Energetic ion bombardment effect at the surface: sputtering, ion-assisted growth

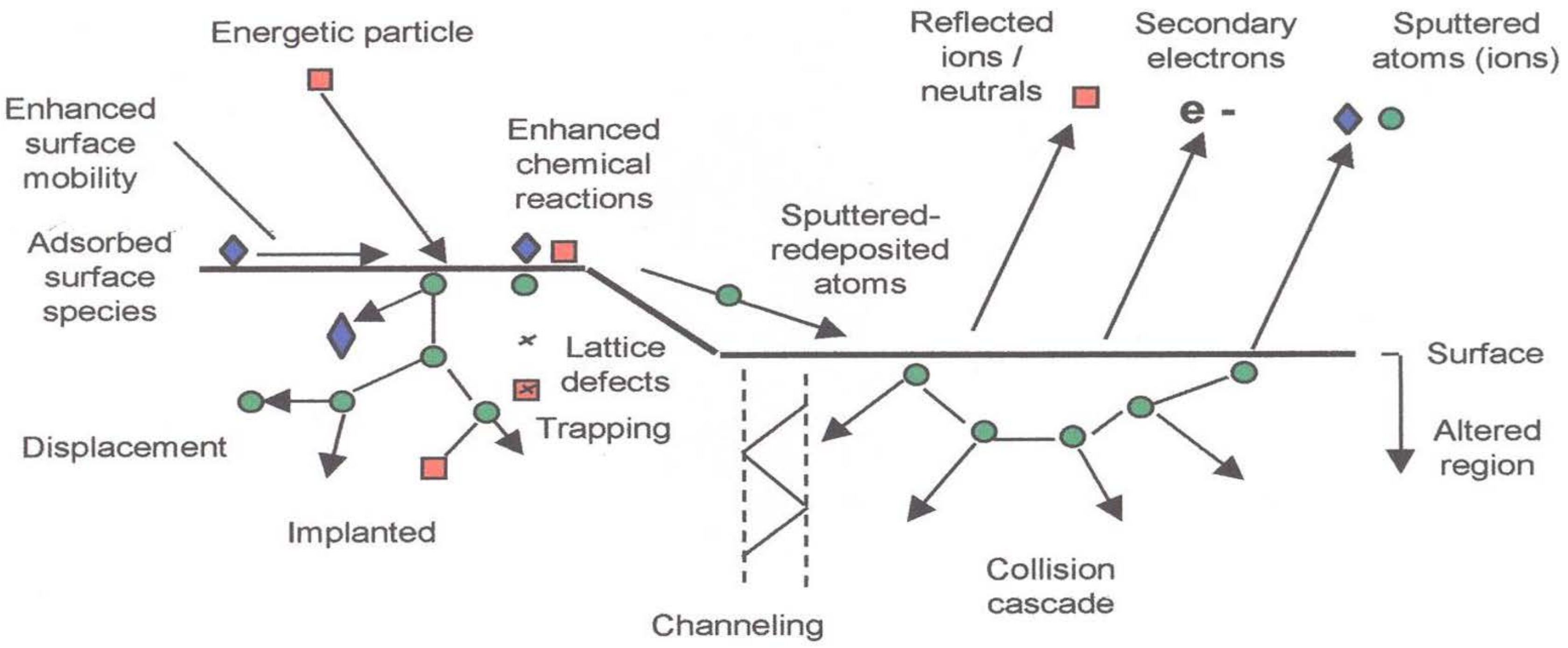

Donald M. Mattox, Handbook of Physical Vapor Deposition (PVD) Processing
Elsevier Science & Technology Books, 2010.

Ion-surface interactions – Sticking probability

Ion beam originating from a plasma

Effects:

- reflection
- adsorption
- diffusion
- sputtering
- incorporation
- surface heating
- chemical reaction
- atom mixing
- change of topography (roughness)

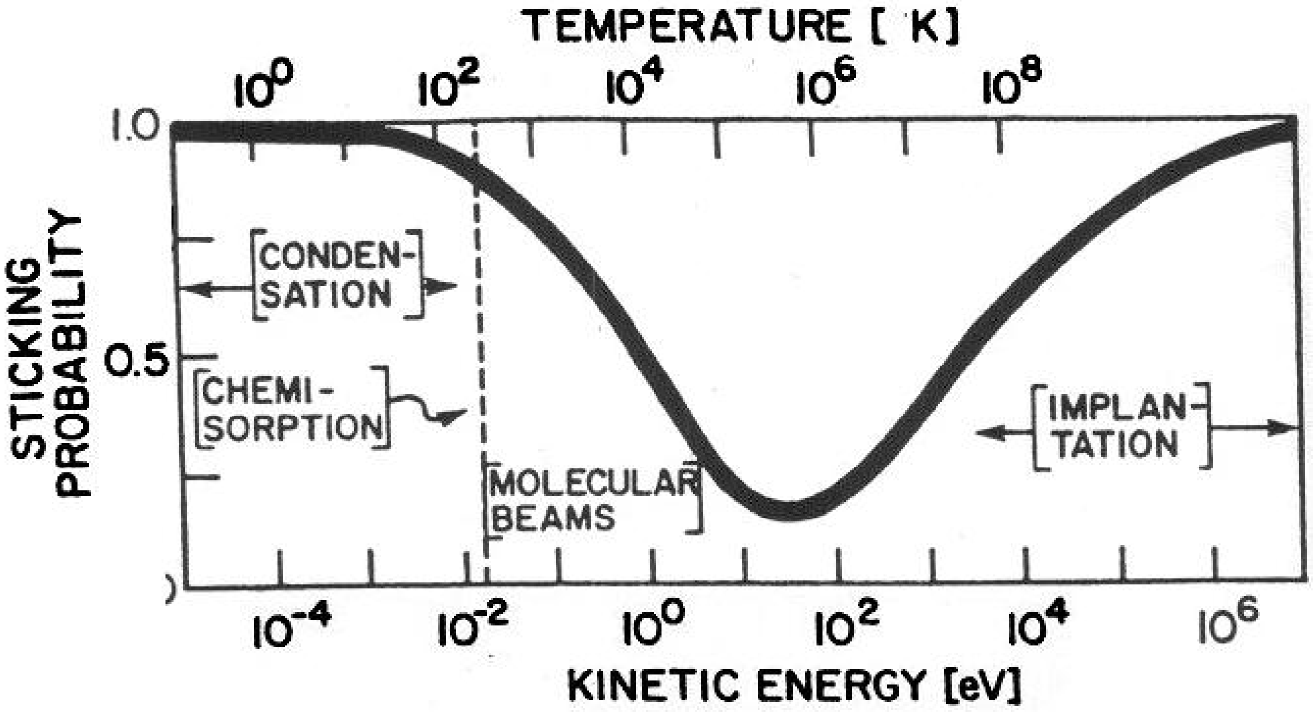

Figure 4-10 Particle-sticking probability as a function of energy. The dashed vertical line corresponds to room-temperature thermal energy. (From S. R. Kasi, H. Kang, C. S. Sass, and J. W. Rabalais, *Surface Science Reports* **10**, Nos. 1/2, p. 1 (1989). Reprinted with the permission of Elsevier Science Publishers and Professor J. W. Rabalais.)

Sputtering

<u>Basic effects:</u>

a) "knock-on"
b) linear cascade
c) thermal spike

E_{th} – threshold energy
U_s – binding energy
(heat of sublimation)
2-5 eV

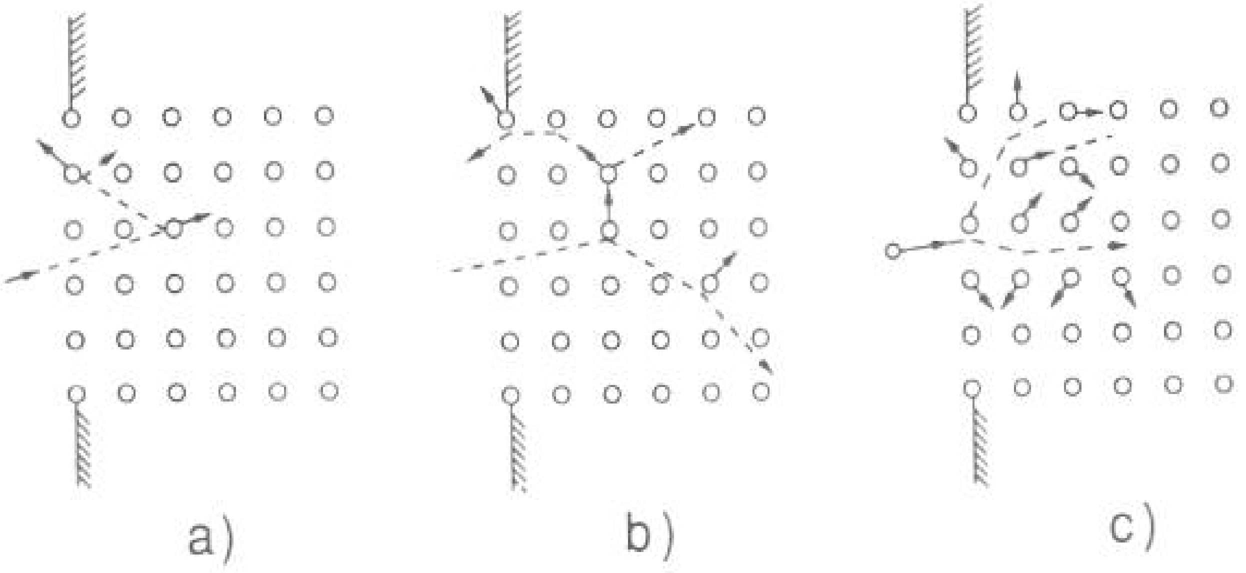

Figure 4-11 Three energy regimes of sputtering. (a) Single knock-on (low energy), (b) linear cascade, (c) spike (high energy). (After P. Sigmund.)

Linear cascade

Sputtering yield

$$S = \frac{3\alpha 4 M_1 M_2 E}{4\pi^2 (M_1 + M_2)^2 U_S} \qquad (E < 1\ \mathrm{keV})$$

$$S = 0.042\alpha S_n(E)/U_s$$

α – efficiency of the mechanical momentum transfer

S_n – Stopping power: energy loss per unit length

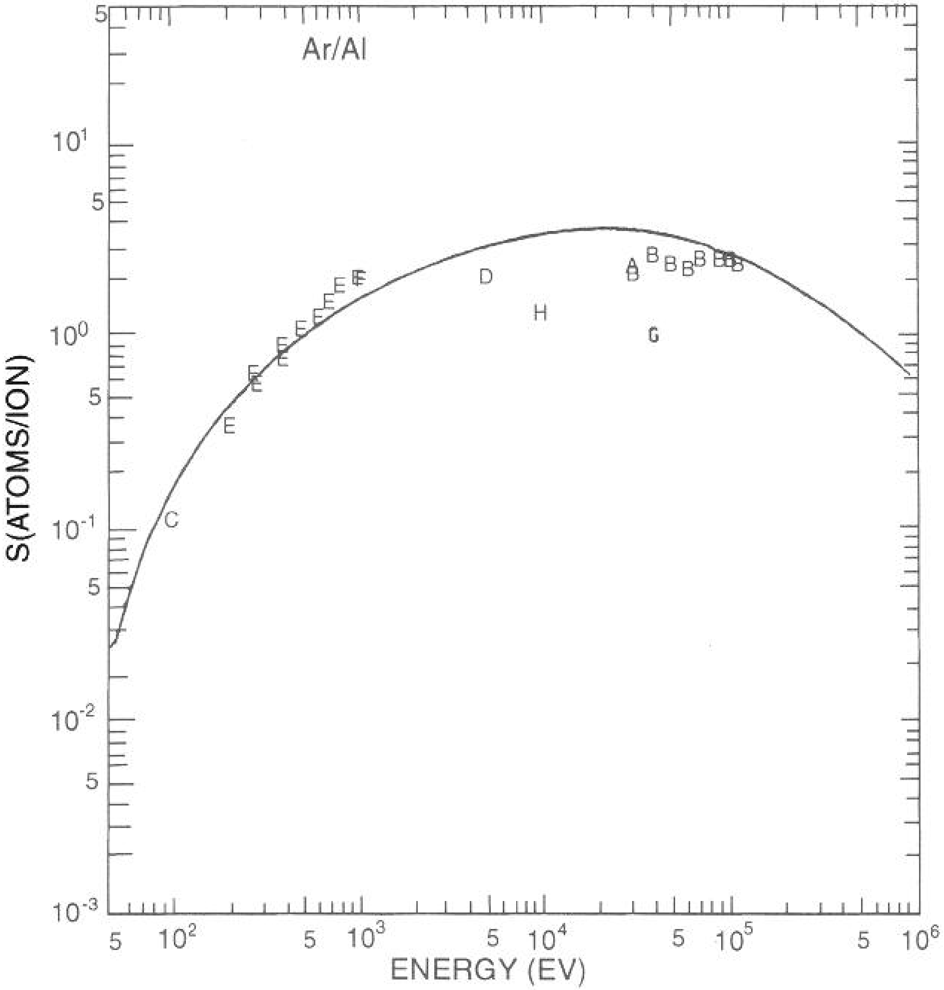

Figure 4-12 Sputter-yield values for Al as a function of energy. Letters on the plot refer to data from the following investigators: A. Yonts, Normand, and Harrison (1960); B. Fert, Colombie, and Fagot (1961); C. Laegreid and Wehner (1961); D. Robinson and Southern (1967); E. Weijsenfeld (1967); F. Oechsner (1973); G. Braun, Emmoth, and Buchta (1976); H. Okajima (1981). (From N. Matsunami, *et al., AT. Data. Nucl. Data Tables* **31**, 1 (1984). Reprinted with the permission of Academic Press, Inc.)

Sputtering yield

S **= number of atoms per incident particle**

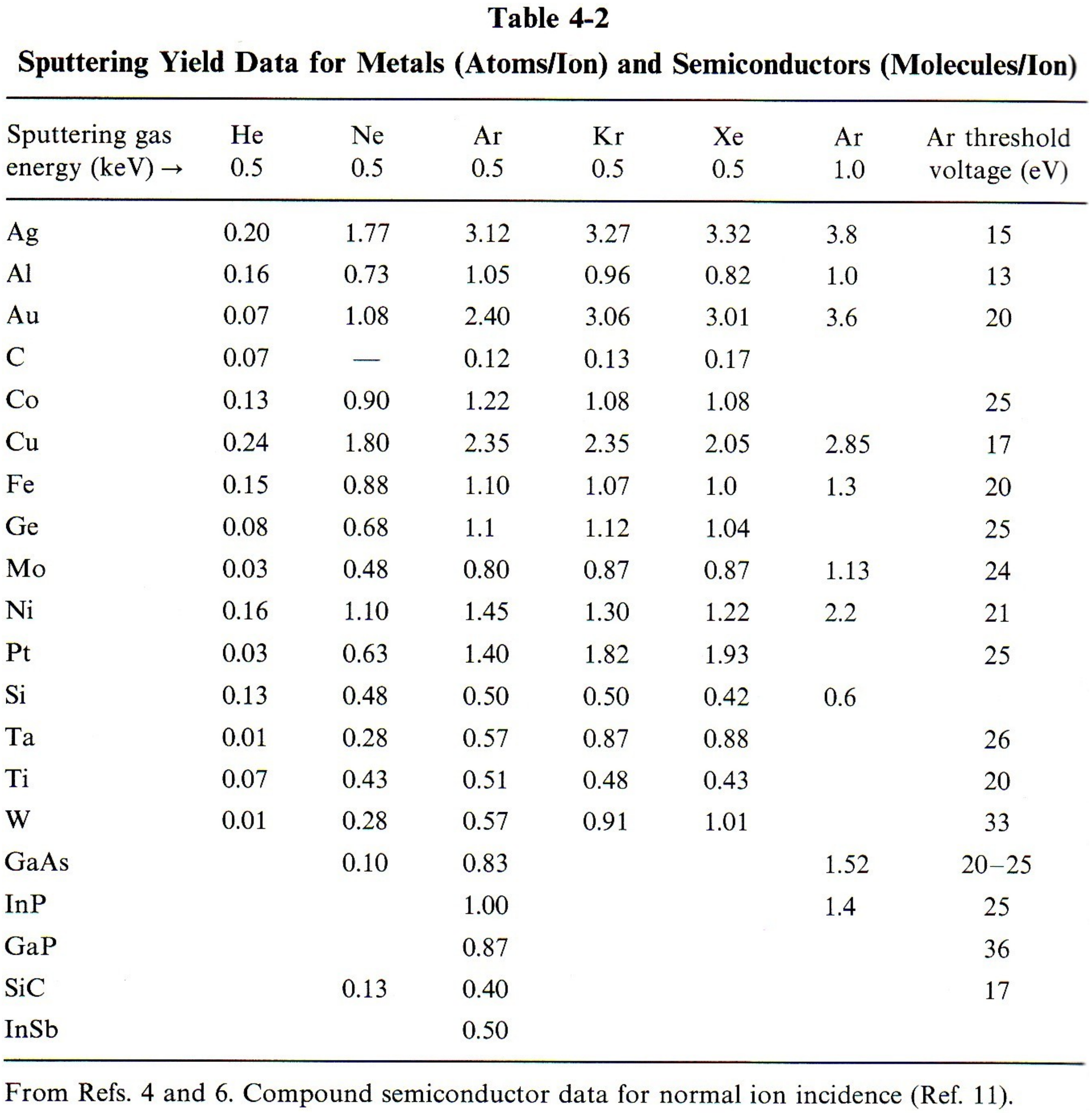

Table 4-2

Sputtering Yield Data for Metals (Atoms/Ion) and Semiconductors (Molecules/Ion)

Sputtering gas energy (keV) →	He 0.5	Ne 0.5	Ar 0.5	Kr 0.5	Xe 0.5	Ar 1.0	Ar threshold voltage (eV)
Ag	0.20	1.77	3.12	3.27	3.32	3.8	15
Al	0.16	0.73	1.05	0.96	0.82	1.0	13
Au	0.07	1.08	2.40	3.06	3.01	3.6	20
C	0.07	—	0.12	0.13	0.17		
Co	0.13	0.90	1.22	1.08	1.08		25
Cu	0.24	1.80	2.35	2.35	2.05	2.85	17
Fe	0.15	0.88	1.10	1.07	1.0	1.3	20
Ge	0.08	0.68	1.1	1.12	1.04		25
Mo	0.03	0.48	0.80	0.87	0.87	1.13	24
Ni	0.16	1.10	1.45	1.30	1.22	2.2	21
Pt	0.03	0.63	1.40	1.82	1.93		25
Si	0.13	0.48	0.50	0.50	0.42	0.6	
Ta	0.01	0.28	0.57	0.87	0.88		26
Ti	0.07	0.43	0.51	0.48	0.43		20
W	0.01	0.28	0.57	0.91	1.01		33
GaAs		0.10	0.83			1.52	20–25
InP			1.00			1.4	25
GaP			0.87				36
SiC		0.13	0.40				17
InSb			0.50				

From Refs. 4 and 6. Compound semiconductor data for normal ion incidence (Ref. 11).

Effet of the fabrication conditions on sputtering

Deposition rate

$$\dot{G}\left(\frac{\mathrm{cm}}{\mathrm{s}}\right) \approx \frac{\bar{\mathscr{P}}_{\mathrm{d}}\langle x_{\mathrm{th}}\rangle}{g\rho(1+\gamma_{\mathrm{e}})E},$$

P_d – power density
x_{th} – thermalisation length of the sputtered atoms
g – anode-cathode distance
ρ – density
γ_e – Townsend coefficient
E – sputtering energy

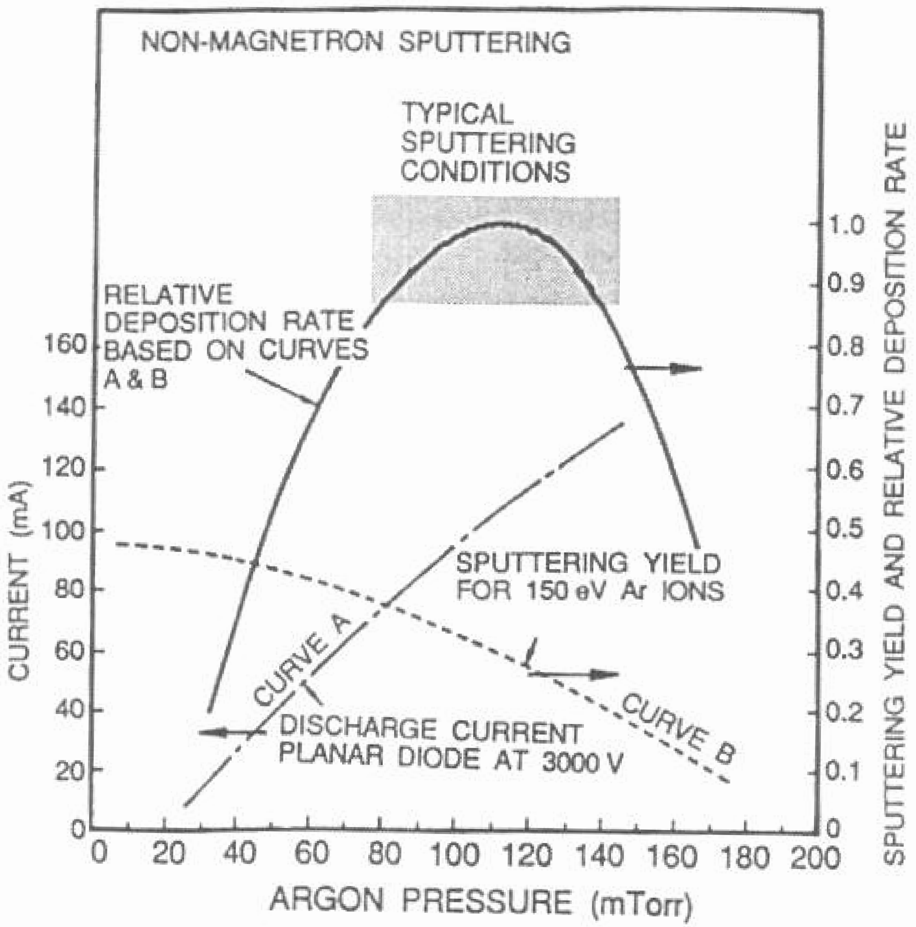

Figure 5-2 Influence of working pressure and current on film deposition rates in nonmagnetron sputtering. (From Ref. 3.)

DC and RF systems (capacitive coupling) - Sputtering

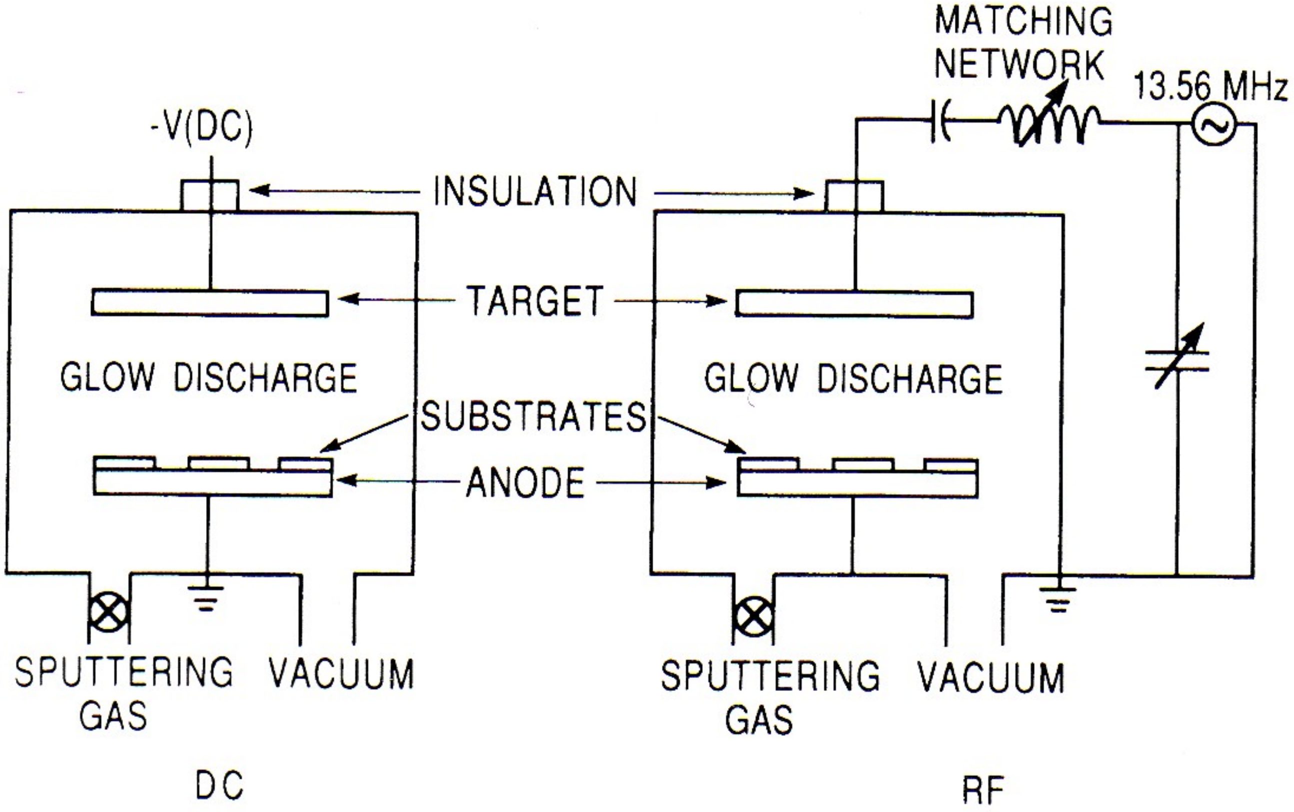

Figure 4-1 Schematics of simplified sputtering systems: (a) DC, (b) RF.

Reactive sputtering

Hysteresis effect

Φ_R: reactive gas flow

1. Oxides (oxygen)—Al_2O_3, In_2O_3, SnO_2, SiO_2, Ta_2O_5.
2. Nitrides (nitrogen, ammonia)—TaN, TiN, AlN, Si_3N_4, CN
3. Carbides (methane, acetylene, propane)—TiC, WC, SiC.
4. Sulfides (H_2S)—CdS, CuS, ZnS.
5. Oxycarbides and oxynitrides of Ti, Ta, Al, and Si.

Deposition rate:

Reactive gas partial pressure:

Cathode voltage:

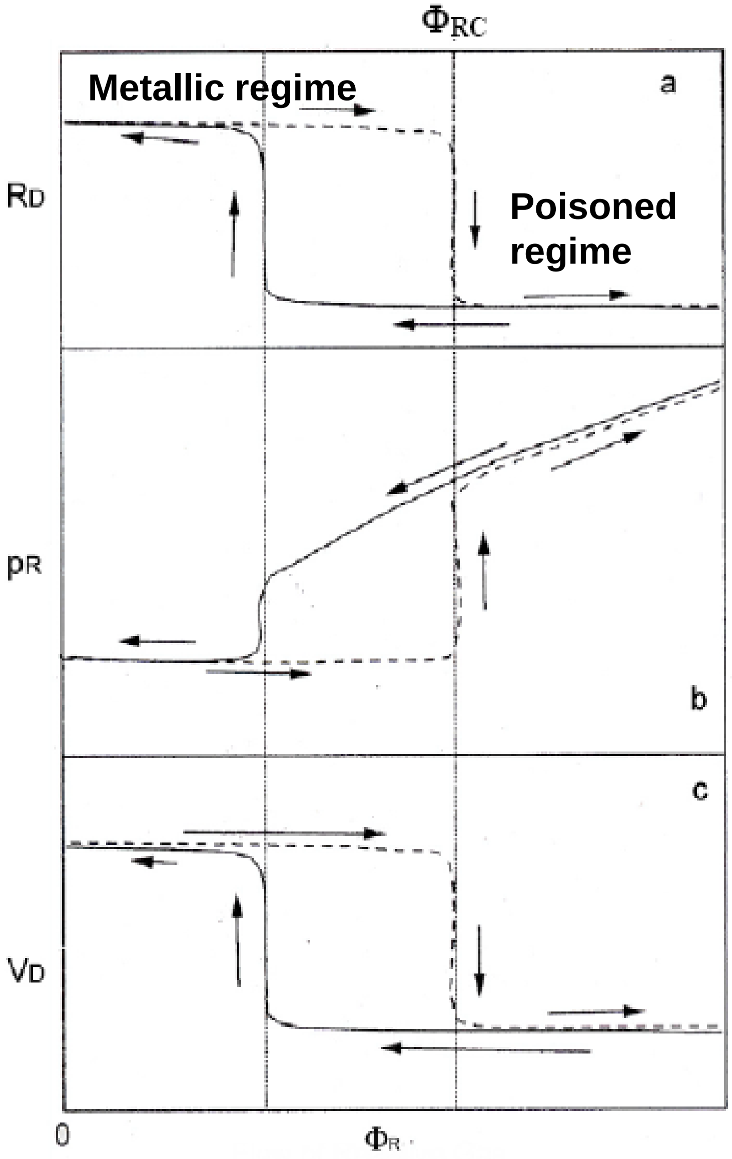

Evolution of R_D (a), p_R (b) and V_D (c) as a function of the **reactive gas flow.**

Berg’s model of reactive sputtering

Assumptions:

a) Metal target – sputtering yield S_m
b) Sputtering due to the inert gas
c) Target compound - S_c
d) Uniform current density at A_t
e) Substrate surface - A_s
f) Compound surface fraction - θ_t
g) Compound surface fraction of the "substrate" - θ_s
h) Sticking: α_t on the target (metal)
0 on the compound

Reactive gas flow toward all surfaces:

$$\Phi_r/N_A = P_R / (2\pi MRT)^{1/2}$$

S. Berg et al, Chapter A5.3 in *Handbook of Thin Film Process technology*”, D.A. Glocker and S.I. Shah, eds., IoP, Bristol 1995

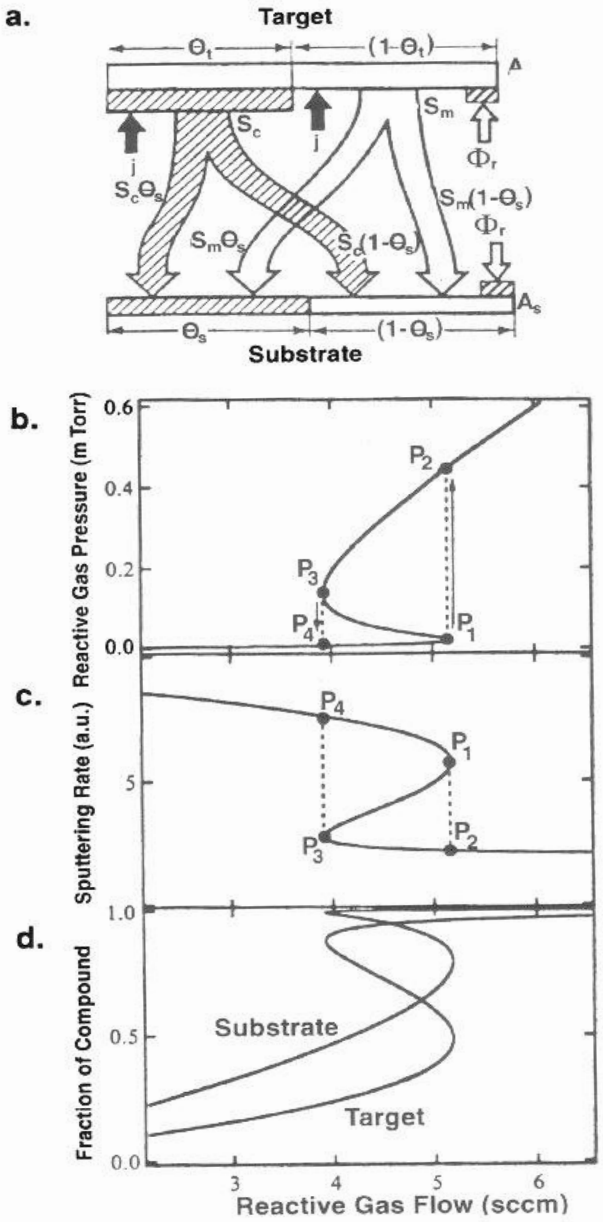

Figure 5-6 (a) Model of reactive sputtering. (b) Simulation of reactive gas pressure vs reactive gas flow. As Q increases, pressure values follow the path $P_1 \to P_2 \to P_3 \to P_4$, tracing out a hysteresis loop. (c) Simulated sputtering rate vs reactive gas flow rate. (d) Simulation of target and substrate composition as a function of reactive gas flow. (From S. Berg *et al.* in *Handbook of Thin Film Process Technology*, edited by D. A. Glocker and S. I. Shah, 1998. Reprinted with the permission of the Institute of Physics Publishing and the authors.)

Reactive sputtering effects

Target: Species formation rate = species sputtering rate:

j ….. Ar$^+$ current density

$$\Phi_r \alpha_t (1 - \theta_t) A_t a = (j/q)\theta_t A_t S_c,$$

Target erosion rate:

$$R_t = (j/q)[S_c \theta_t + S_m(1 - \theta_t)]A_t$$

Equilibrium of the arrival rates :

1. Sputtering rate, deposition rate on the metal and on the substrate;

   α_S – gas sticking coefficient
2. Metal reaction with the reactive gas
3. Metal sputtered from the target

$$\overset{1}{(j/q)[S_c \theta_t A_t](1 - \theta_s)} + \overset{2}{\Phi_r \alpha_s (1 - \theta_s) A_s b} = \overset{3}{(j/q)[S_m(1 - \theta_t)A_t]\theta_s / b}$$

Gas phase equilibrium:

$$Q = Q_t + Q_s + Q_p,$$

Reaction on the target: $Q_t = \Phi_r \alpha_t (1-\theta_t) A_t$
Reaction on the substrate: $Q_S = \Phi_r \alpha_s (1-\theta_s) A_s$
Pumped flux, S – pumping speed: $Q_p = P_r S$

Effet of reactive gas on the deposition rate: stoechiometry and properties

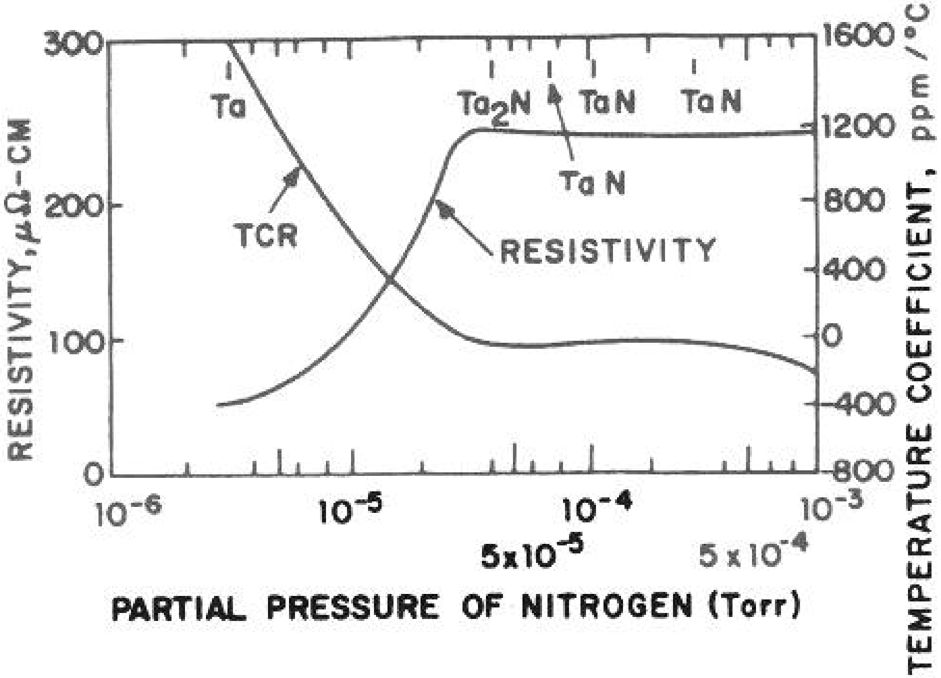

Figure 5-7 Influence of nitrogen on composition, electrical resistivity, and temperature coefficient of resistivity of reactively sputtered Ta films. (From Ref. 19.)

TaN – resistence in electric circuits;
DC sputtering at 3 - 5 kV, thermal coeff. of resistivity: $\rho = \rho_0(1 + \alpha T)$

Plasma system and process control

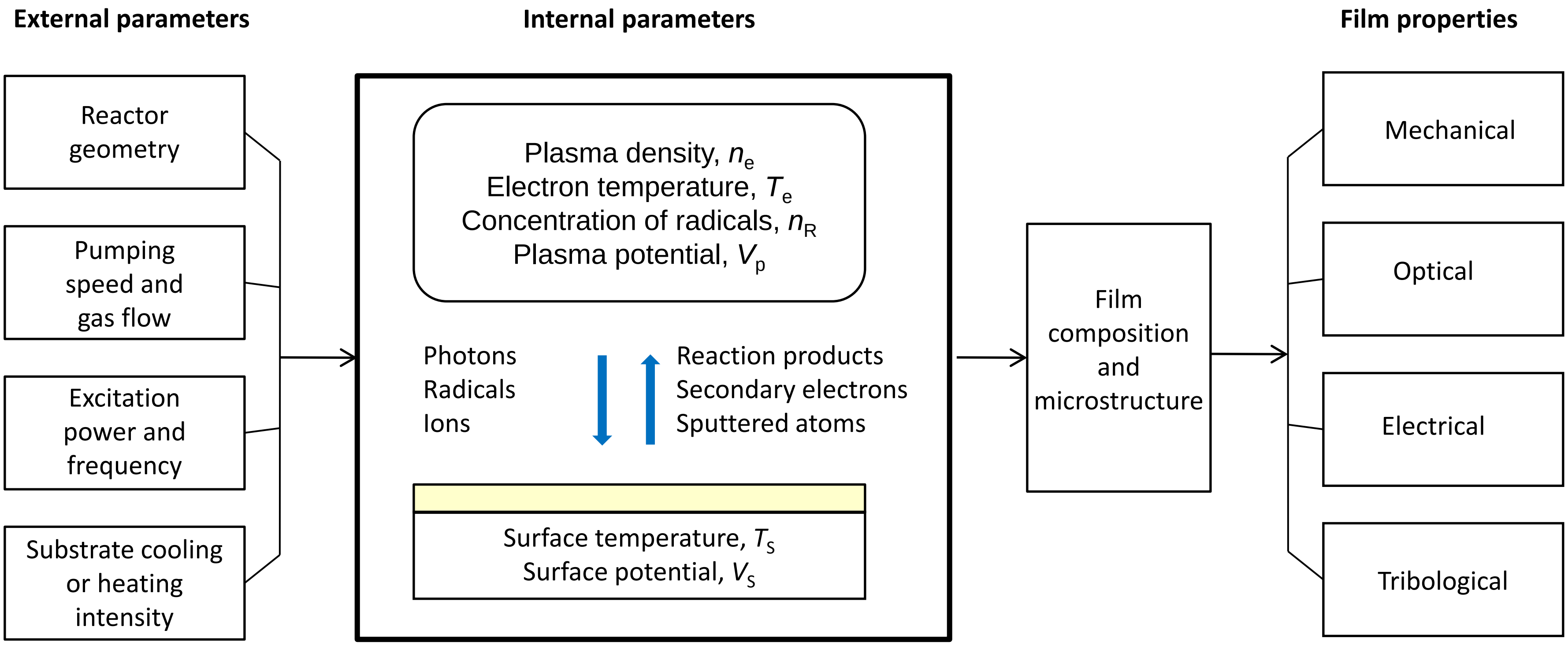

External parameters

- Reactor geometry
- Pumping speed and gas flow
- Excitation power and frequency
- Substrate cooling or heating intensity

Internal parameters

Plasma density, n_e
Electron temperature, T_e
Concentration of radicals, n_R
Plasma potential, V_p

Photons
Radicals
Ions

Reaction products
Secondary electrons
Sputtered atoms

Surface temperature, T_S
Surface potential, V_S

Film composition and microstructure

Film properties

- Mechanical
- Optical
- Electrical
- Tribological

Today:

Reactive sputtering
Microstructural evolution during the film growth – Structure zone model
Plasma diagnostics

L. Martinu et al., Chapter 9 in "*Handbook of Thin Film Process Technology*", P.M. Martin, ed., Elsevier, 2010.

Thin film growth models

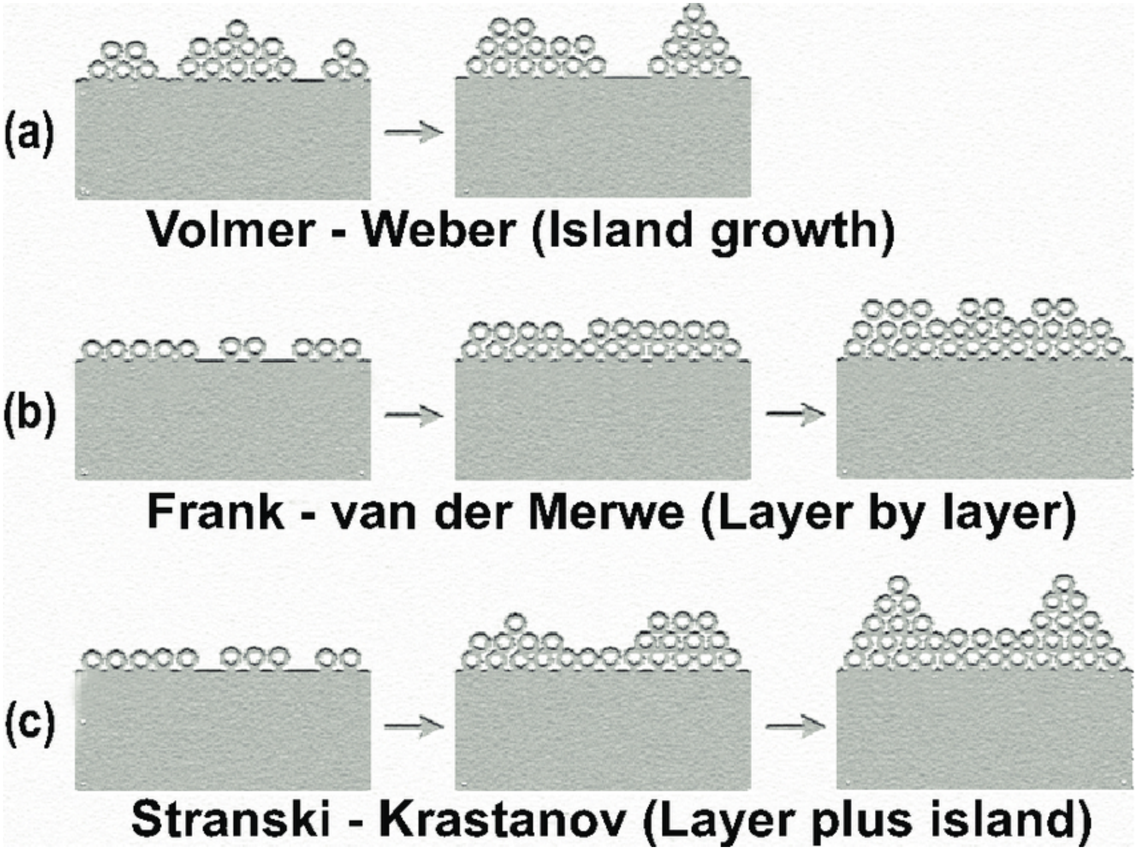

Structure zone model - SZM

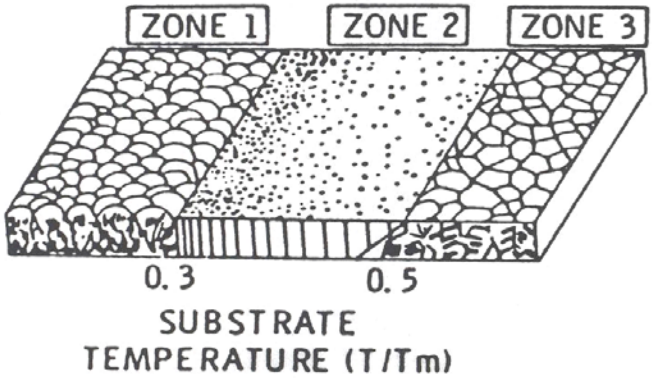

B.A. Movchan and A.V. Demchishin, Fiz. Metal. Metalloved., 28 (1969) 653.

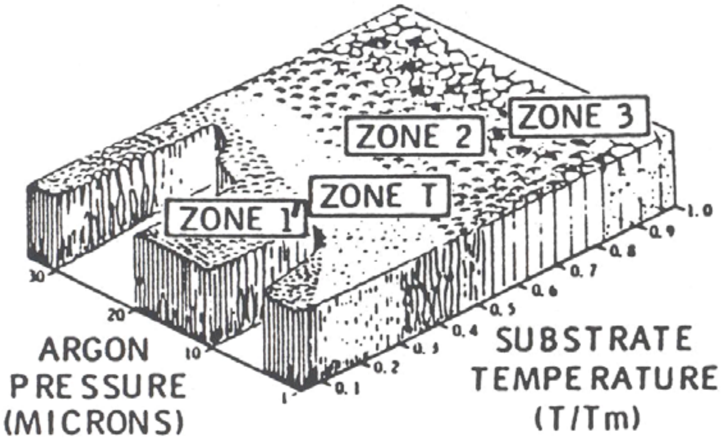

J.A. Thornton, J. Vac. Sci. Technol., 11 (1974) 666.

Microstructural evolution according to the SZM

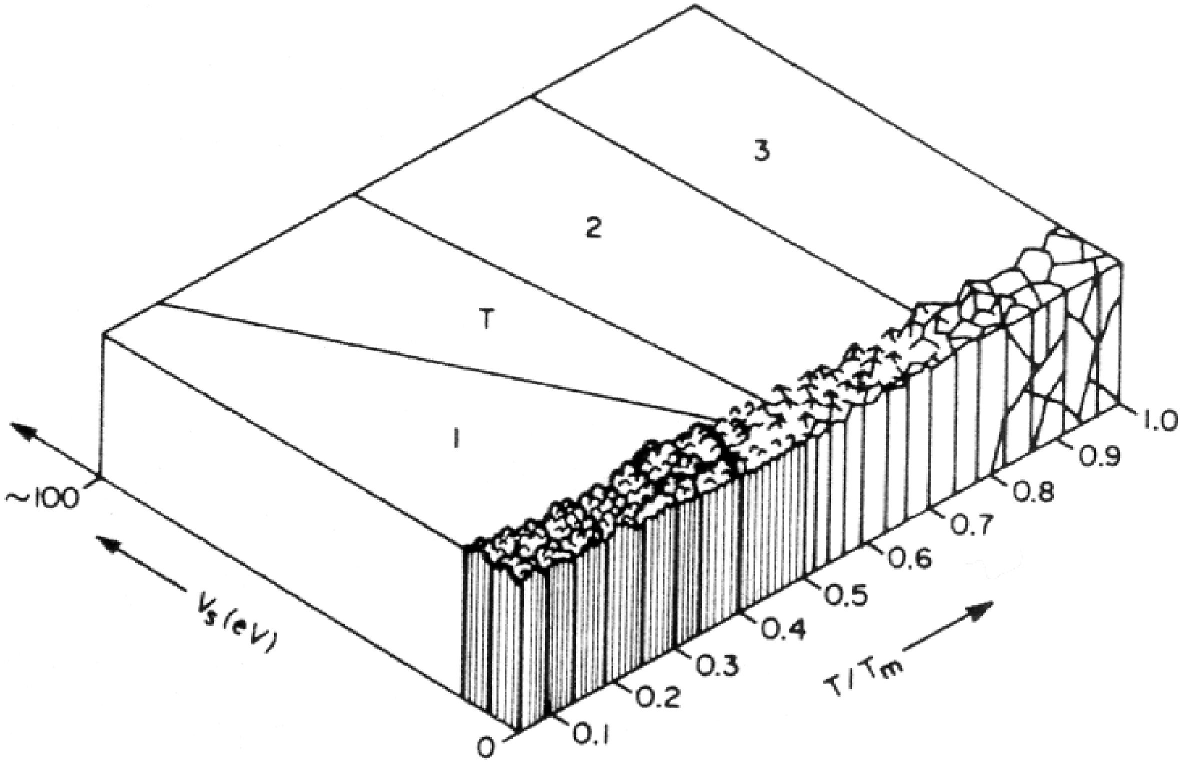

Messier, Giri, and Roy [Messier, 1984];

Structure zone diagram including plasma based deposition and ion etching

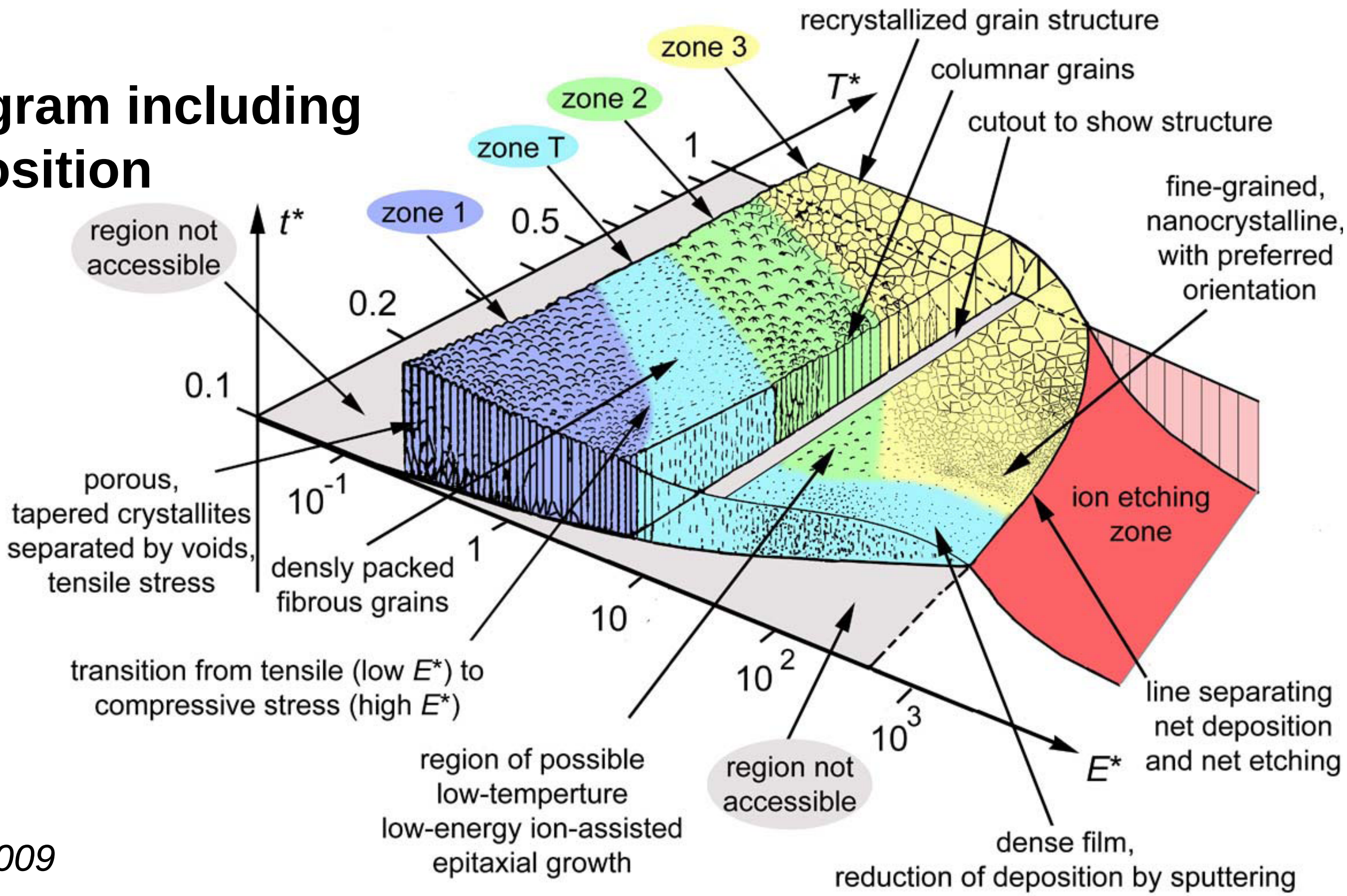

A. Anders, Thin Solid Films, 2009

(I) The linear axis is replaced with a generalized temperature, which includes the homologous temperature plus a temperature shift caused by the *kinetic energy of particles arriving on the surface.*

(II) The linear pressure axis is replaced with a logarithmic axis for a normalized energy, describing displacement and heating effects caused by the *kinetic energy of bombarding particles.*

(III) The until now unlabeled z-axis is replaced with a net film thickness, which allows one to illustrate film structure, thickness reduction by densification/sputtering, and “negative thickness” (ion etching).

Growth control by the ion bombardment energetics

1. Ion bombardment effets

$E_p \sim E_i \;.\; \Phi_i / \Phi_n$ *- energy per deposited particle*

$E_i < 1$ keV, IEDF, Φ_i ion flux, Φ_n flux of the condensing particles, SZM

Control of E_i and Φ_i / Φ_n :

$$\Phi_N = r_D \frac{\rho N_A}{m_A}$$

- Surface biasing
- Unbalanced magnetrons
- Gas phase ionization (plasma assistence)
- Ionization / biasing (IBAD, PA-EBE, ECR, PECVD, MW/RF)
- Pulsed plasma (HiPIMS)

2. UV and VUV radiation

- Strong radiation below $\lambda = 200$ nm
- Polymer crosslinking, surface volatilization

Vacuum ultraviolet (VUV) spectra

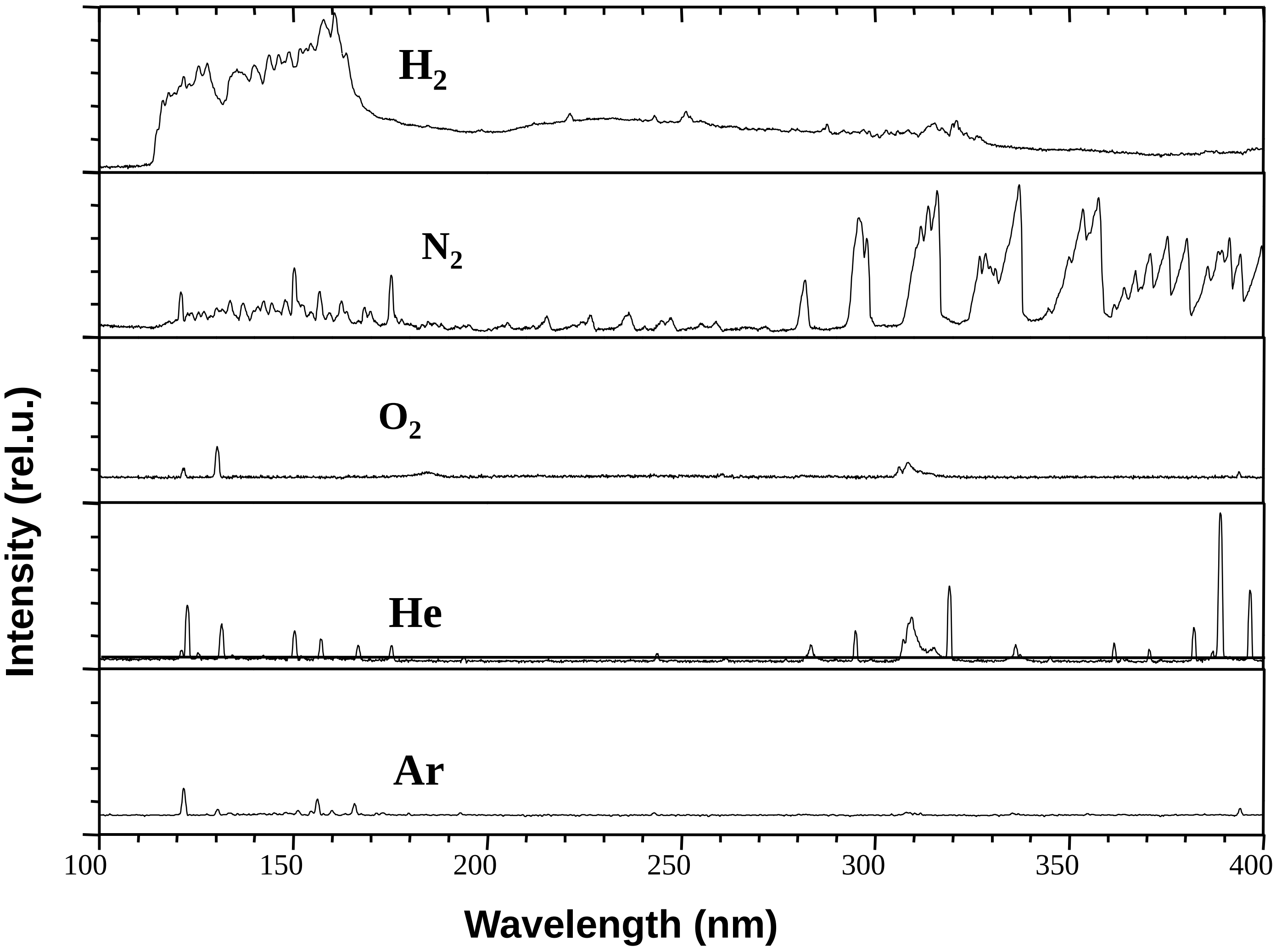

A. Hollander et al., J. Polym. Sci., Polym. Chem., 1995

Critical ion energy and ion flux

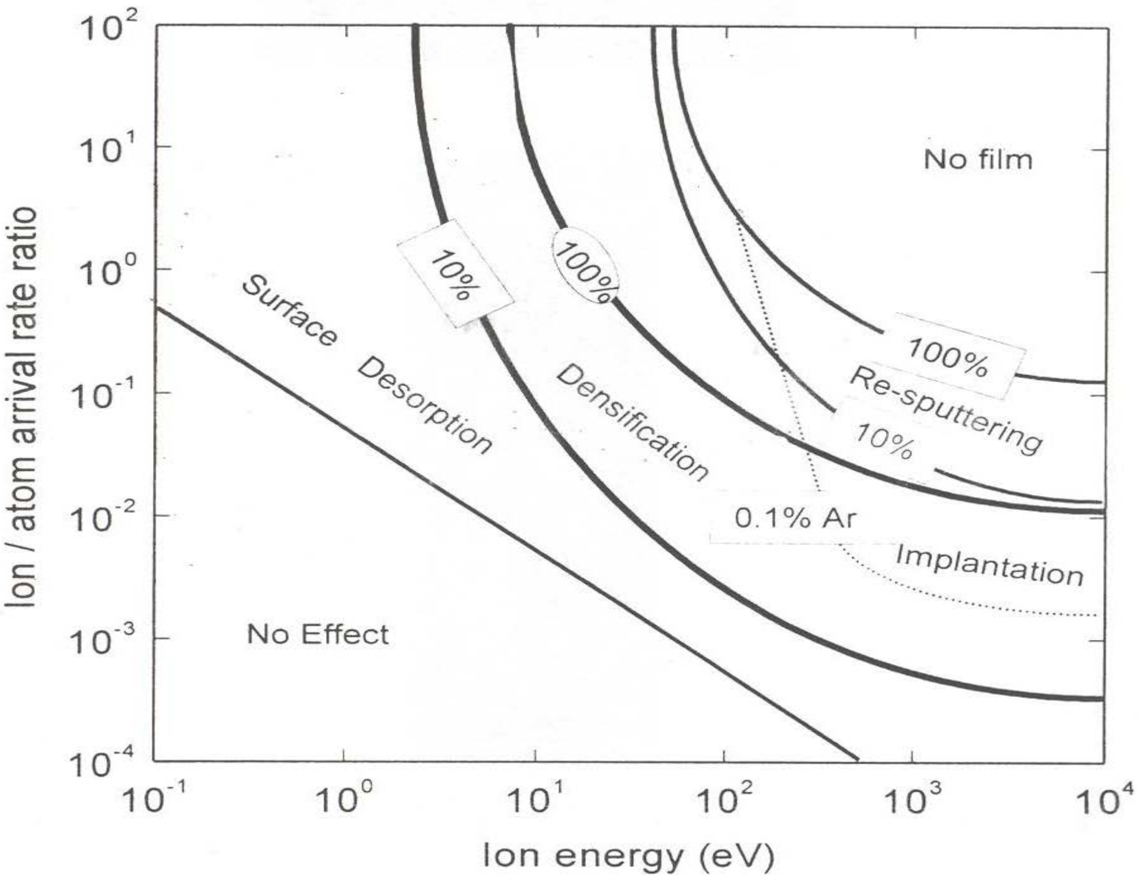

(After Ref. [Roy89], adapted from Ref.[Harper84] for IAD of metals).

Multi-grid ion energy analyser

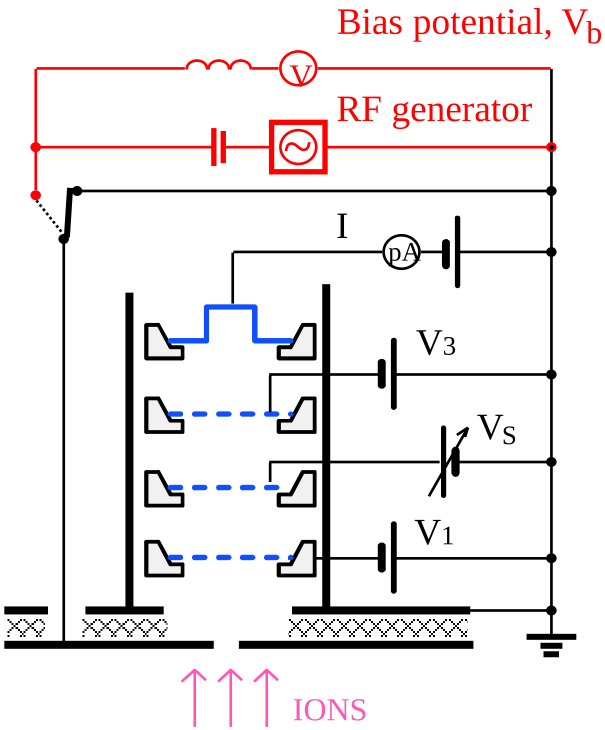

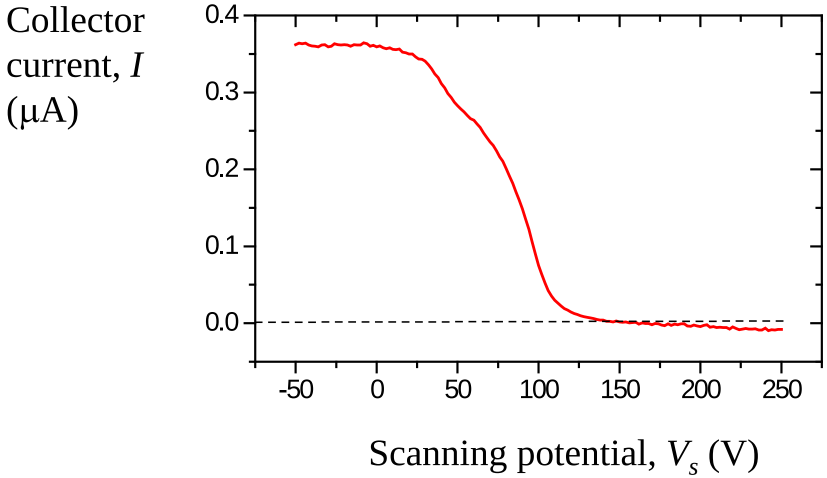

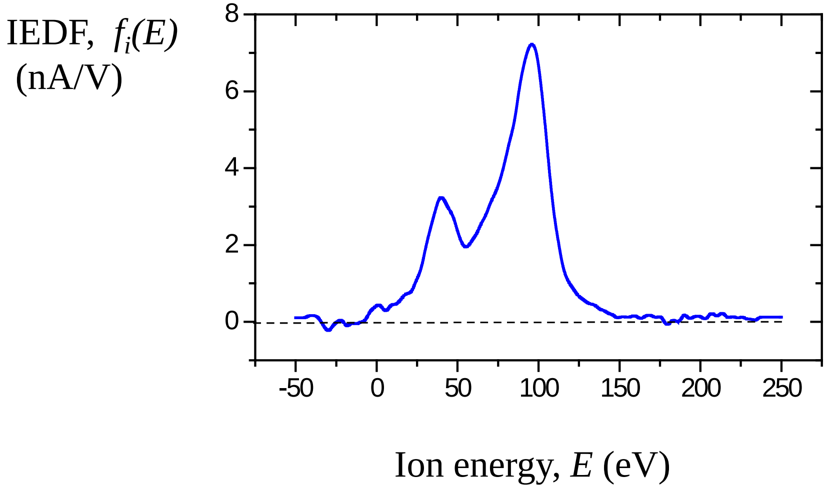

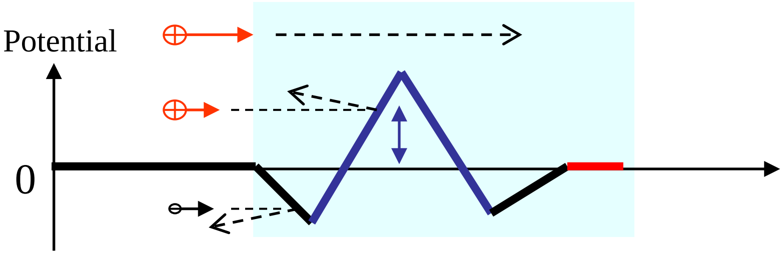

O. Zabeida, PhD Thesis, Polytechnique Montreal, 2000

PECVD in the dual-frequency MW/RF discharge

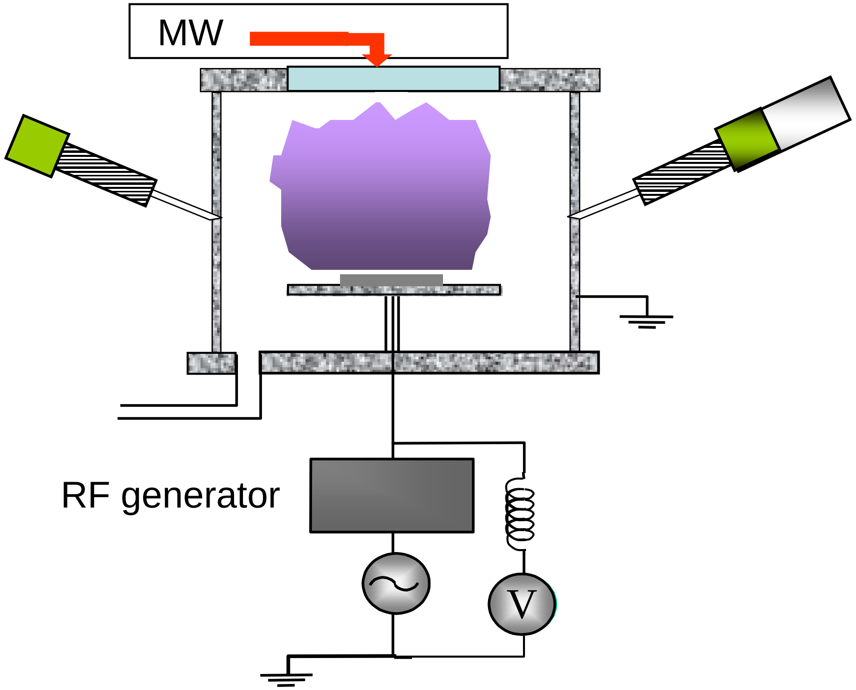

- Principal microwave (2.45 GHz) plasma
- RF (13.56 MHz) radiofrequency applied to the substrate holder - V_B

MW/RF dischharge: Ion flux vs. bias voltage in CH_4

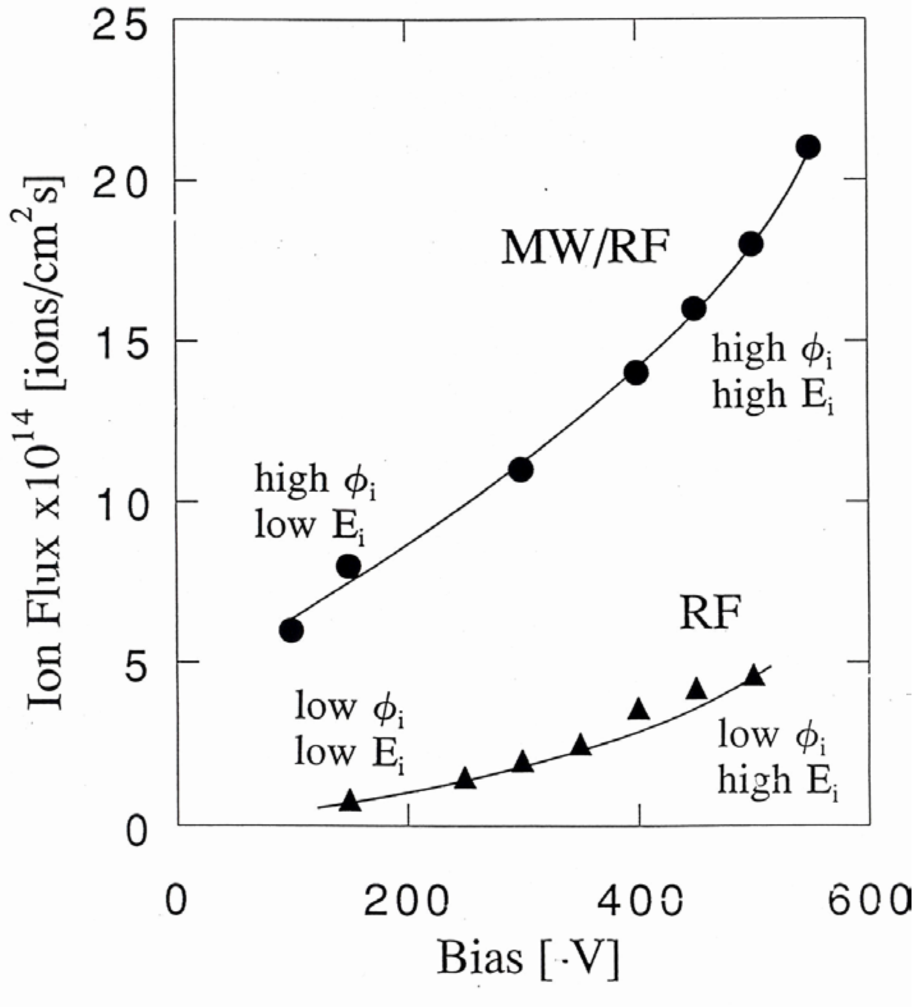

L. Martinu et al., J. Vac. Sci. Technol. A, 12 (1994) 1360

Ion energy distributions, IED

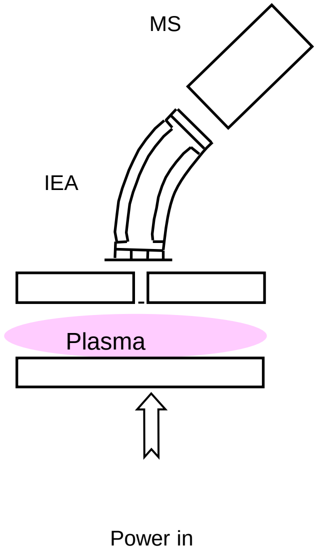

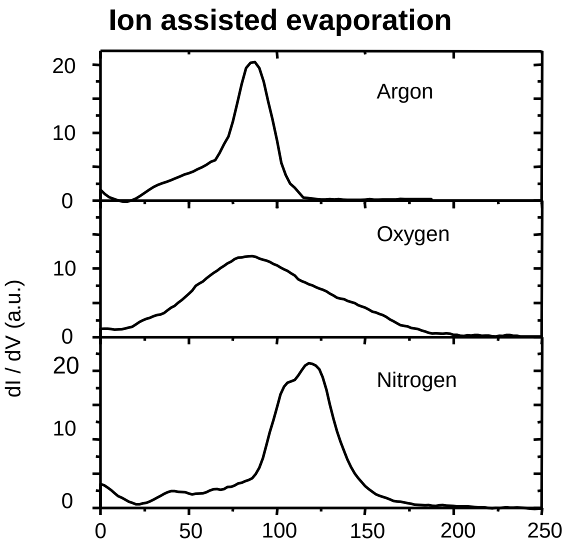

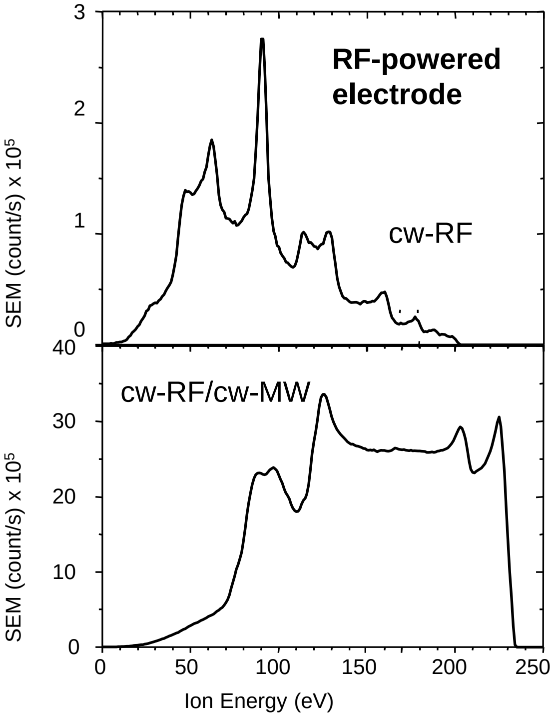

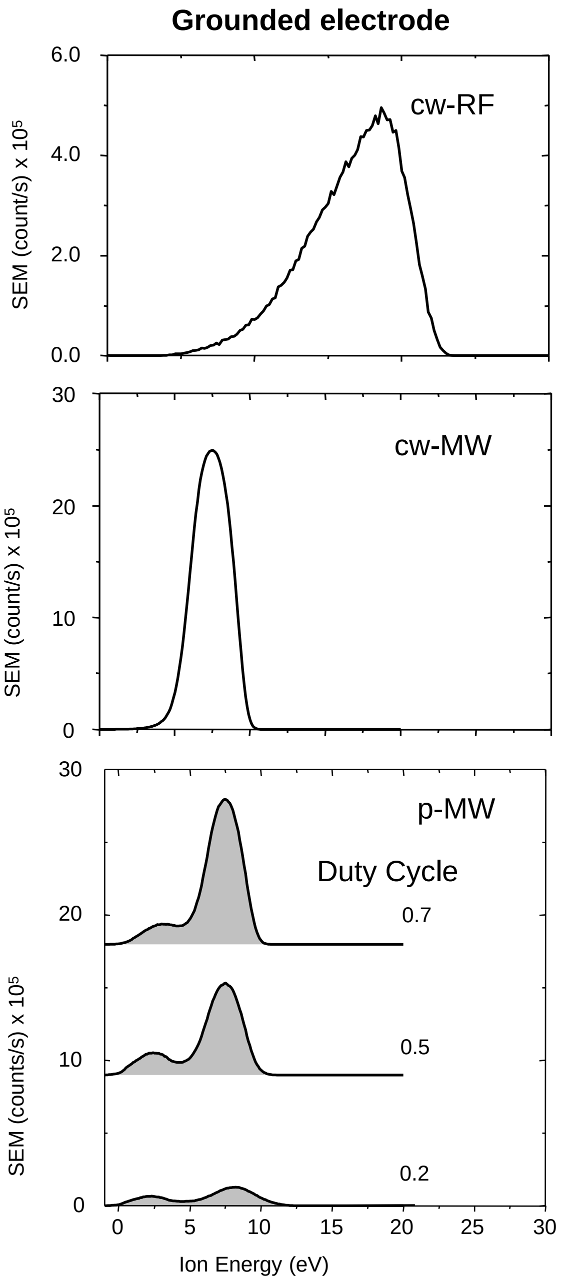

Effet of ion bombardment in Si_3N_4

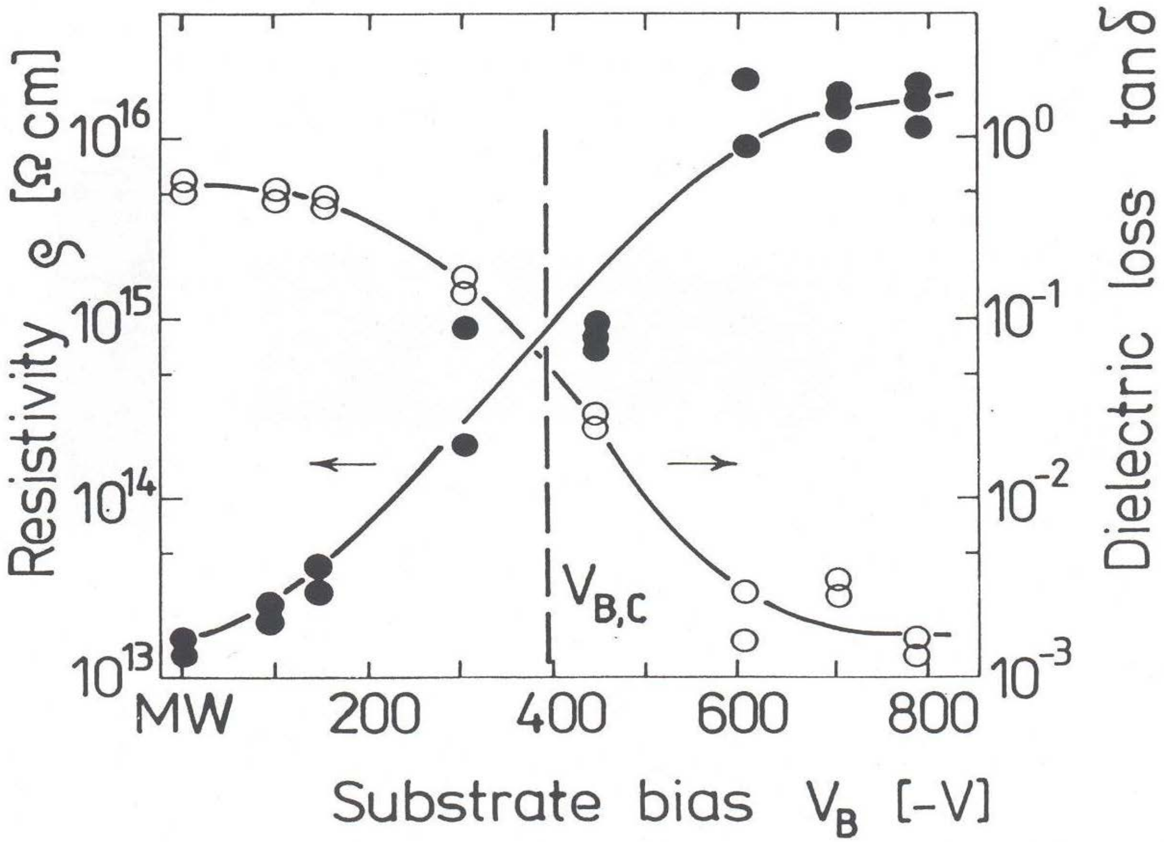

Critical ion energy - E_c

Mechanical stress in PECVD films

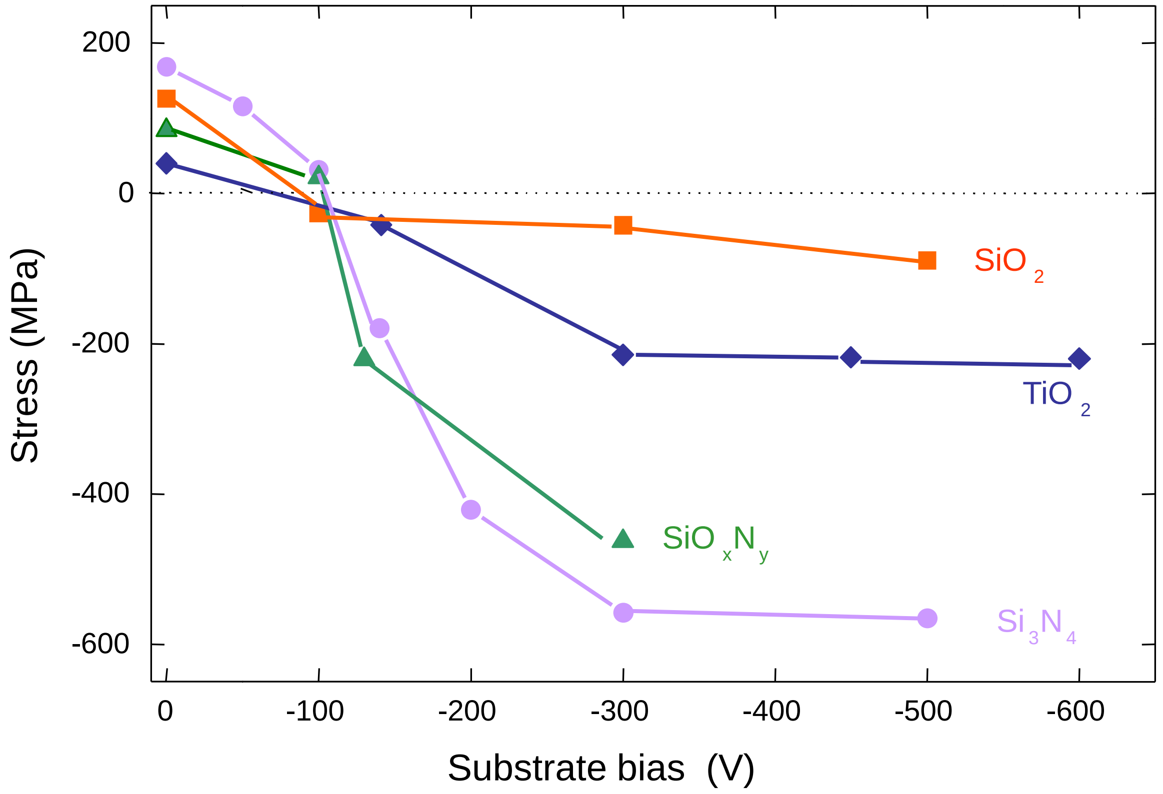

J.E. Klemberg-Sapieha et al., SVC Proc., 2000

Critical ion energy and ion flux

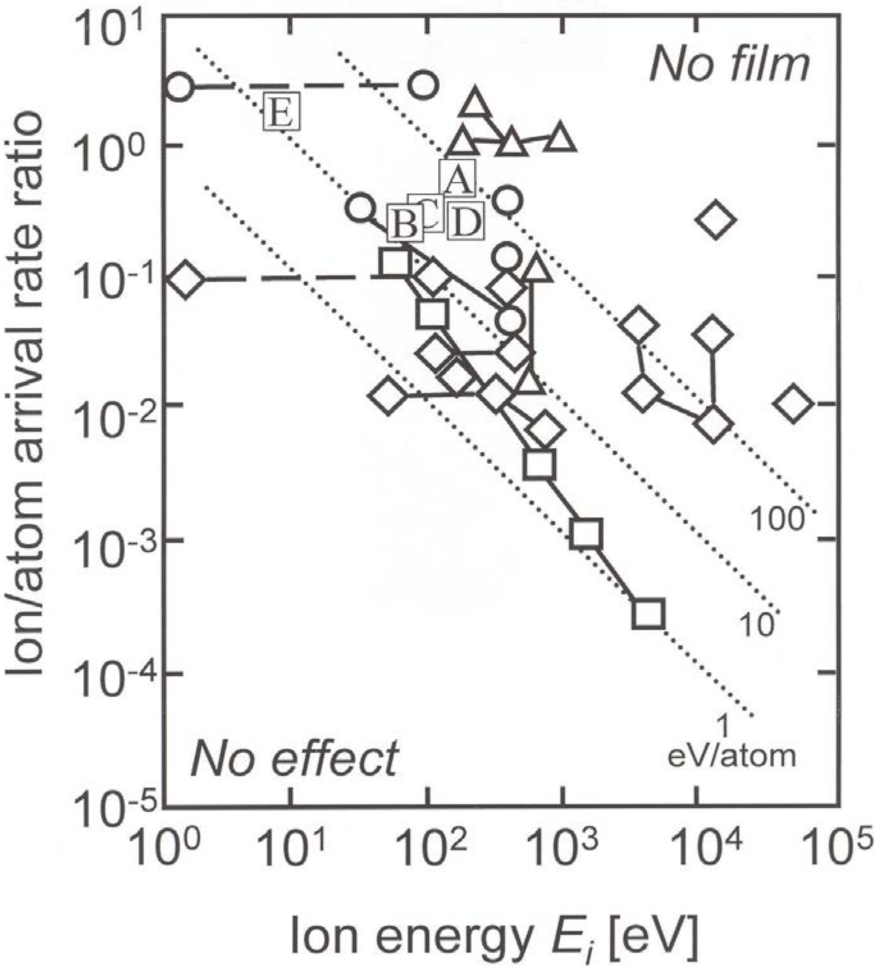

A: $SiN_{1.3}$; **B**: SiO_2; **C**: a-C:H; **D**: TiO_2 (MW/RF); **E**: TiO_2 (PICVD)
and different PVD dielectrics, metals and semiconductors

L. Martinu et al., J. Vac. Sci. Technol. A, 12 (1994) 1360

Ion bombardment and thin film growth

Layer-by-layer
(Franck-van der Merwe)

Island
(Vollmer-Weber)

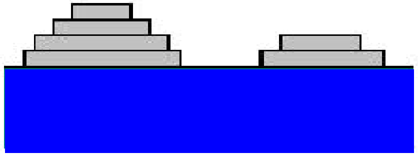

Mixed
(Stranski-Krastanov)

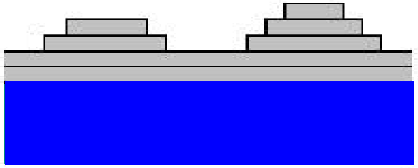

Surface effects

Enhanced surface mobility
Island dissolution
Surface defects
Surface activation

➔

Homogeneous nucleation
Early coalescence
Surface morphology
Compound formation

Interface mixing

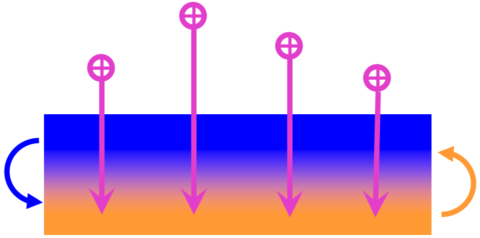

Subplantation

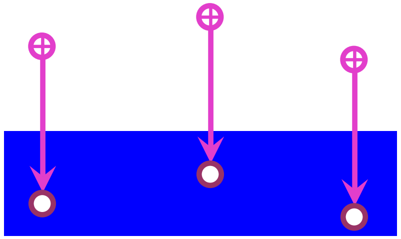

Lifshitz *et al. PRL* 62 (1989) 1290.

Growth below surface:
➔ Film-forming ions
➔ Film densification
➔ Stress formation

Ion bombardment effects in a plasma environment: sub-surface transport and its effects.

Complex optical interference filters

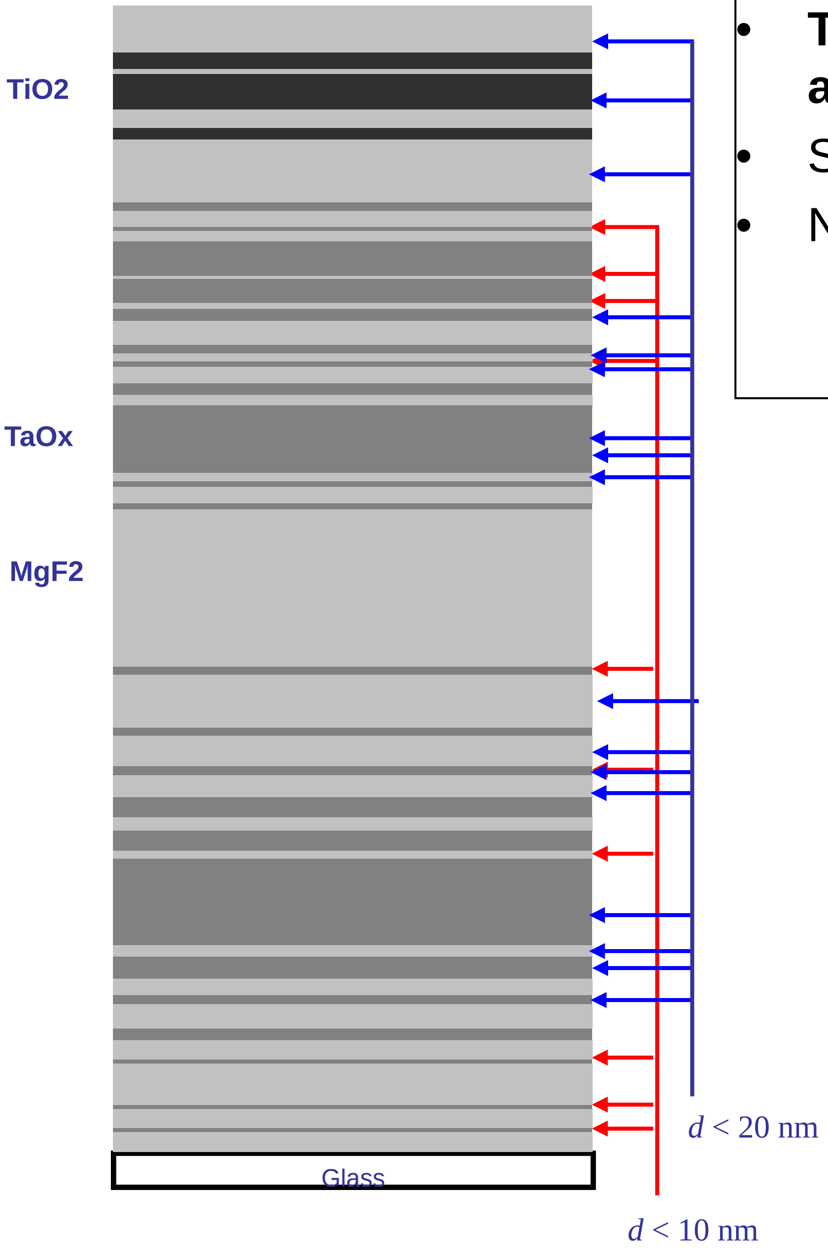

- **Today’s advanced optical interference filters are synthesized, not designed**
- Synthesis techniques: Flip-Flop and Needle
- New challenges on films and processes:
  - Ultra-thin films with abrupt interfaces
  - Non quarter-wave films require control

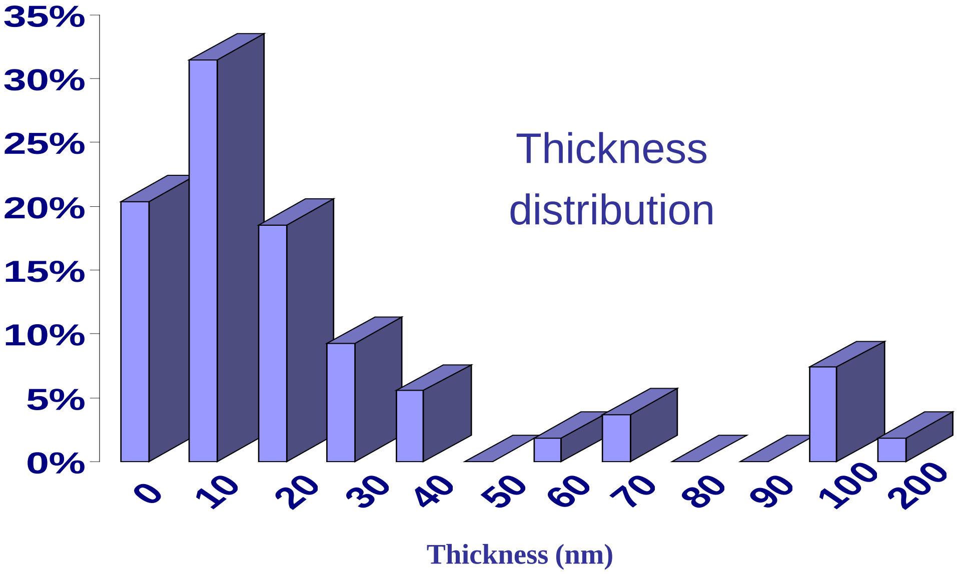

- **53 layer broad-band AR coating** for photographic lens synthesized by Flip-Flop method
- Berlin ’91 design contest winner: W. H. Southwell

Initial growth of TiO_2 on SiO_2: *In situ* RTSE

Addition of $TiCl_4$ to O_2

PECVD Deposition
V_B = - 450 V
in O_2 + $TiCl_4$
P_{TiCl4}/P_{O2} = 0.005

Ion Bombardment
E_{max} ~ 480 eV
E_m ~ 150 eV

Optical model

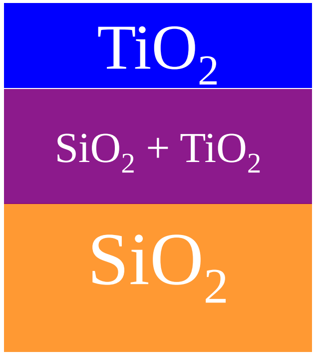

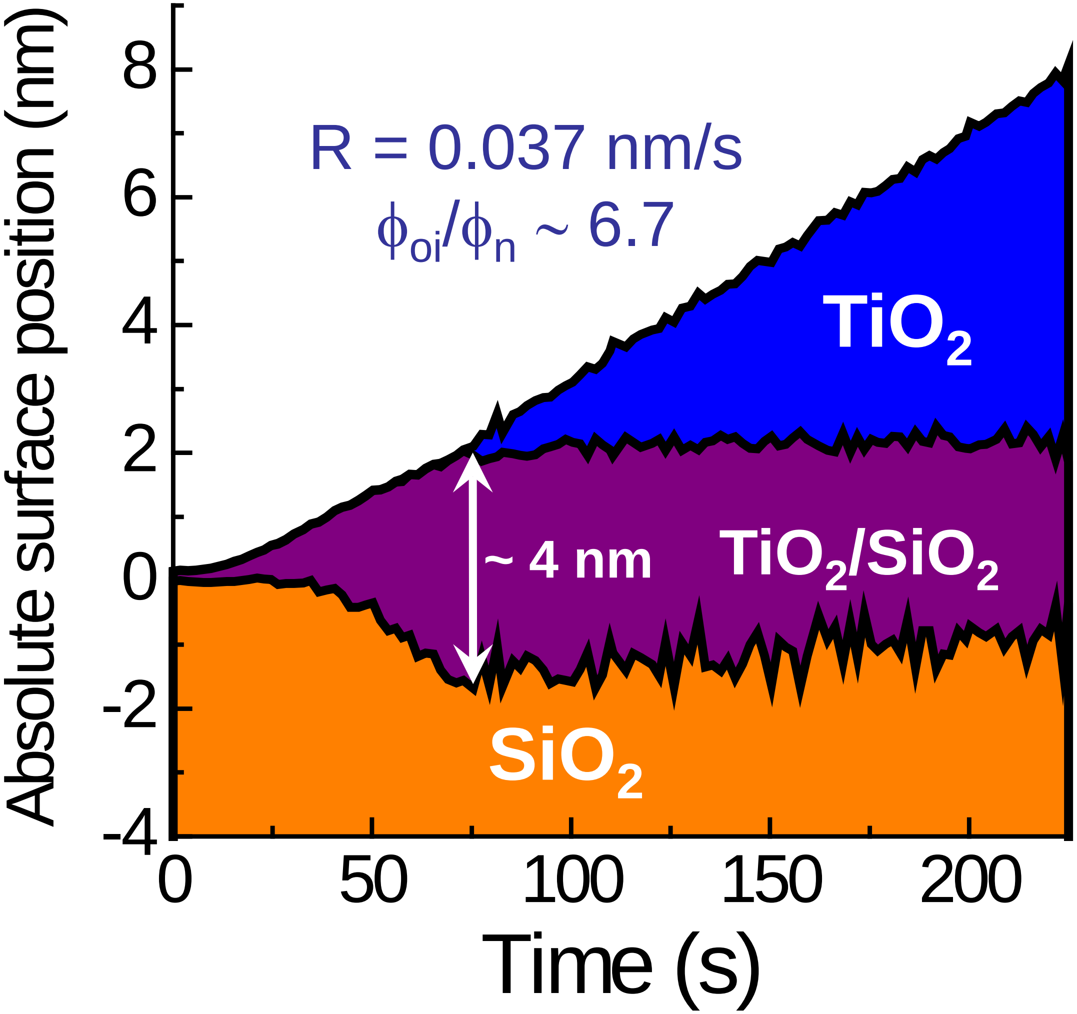

- Interface broadening during initial growth => steady state thickness
- We want to understand interface formation and to control it!

Interface broadening: TRIDYN simulation

Interface Mixing: $\phi_i/\phi_n \sim 6.3$; R = 0.04 nm/s

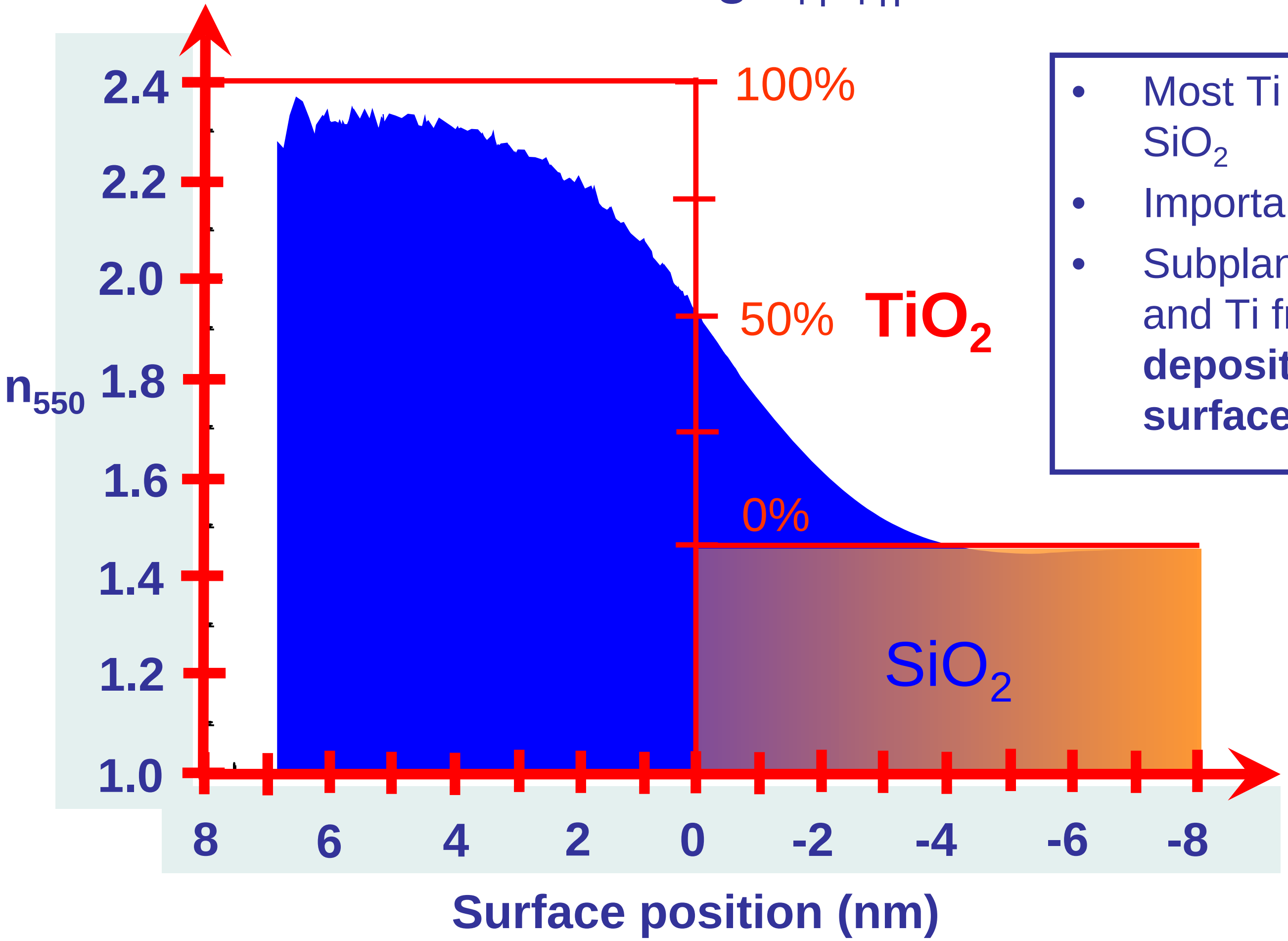

- Most Ti atoms are knocked into SiO_2
- Important ion mixing
- Subplantation of O from plasma and Ti from surface ⇒ **film deposited below growth surface**

We must increase Ti flux (r_D)!

Interface broadening: TRIDYN simulations

Interface Mixing: $\phi_i/\phi_n \sim 0.063$; R = 4 nm/s

$V_B = -450$ V

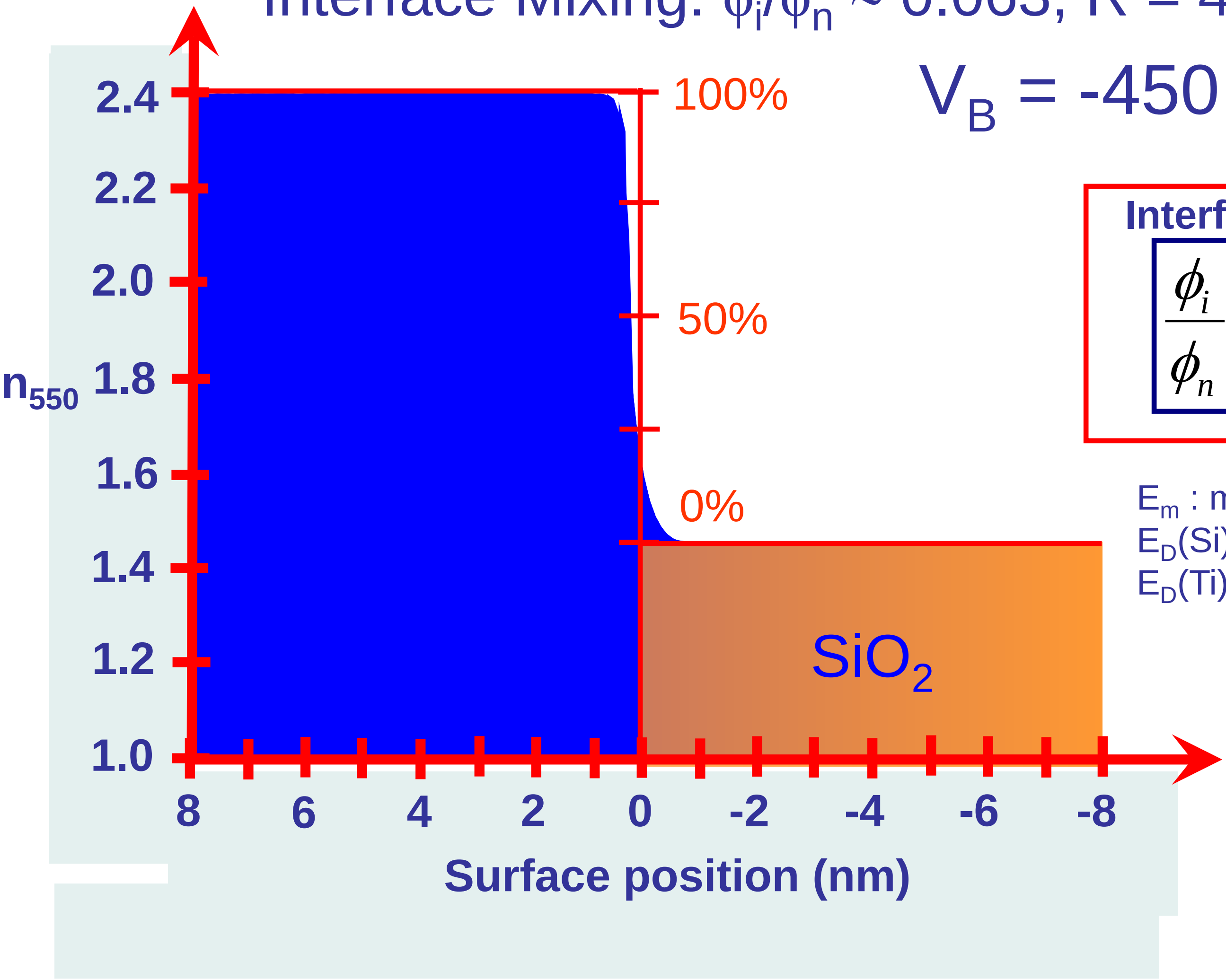

Interface ≤ 1 nm

$$\boxed{\frac{\phi_i}{\phi_n}\frac{E_m}{2E_D} < 1}$$

E_m : mean ion energy
$E_D(Si) \sim 12$ eV
$E_D(Ti) \sim 20$ eV

POLYTECHNIQUE MONTRÉAL
UNIVERSITÉ D'INGÉNIERIE

Interface broadening:

HRTEM, comparison with simulation

EELS
Ti signal

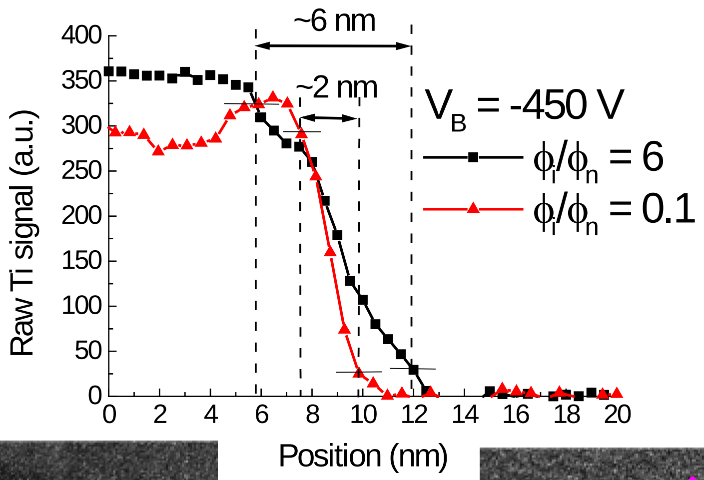

HRTEM

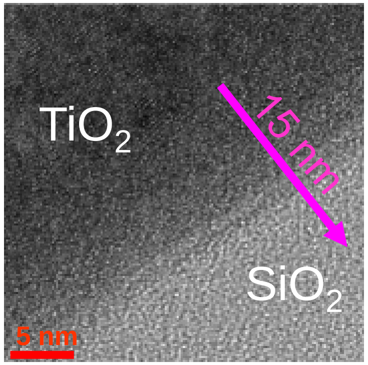

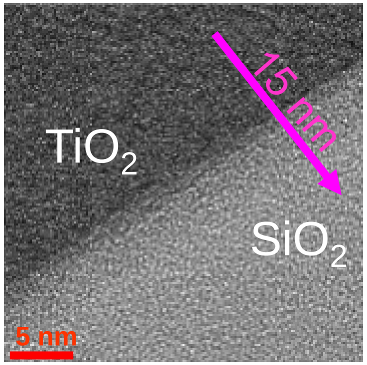

$\boldsymbol{\phi_i/\phi_n = 6}$

TRIDYN

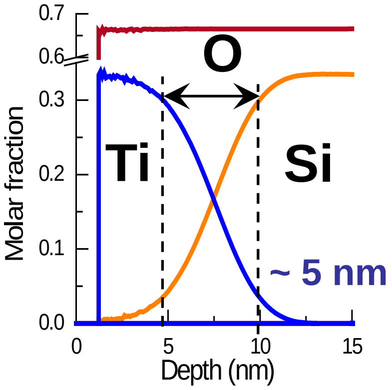

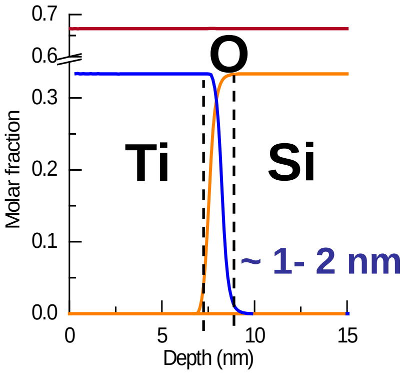

$\boldsymbol{\phi_i/\phi_n = 0.1}$

Interface engineering of Si nitrides – MW/RF plasma

- **PECVD deposition system**
  - Gas mixtures: SiH_4, N_2, Ar
  - Pressure: 20-200 mTorr
  - RF and MW power levels: ≈ 100 W
  - Substrate bias: ~ 0 – 800 V
- ***In-situ* spectro-ellipsometry**
  - Dynamic Monte Carlo simulations SRIM: www.srim.org
  - A. Amassian, JAP, 2006
- ***Ex-situ* characterization:**
  - UV-VIS-NIR-IR VASE: 260 nm – 33 μm, Spectrophotometry
  - FTIR, XPS, XRD, AFM, ERD-TOF

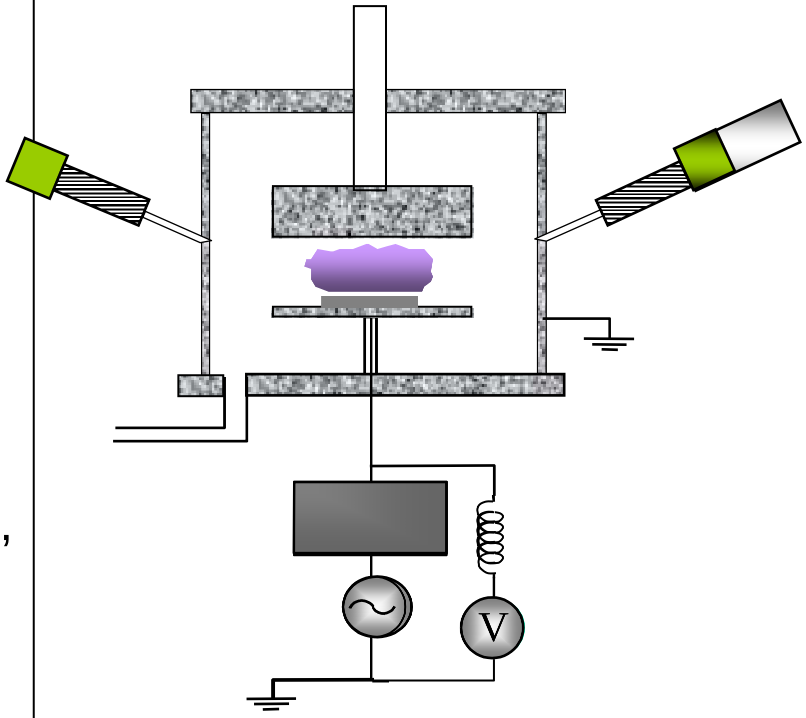

Ion bombardment and properties of Si_3N_4

IEDF

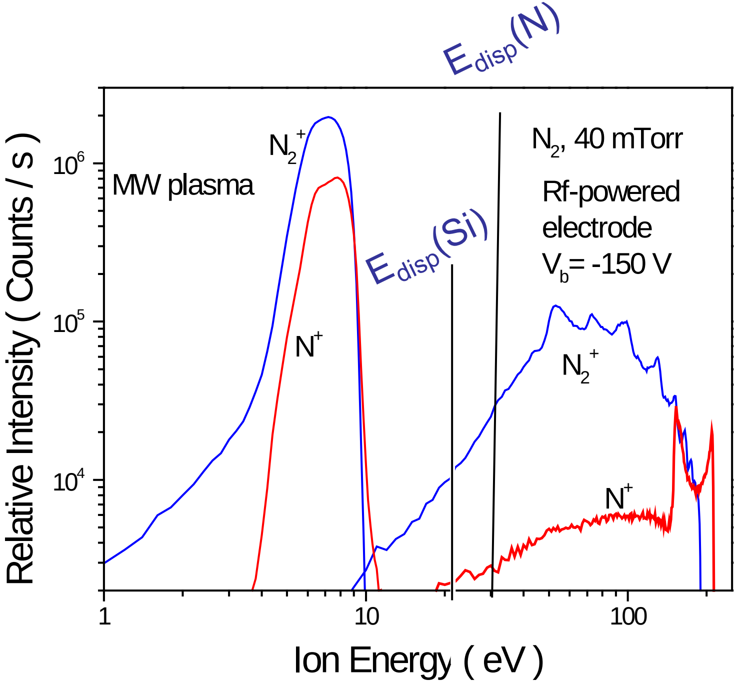

Si rich:
Filters in IR

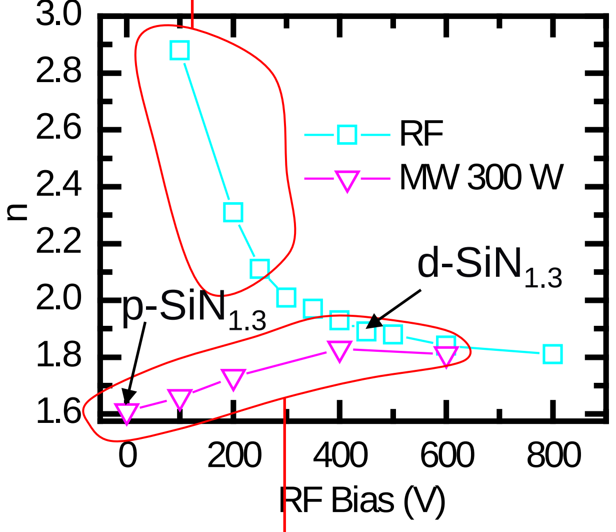

Transparent:
filters in visible

Energy per deposited particle: $\boldsymbol{E_p \approx E_i \times \phi_i / \phi_n}$

<u>Surface</u>

$E_b(Si) \approx E_b(N) \sim 2$ eV < E_{max} (MW) <

<u>Bulk displacement</u>
$E_{disp}(Si) \sim 20$ eV
$E_{disp}(N) \sim 28$ eV

<< E_{max} (RF)

L. Martinu, JVST A, 2000
A. Hallil et al, JVST A, 2000

Single-material (Si_3N_4) rugate filter

- A single material is used to provide low, high and all intermediate refractive indices
- n dependent on the microstructure and porosity
- Microstructure and porosity dependent on ion bombardment energy, E_i, and incident flux, Φ_I
- Dual-mode RF/MW PECVD flexible enough to produce $SiN_{1.3}$ films with n_{550} ~ 1.2 – 2.0
- Graded-index optical filters have been fabricated

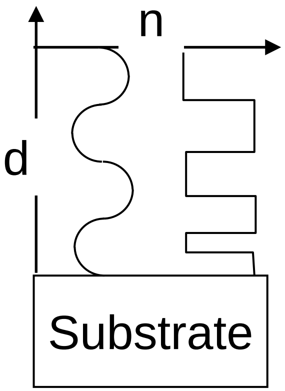

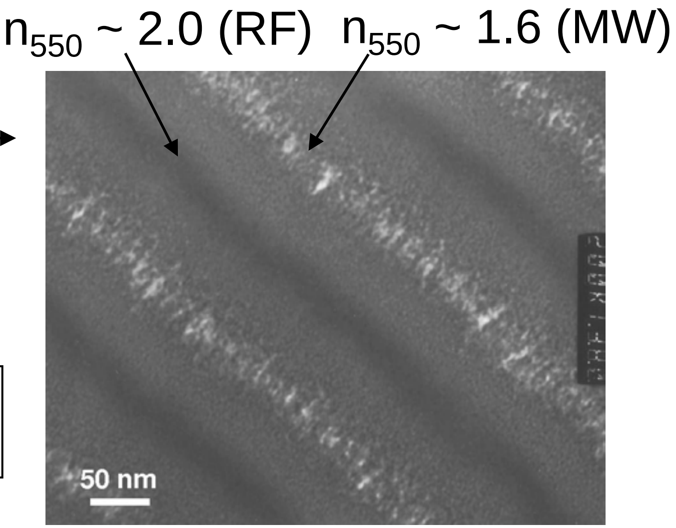

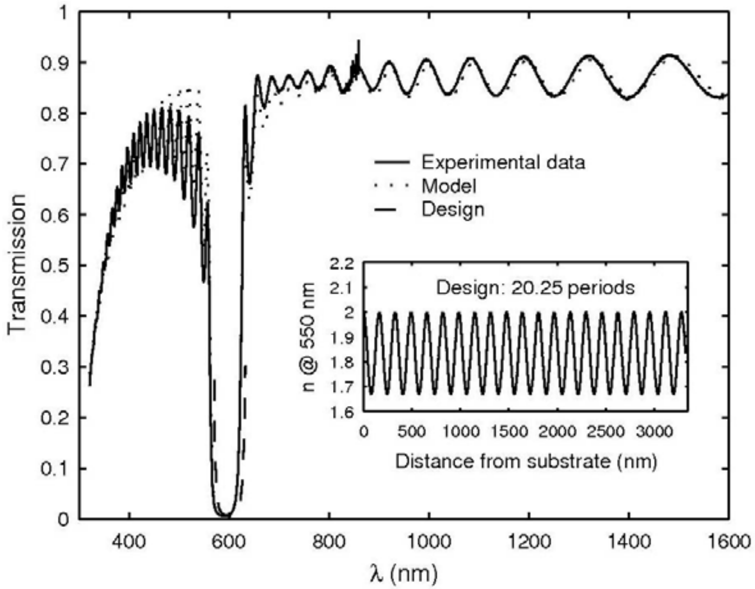

R. Vernhes et al., Appl. Opt. 43 (2004) 97

Fabry-Perot porous/dense OIF sensor

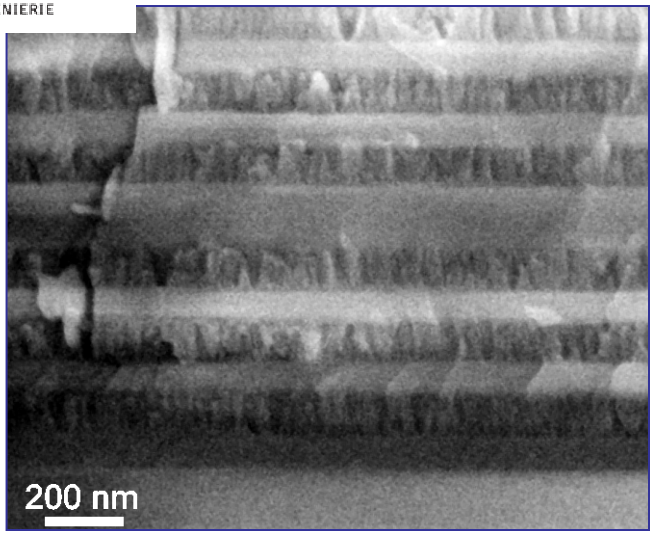

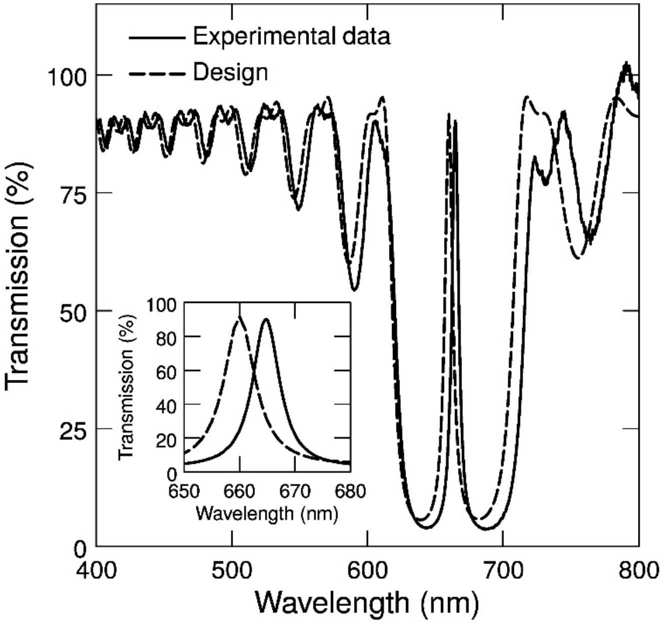

Optical transmission

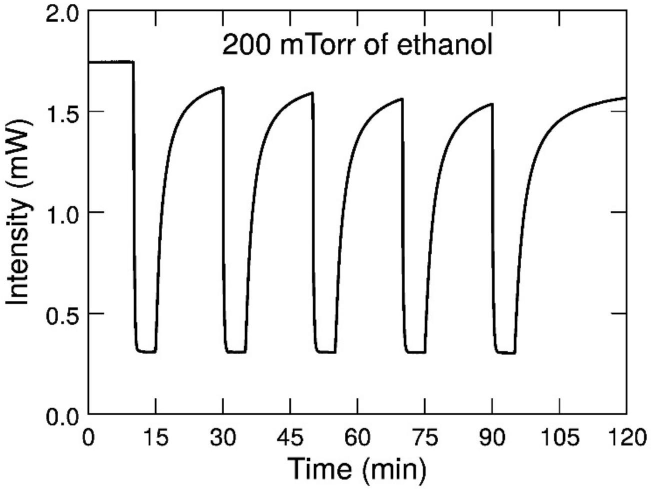

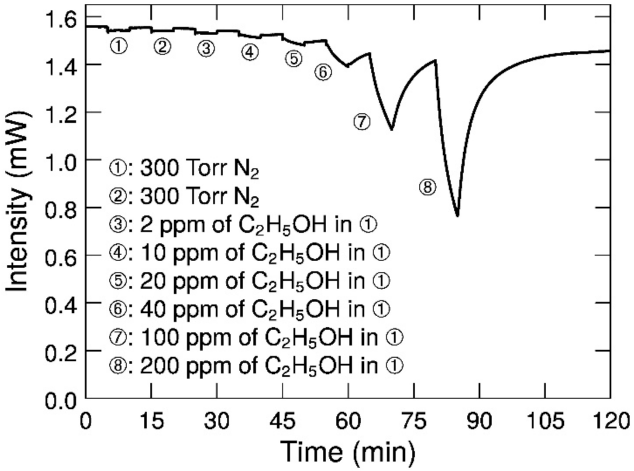

R. Vernhes et al., Sensors and Actuators B 185 (2013) 504– 511

Plasma system and process control

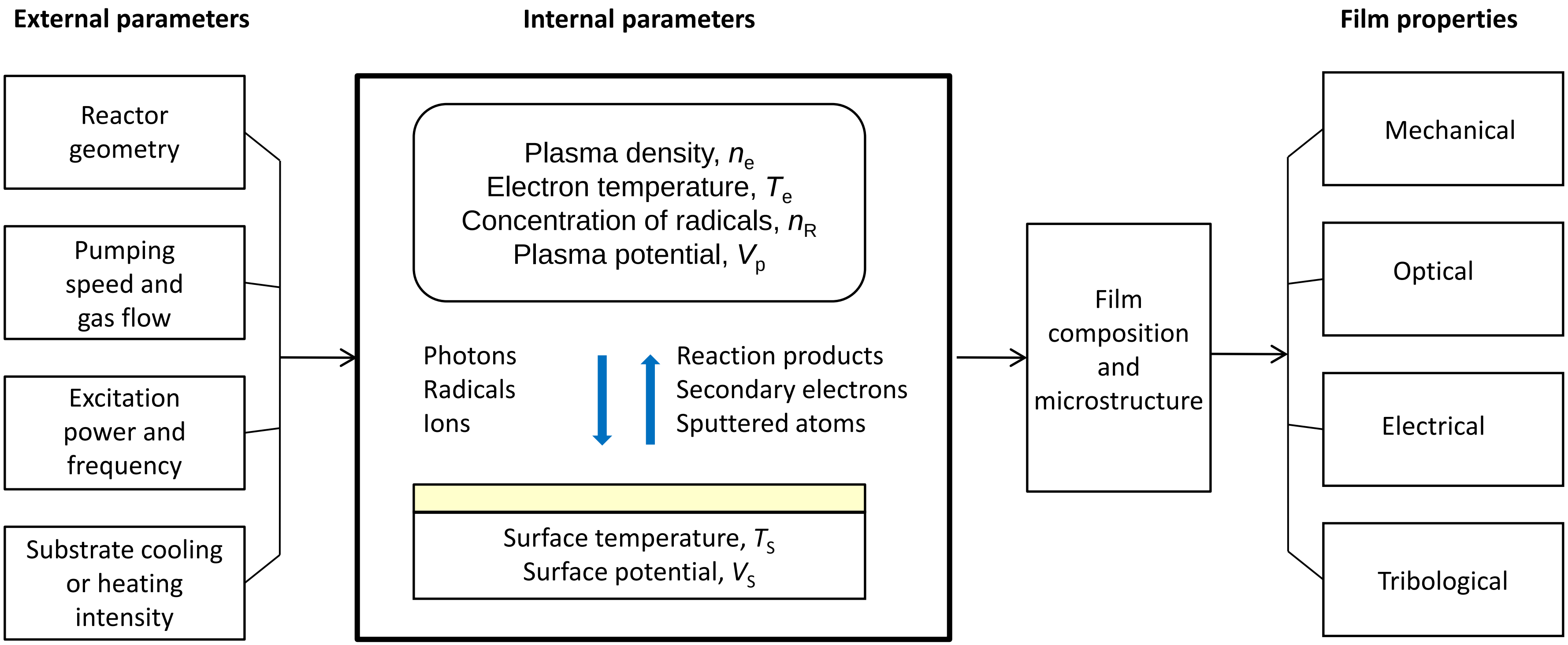

External parameters

- Reactor geometry
- Pumping speed and gas flow
- Excitation power and frequency
- Substrate cooling or heating intensity

Internal parameters

Plasma density, n_e
Electron temperature, T_e
Concentration of radicals, n_R
Plasma potential, V_p

Photons
Radicals
Ions

Reaction products
Secondary electrons
Sputtered atoms

Surface temperature, T_S
Surface potential, V_S

Film composition and microstructure

Film properties

- Mechanical
- Optical
- Electrical
- Tribological

<u>Today:</u>

Reactive sputtering
Microstructural evolution during the film growth – Structure zone model
Plasma diagnostics

L. Martinu et al., Chapter 9 in “*Handbook of Thin Film Process Technology*”, P.M. Martin, ed., Elsevier, 2010.

Plasma diagnostic techniques

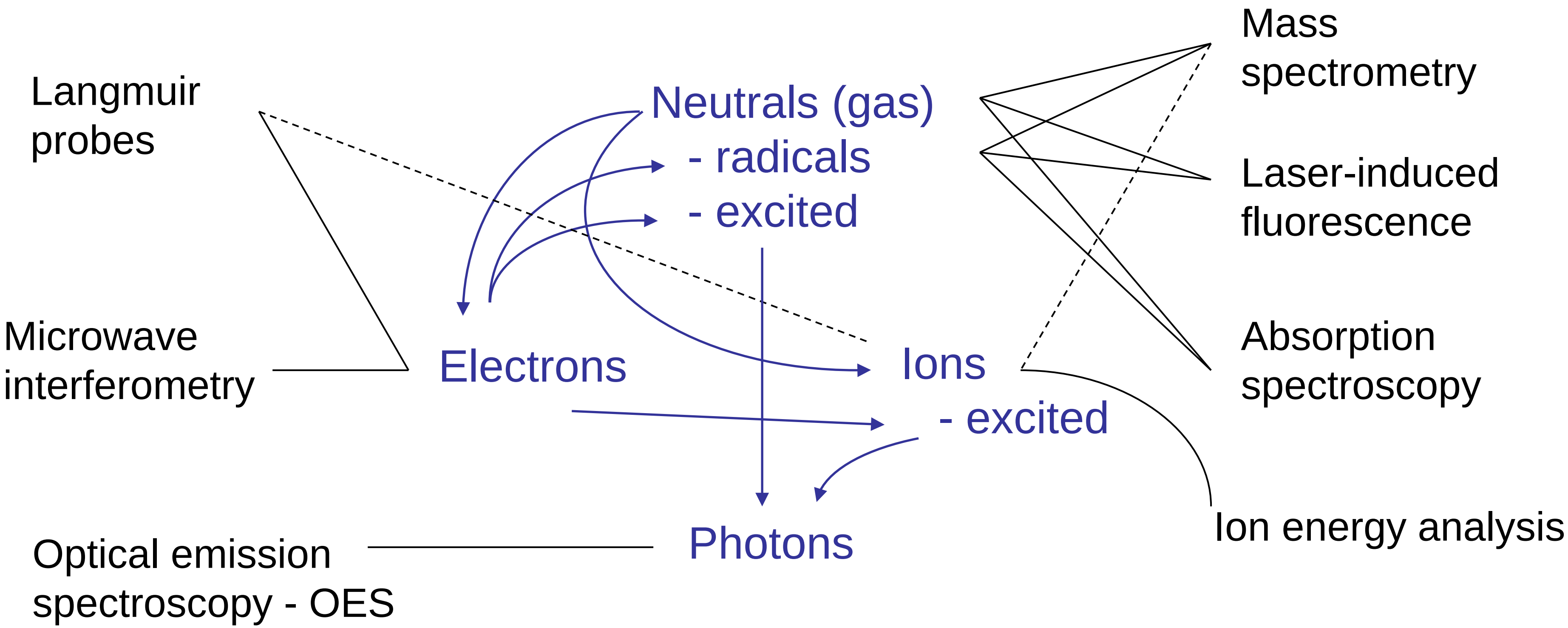

Langmuir probes

Microwave interferometry

Optical emission spectroscopy - OES

Neutrals (gas)
- radicals
- excited

Electrons

Ions
- excited

Photons

Mass spectrometry

Laser-induced fluorescence

Absorption spectroscopy

Ion energy analysis

Plasma diagnostic techniques provide information about the concentration and energy of the species

Diagnostic methods and their capabilities suitable for advanced analysis and control of the plasma processes.

a) Plasma bulk:

Diagnostics method	**Measured parameters**	**Derived characteristics**	**Perturb the plasma**	**Time resolution**	**Space resolution**	**Cost**	**Contami-nation is a problem**	**Advantages**	**Shortcomings**
Langmuir probes	I-V characteristics; Ion and electron currents	n_e, T_e, V_p, λ_D, EEDF	slightly	10^{-5} s	5 mm	$ - $$	+++	Simple instrumentation	Complex interpretation
Mass-spectrometry	Mass-selective intensity	Concentrations of atoms, molecules and fragments	slightly	10^{-3} s	1 cm	$$ - $$$	++	Many species, straightforward	Differential pumping, short lived species
Ion energy analysis	Ion current	IEDF	slightly	10^{-4} s	1 cm (0.1 mm)	$	+++	Direct ion flux	No mass resolution
Optical emission spectroscopy	Spectrally resolved emission intensity,	Concentrations of atoms, molecules and fragments; Vibrational and rotational temp., partial info. on the EEDF	no	10^{-9} s	1 mm x 10 cm	$-$$$	+	Easy to set up	Indirect, convoluted interpretation
Absorption spectroscopy	Spectrally resolved absorption	Concentrations of atoms, molecules and fragments	no	10^{-9} s	1 mm x 10 cm	$$$	+	Access to radical densities	Bulky, limited set of species
Laser induced fluorescence	Induced light intensity	Concentrations of atoms, molecules and fragments,	no	10^{-9} s	1 mm x 10 cm	$$$	+	Access to radical densities	Bulky, limited set of species
Plasma impedance	Current, voltage, phase shift	Resistance, Capacitance, n_e	no	10^{-3} s	none	$	-	Simple	Indirect, convoluted interpretation

b) In situ real time film growth monitoring :

Monitoring method	**Measured parameters**	**Derived characteristics**	**Perturb the plasma**	**Time resolution**	**Precision in assessing thickness**	**Cost**	**Contami-nation problem**	**Advantages**	**Comments**
Quartz crystal microbalance	Vibration frequency	Mass, d, r_D, density (indirect)	slight	1 s	1-5 nm	$	-	Simple	Sensitive to heating and to electric fields
Interferometry	Light intensity in transmission or reflection	d, n, r_D	no	10^{-3} s	1-5 nm	$ - $$	+	Simple	Single wavelength or multiwavelength; transparent films
Spectroscopic reflection / transmission	Spectrally resolved light intensity	d, n, r_D	no	10^{-3} s	1-5 nm	$$	+	Wide range of λ	Partially transparent films
Spectroscopic ellipsometry	Ellipsometric angles $\Psi(\lambda)$ and $\Delta(\lambda)$	d, n, k, r_D	no	10^{-1} s	0.2 nm	$$$	+	Precise assessment of n and k in a wide range of λ	Costly, only for at least partially transparent films.
Resistivity	Current, Resistance	d	no	10^{-3} s	Depends on knowledge of the resistivity	$	-	Simple	Only for conductors, affected by electric fields

L. Martinu et al, in the "Handbook on Thin Film Deposition Technologies", P.M. Martin, ed., Elsevier, Amsterdam, 2010, pp. 394-467

1. Langmuir probes (electrostatic): diagnostics of the main plasma characteristics:

Simple probe – EEDF, n_e, V_p, V_f

Double probe - EEDF, n_e

Emissive probe - V_p

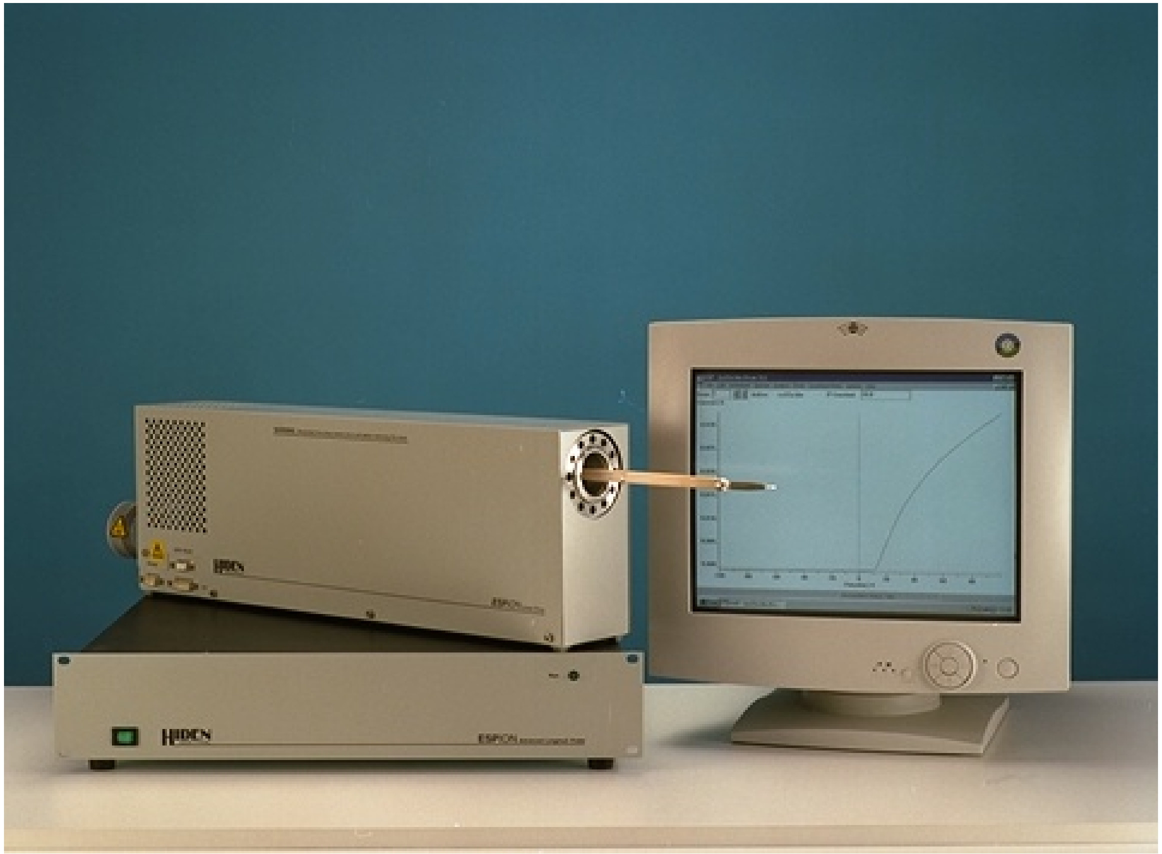

Single Langmuir probe

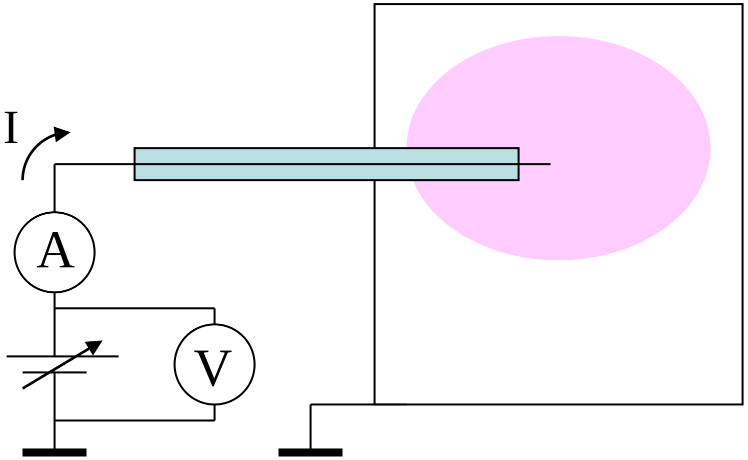

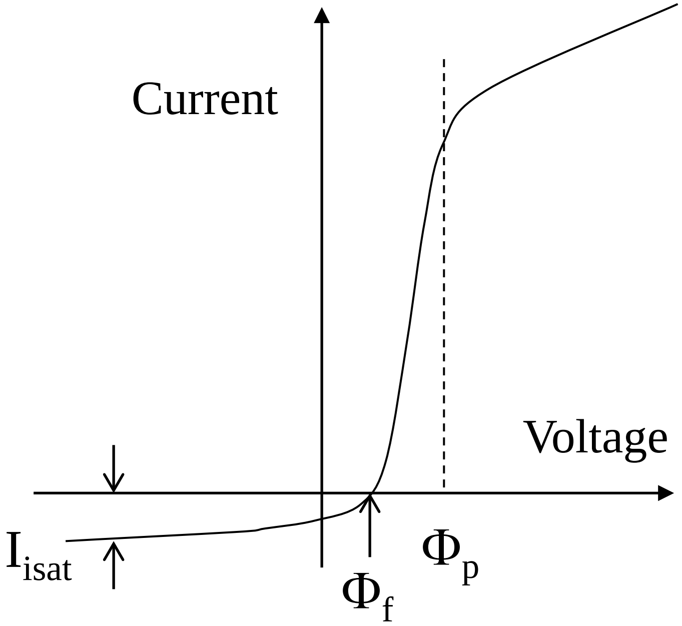

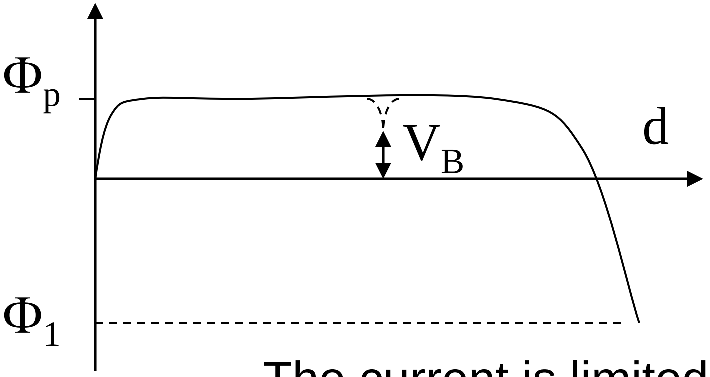

The current is limited by space charge

Collection surface is a function of the applied potentiel and of the probe geometry

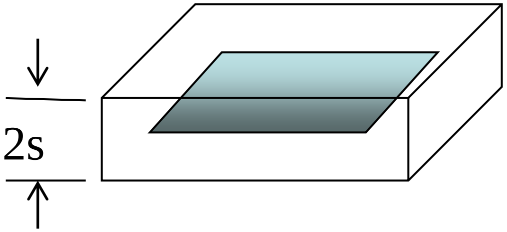

$A \approx 2LW$

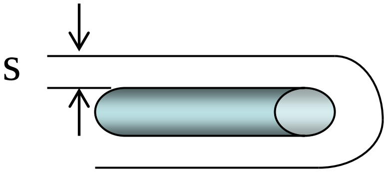

$A \approx 2\pi\,(s+a)\,L$

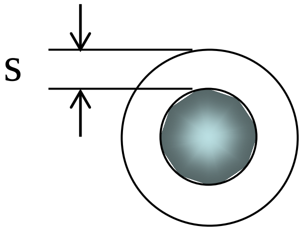

$A = 4\pi\,(s+a)^2$

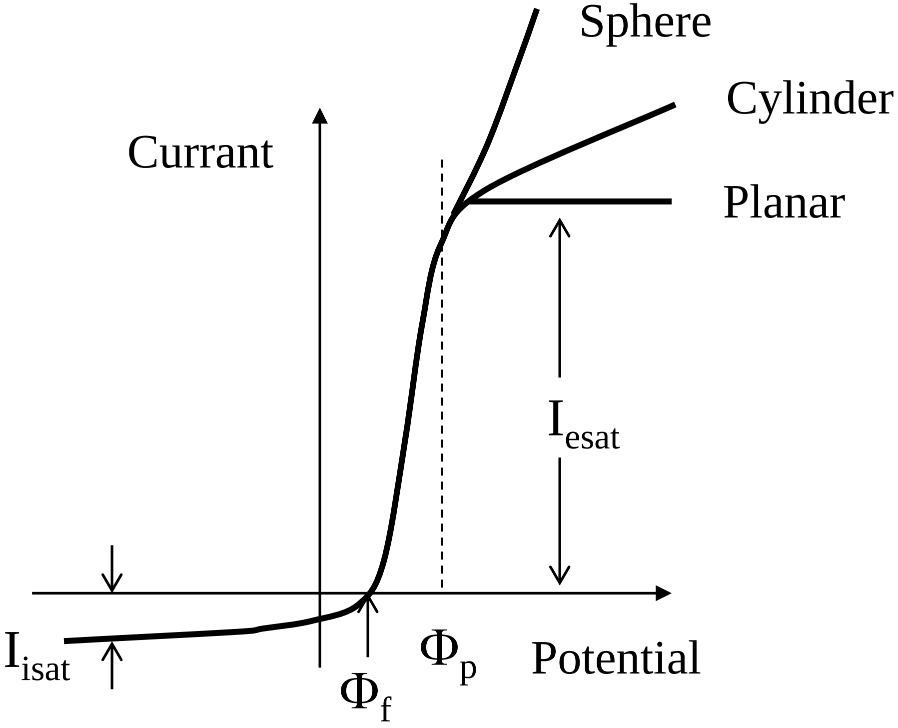

2. Mass spectrometry

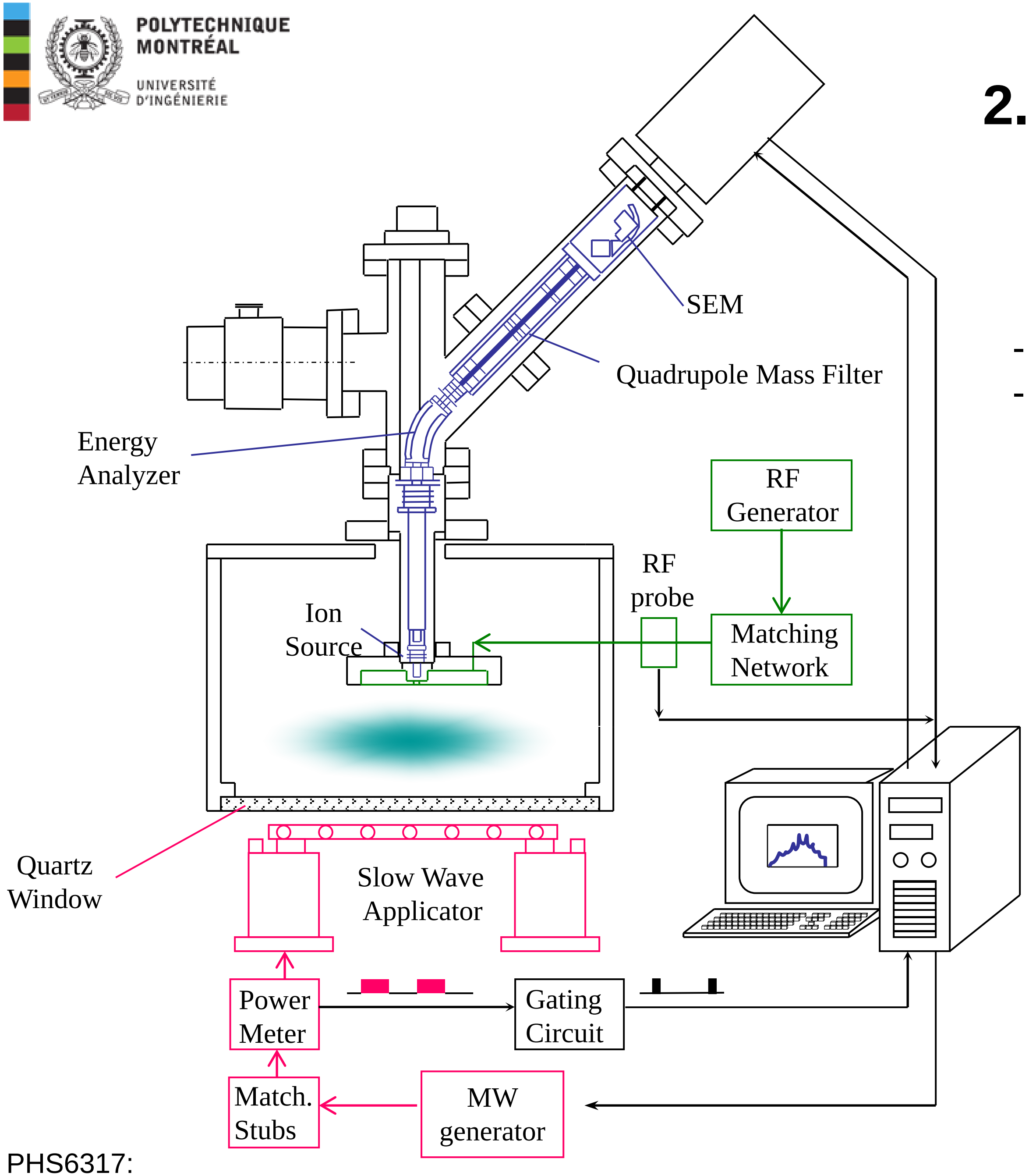

- Hiden EQP-1000 plasma probe:
- mass- and time-resolved energy distributions of
    - positive ions,
    - negative ions,
    - neutrals.

Quadrupole mass analyser

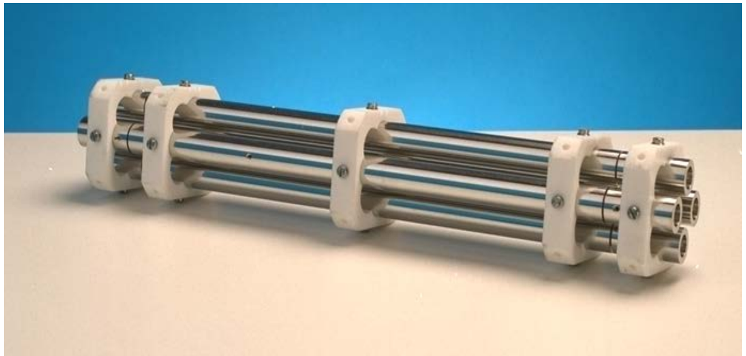

Quadrupoles are four precisely parallel rods with a direct current (DC) voltage and a superimposed radio-frequency (RF) potential. And by scanning a pre-selected radio-frequency field one effectively scans a mass range.

Quadrupole mass analyzers have been used in conjunction with electron ionization sources since the 1950s and are the most common mass spectrometers in existence today. Quadrupoles have three primary advantages:

First, they are tolerant to a relatively poor vacuum (~5×10^{-5} Torr)

Secondly, quadrupoles are now capable of routinely analyzing up to a m/z of 3000, which is useful, e.g., for the analysis of polymers and biomolecules.

Finally, the relatively low cost of quadrupole mass spectrometers makes them attractive for use in many applications.

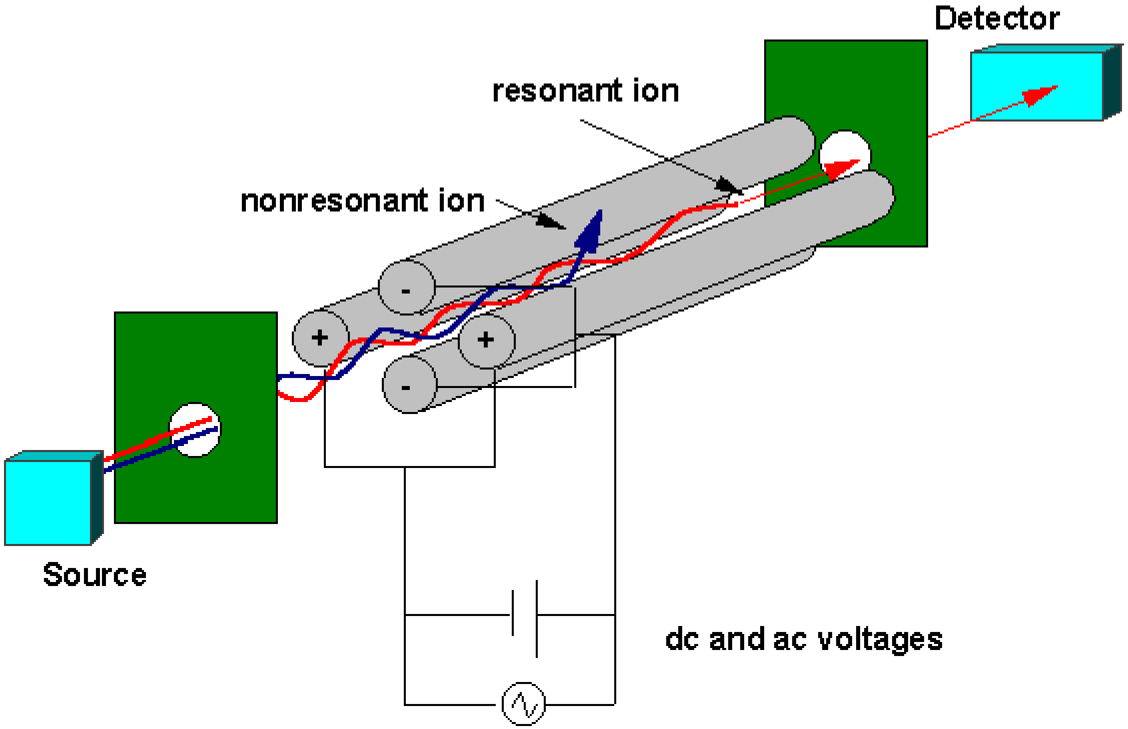

Separation by v → par M/Z
i.e.
Ar^{++} M/Z=40/2=20
and
Ne^{+} M/Z=20/1=20
are not resolved

RGA mode (Residual Gas Analysis)

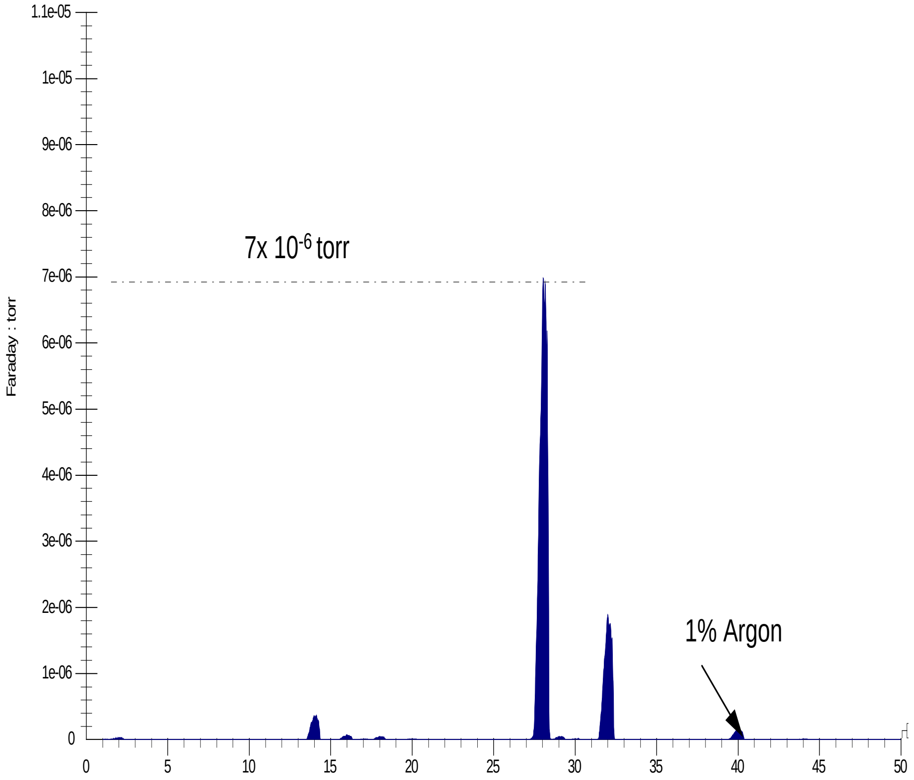

Analysis of the neutrals

Gas composition

Detection of impurities

Process kinetics

‘End point detection’

Real and virtual leaks

Mass-spectrometry - application

Polymer (PP) treatment in N_2 plasma

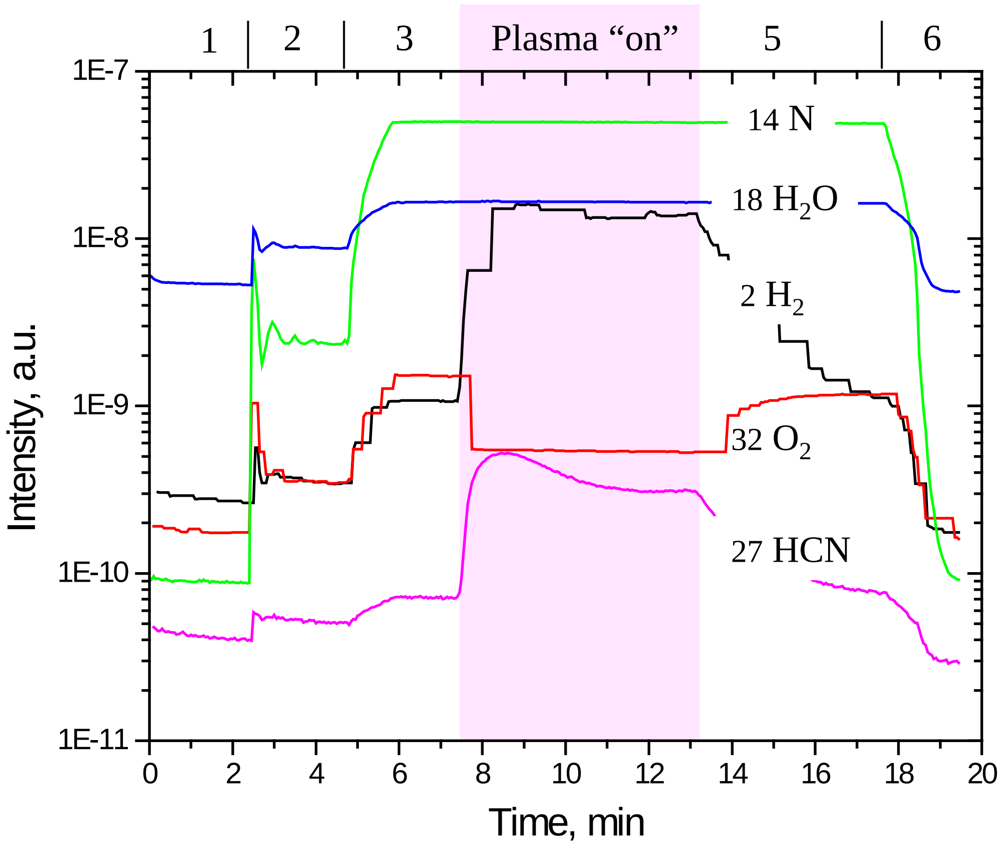

1- residual gas
2- N_2 15 sccm, p = 20 mTorr
3- throttle valve activated, p = 200 mTorr
4- Rf 50/1 W, V_b = -233….-207 V
5- Rf "off"
6- valve open, after 1 min gas is closed

Example: results from Polytechnique

3. Multigrid electrostatic ion energy analyzer

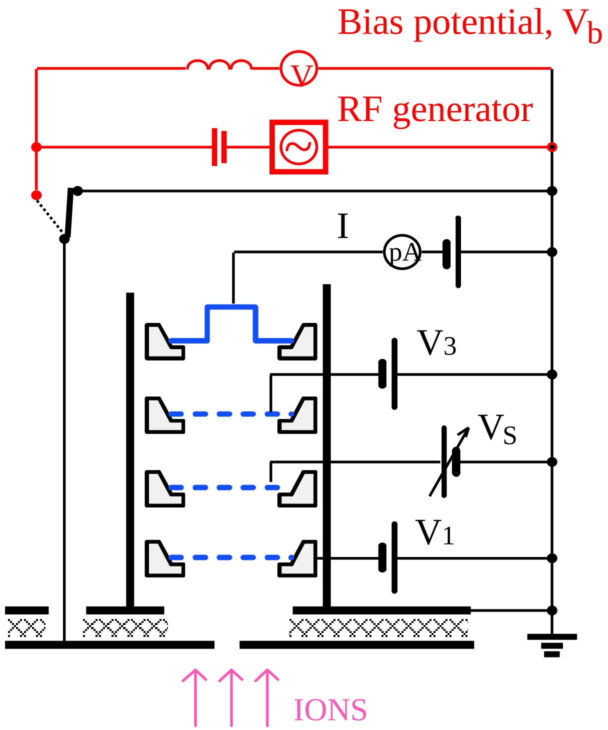

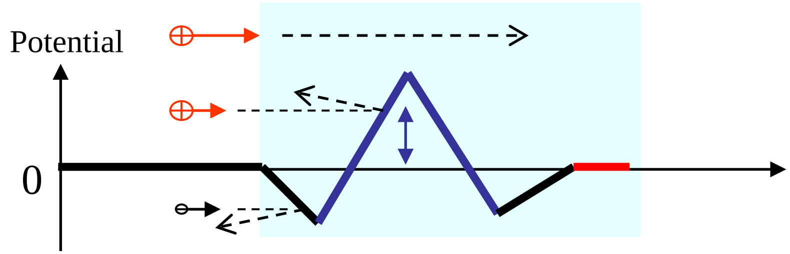

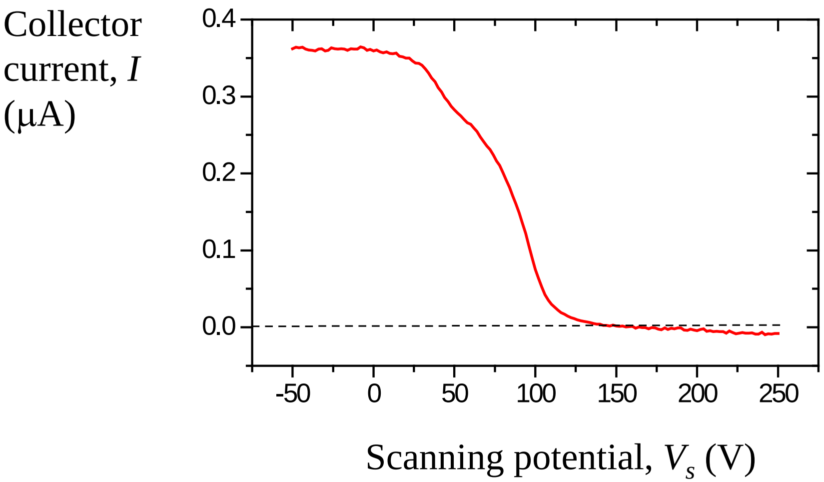

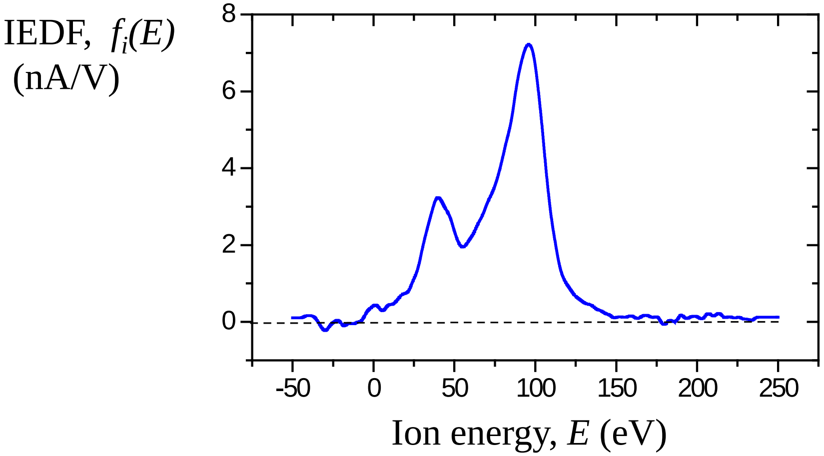

Example: results from Polytechnique

IEDF on the RF-powered electrode

$$E_{max} = |V_b| + V_p + (\Delta E/2) > |V_b|$$

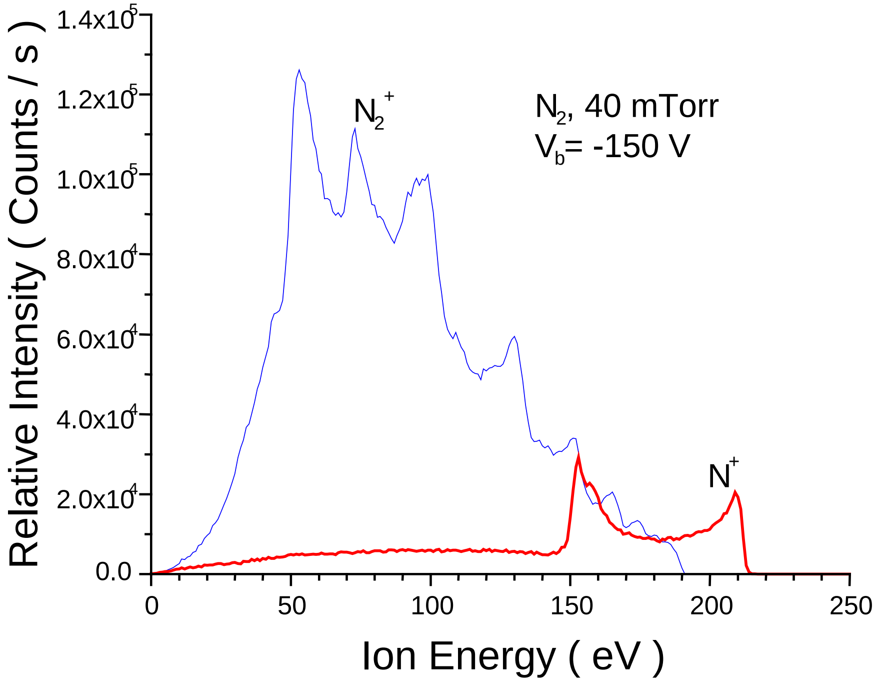

MW/rf plasma

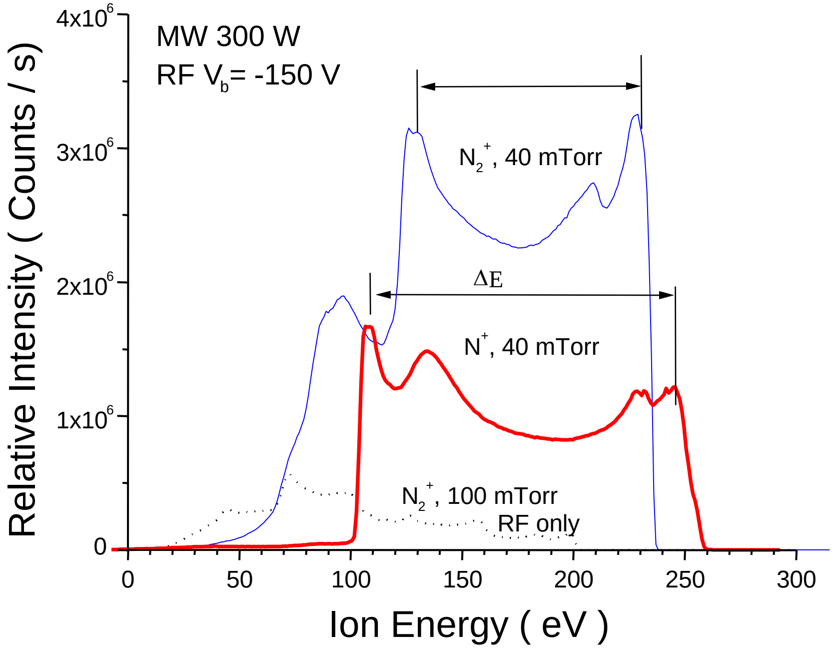

Les ions N_2^+ subissent plus des collisions dans la gaine à cause de procédés résonants de transfert de la charge

La gaine plus petite dans les plasmas denses mène à des énergies des ions plus importantes:
- moins des collisions
- plus de modulation

Example: results from Polytechnique

4. Quartz crystal microbalance

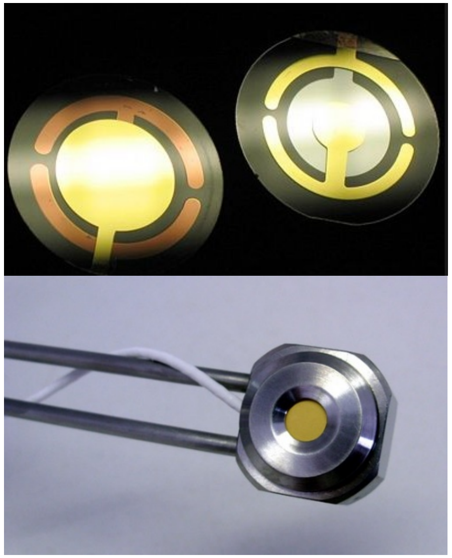

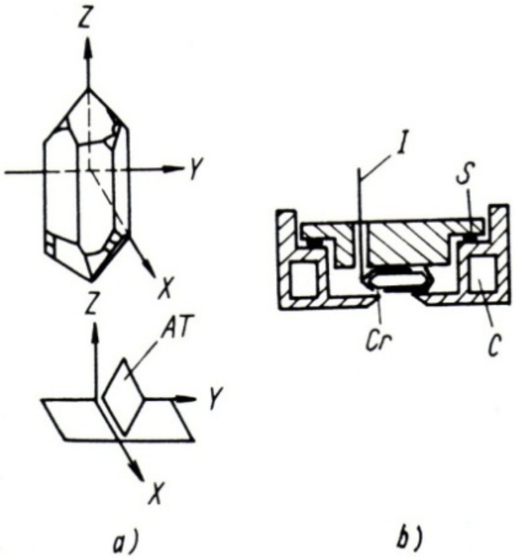

Fig. 45: (a) orientation of AT cut in quartz; (b) crystal holder: I – inlet bushing, S – seal, Cr – crystal, C – cooling.

Incrément d'épaisseur:

$$dt = \frac{1}{\rho_K S} dm$$

Sauerbrey equation:

$$\Delta f = - \Delta m/A \, (f_0^2 / N \rho_q)$$

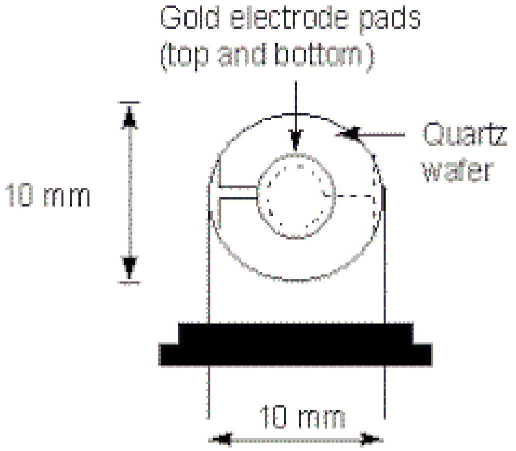

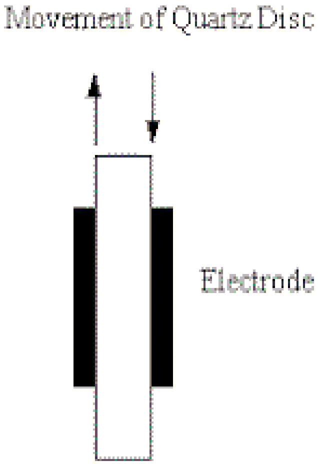

Completing the story:

$$E_p \sim E_i \; . \; \Phi_i / \Phi_N$$

$$\Phi_N = r_D \frac{\rho N_A}{m_A}$$

5. Optical diagnostics

- HIPIMS discharge
- Cr target
- 50 Hz – 200 µs pulses

- 2 configurations:
  - 2.2 mTorr Ar
  - 2.2 mTorr Ar + N_2 (reactive mode)

Images courtesy of Matěj Hála (LaRFIS)

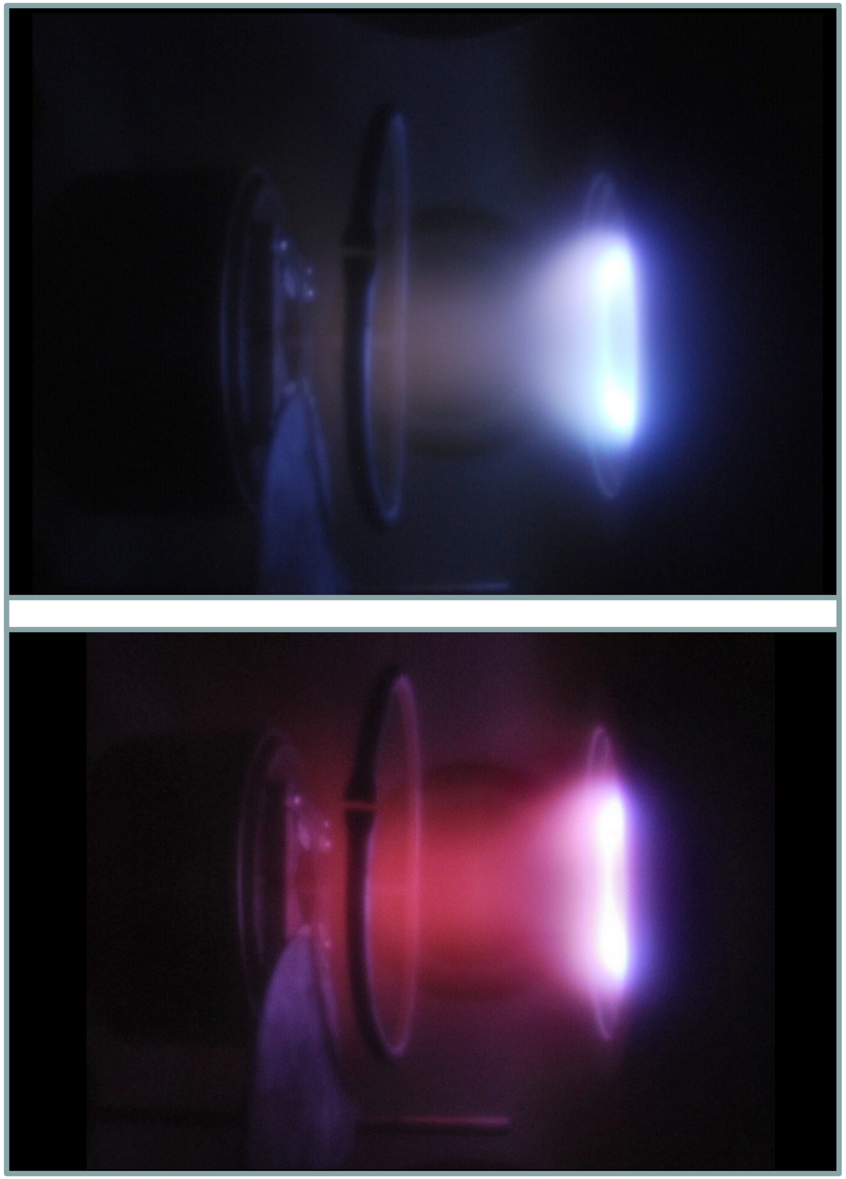

Optical emission spectroscopy - OES

Assessment of the light emission in the NIR-VIS-nearUV range (200 – 1000 nm or 1-5 eV).

Emission from the electronically excited states of atoms, radicals, ions, molecules.

Identification of species based on the wavelength of the peaks (bands) and the knowledge of the spectroscopy.

Usual wavelength resolution between 0.1 et 1 nm.

Simple to install, frequently used for qualitative approches (e.g., end point detection during etching, identification of impurities etc.).

Space- and time- resolved OES

Examples for the discharges in Ar and N_2

C M Ferreira and J Loureiro

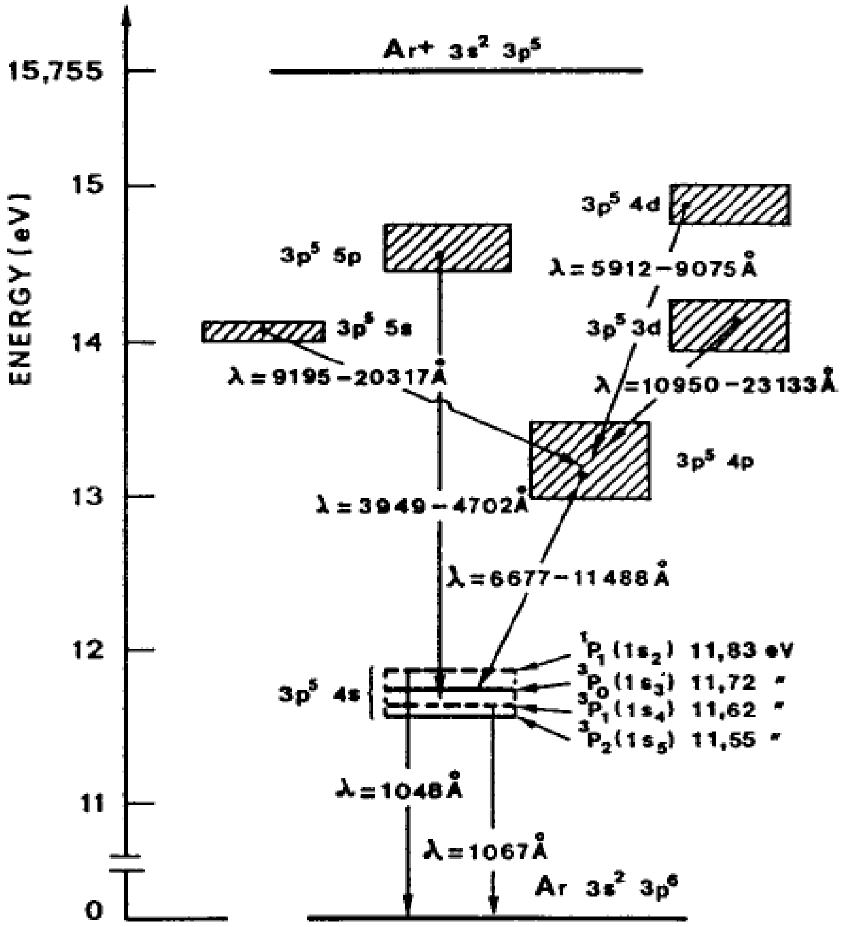

Figure 1. Energy levels of Ar.

C M Ferreira and J Loureiro

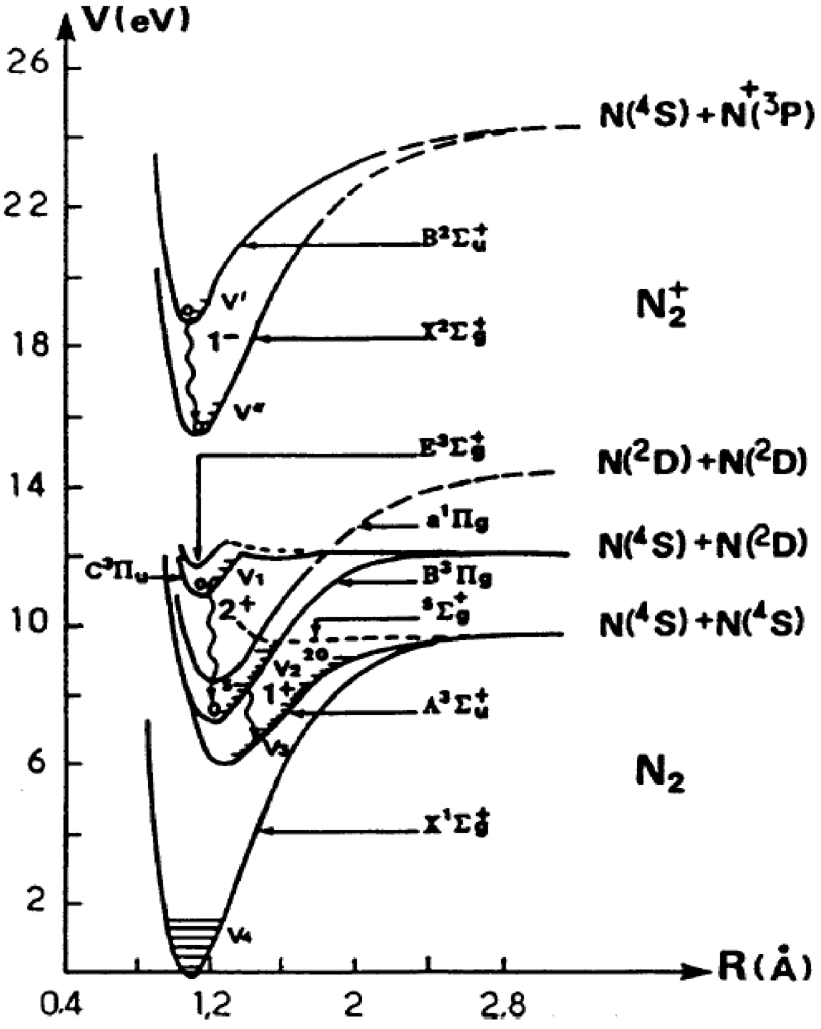

Figure 9. Energy level diagram of N_2.

Optical spectrometer

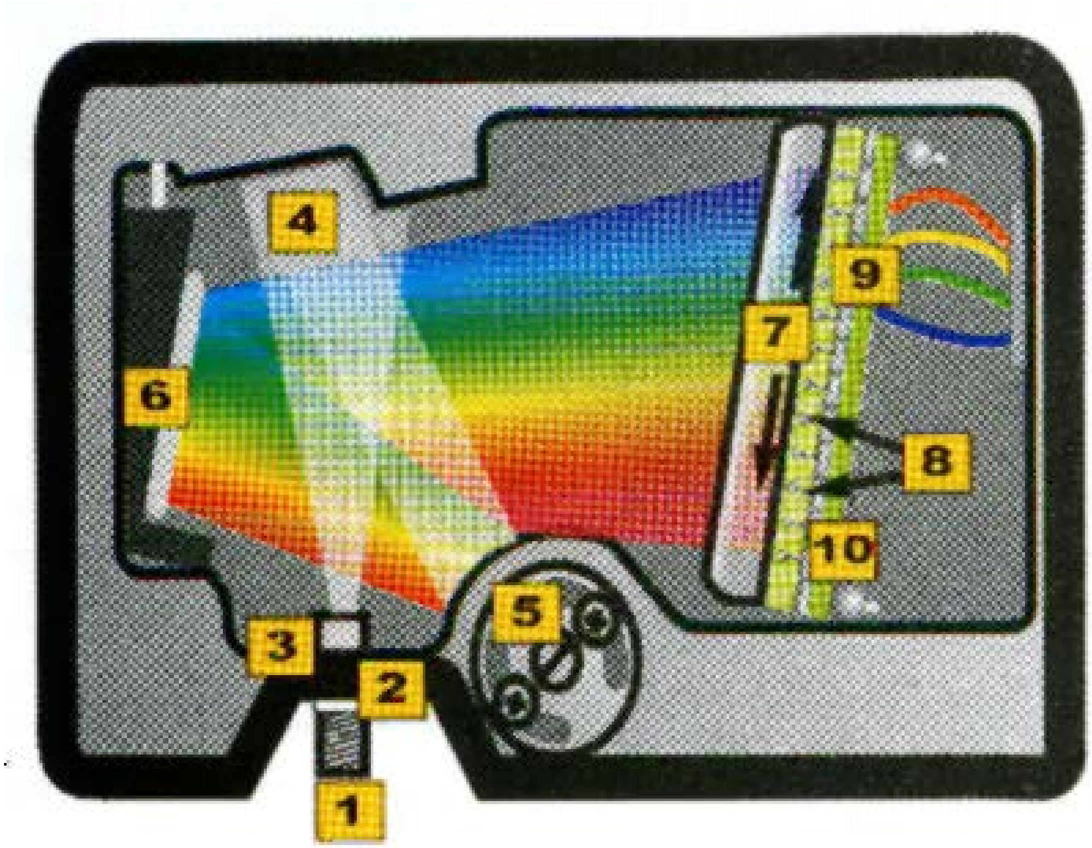

1 Entrance
2 Entrance slit
3 Filter
4 Collimation mirror
5 Dispersive element (grating)
6 Focusing mirror
7 Collection lenses
8 Harmonics optical filters
9 UV-option
10 Detector

Spectrometer resolution

$\Delta\lambda = 2$ nm

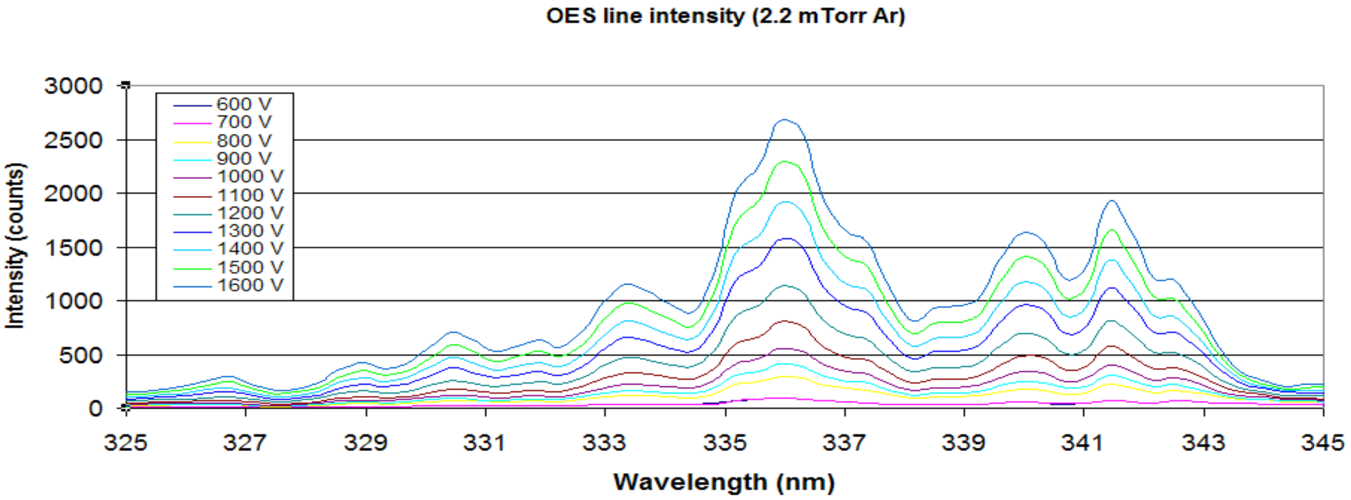

$\Delta\lambda = 0.2$ nm

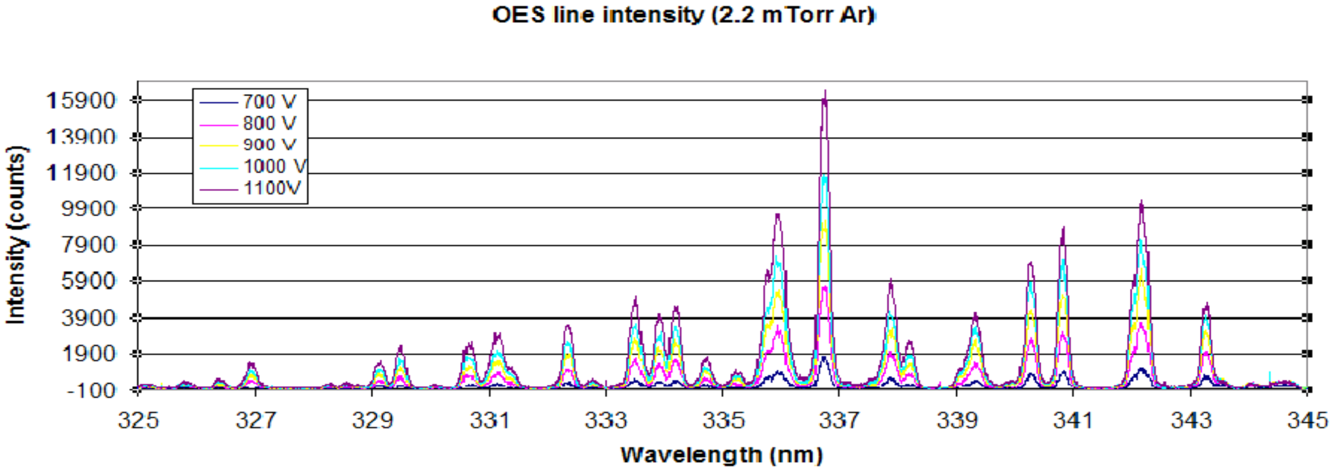

Nicolas Viau & Matej Hala – unpublished (LaRFIS)

Line assignment

NIST Atomic Spectra Database

http://www.nist.gov/srd/atomic.htm

Kurucz Atomic Line Database

http://www.cfa.harvard.edu/amp/ampdata/kurucz23/sekur.html

PLASUS SpecLine software

http://www.plasus.de

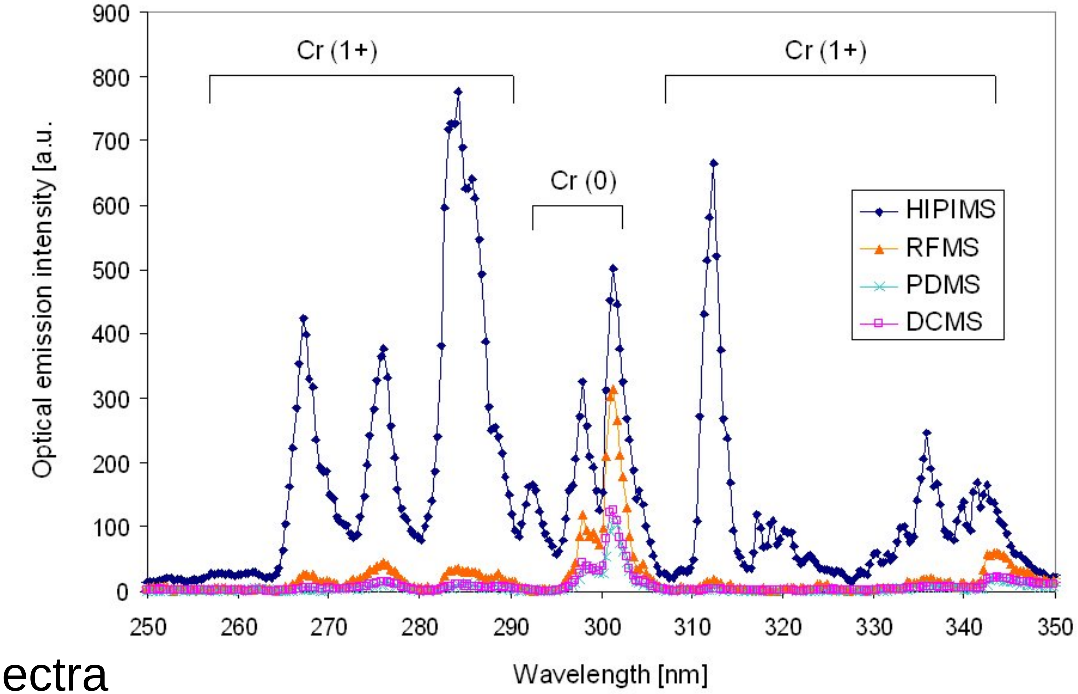

The Identification of Molecular Spectra
Reginald William Blake Pearse, Alfred Gordon Gaydon
London: Chapman and Hall, 1976, 4th ed.

Nicolas Viau & Matej Hala – unpublished (LaRFIS)

Emissions from impurities

Species	Wavelength (nm)	Source of impurity
CO	292.5, 302.8, 313.8, 325.3	Polymer oxidation, carbon
N2	315.9, 337.1	Air leak, nitride etching
OH	281.1, 306.4	Water, alcohol, degassing
NO	288.5, 289.3, 303.5, 304.3, 319.8, 320.7, 337.7, 338.6	Polyimide, nitride oxidation
Al	308.2, 309.3	Sputtering of Al
Cu	324.8, 327.4	Etching of Cu or brass
CN	289.8, 304.2	Nitride etching, sputtering of polyimide
Si	288.2	Sputtering of Si, dissociation of silane (SiH_4)

G.S. Selwin, Optical diagnosic techniques for plasma processing, AVS monograph Series, M-11, AVS 1993.

Actinometry: measurement of the radical density

Addition of a « small » known quantity of innert gas [Act], e.g., Ar

$$\mathbf{I(X^*) \propto K_e n_e [X]}$$

$$\frac{\mathrm{I(X^*)}}{\mathrm{I(Act^*)}} = \frac{\mathrm{k_D(\lambda_x)}}{\mathrm{k_D(\lambda_{Act})}} \frac{\mathrm{[X]}}{\mathrm{[Act]}} \frac{\mathrm{K_{eX}}}{\mathrm{K_{eAct}}}$$

$\nearrow$

Instrument's response

$\Downarrow$

[X]

High Power Impulse Magnetron Sputtering - HiPIMS

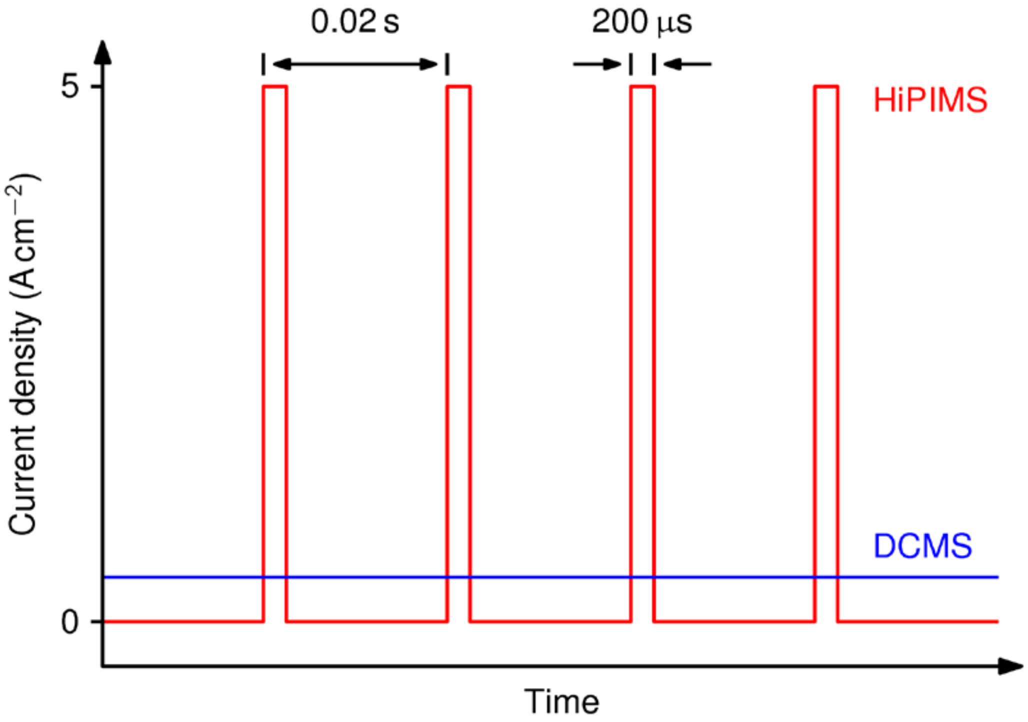

New coating properties due to:

- high density plasmas – films obtained from ionized species
- high ion fluxes toward the substrate
- effect of ion bombardment on the microstructural evolution

Pulsed discharges

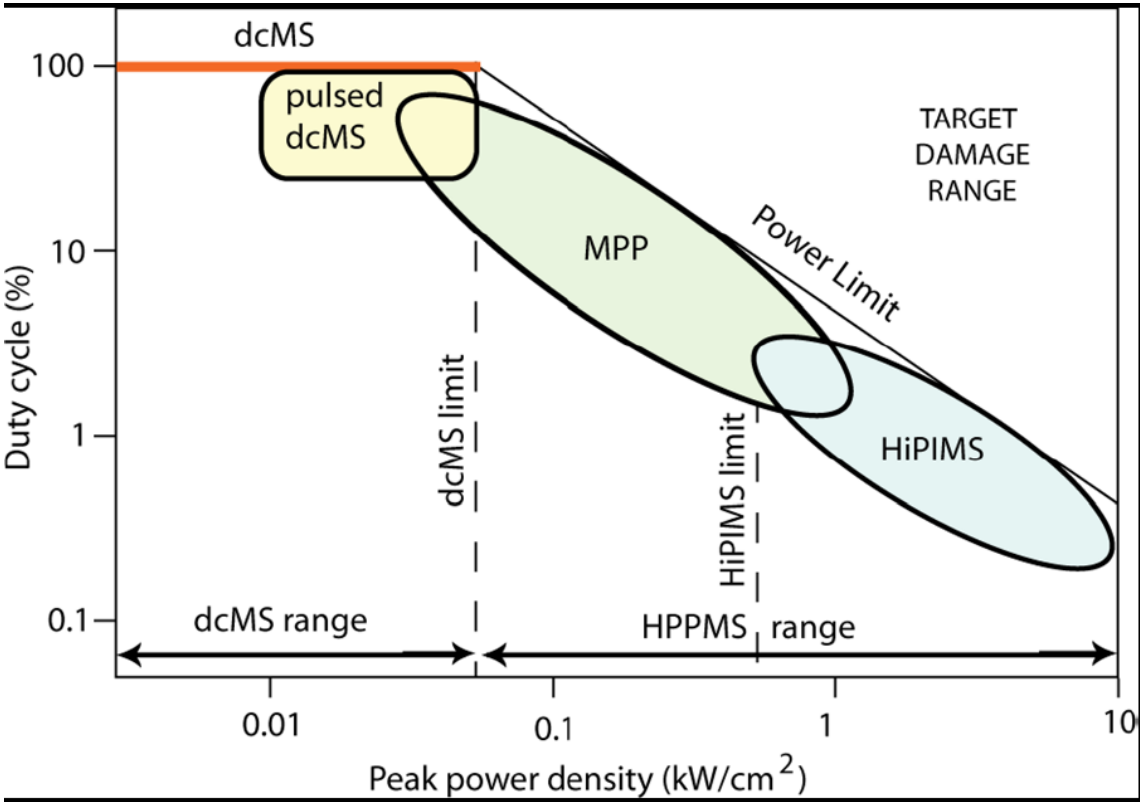

Nomenclature for pulsed discharges

Recent review articles and comparisons:

- J.T. Gudmundsson, N. Brenning, D. Lundin and U. Helmersson, J. Vac. Sci. Technol. A 30 (2012) 030801-1-35 (above)
- A. Anders, Surf. Coat. Technol. (2011), J. Vac. Sci. Technol. A 28 (2010) 783
-K. Sarakinos et al., Surface & Coatings Technology, 204 (2010) 1661

- MPP vs. HiPIMS: M. Hala et al, SCT 2012, JPD-AP, 45 (2012) 055204

HiPIMS process optimization

Parameter space

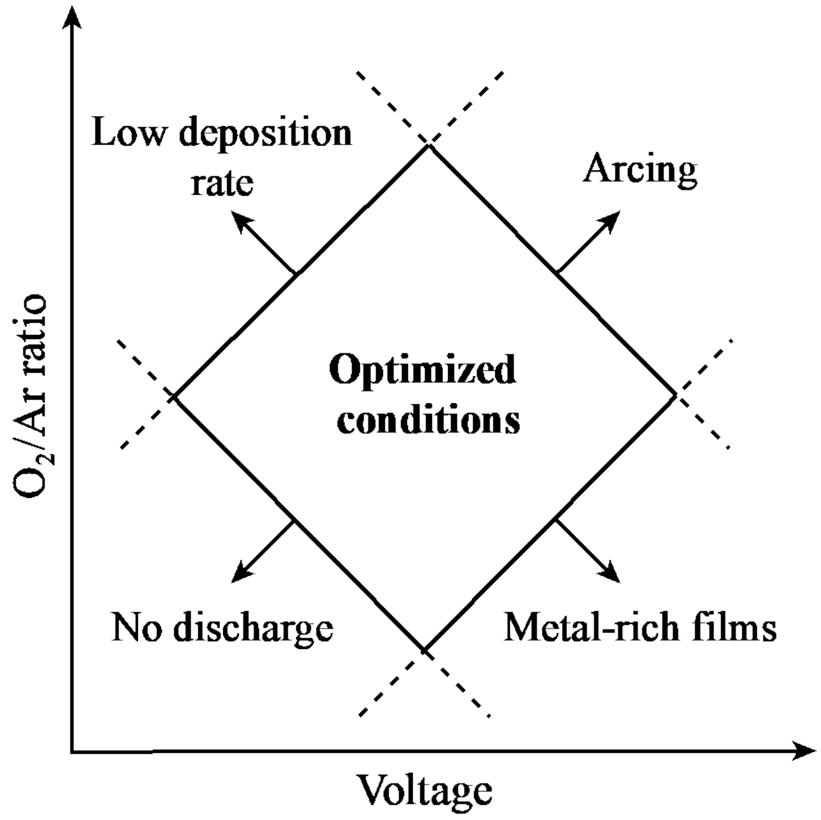

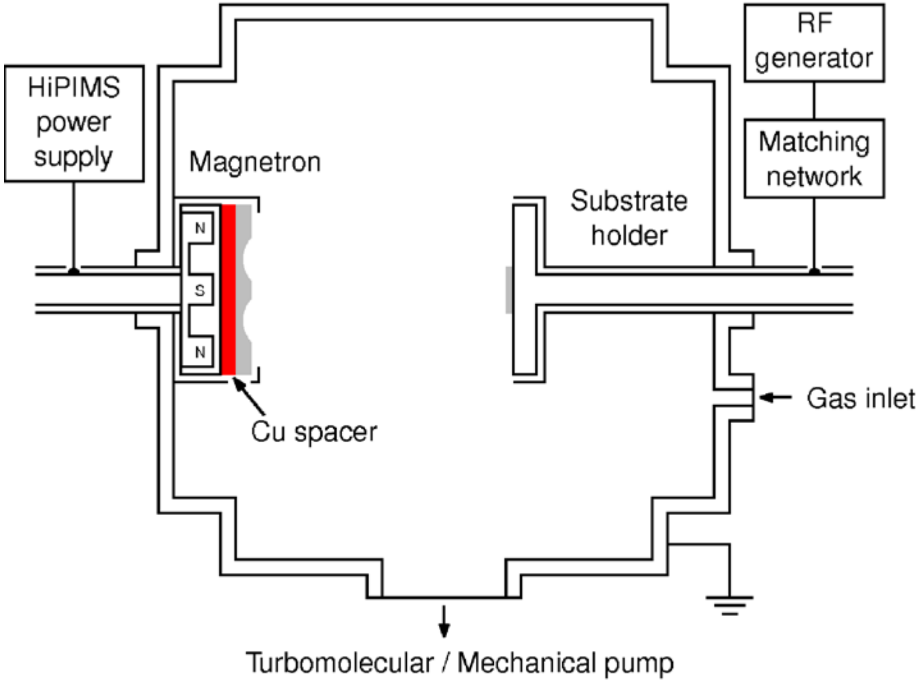

Effect of magnetic field:
J. Capek et al., J. Appl. Phys., 111 (2012)

Hysteresis suppression:
M. Hala et al., J. Phys. D: Appl. Phys., 45 (2012)
M. Hala et al., Surf. Coat. Technol. 2012

Time and space resolved OES:
M. Hala et al., IEEE Trans. Pl. Sci., 38 (2010)

OES diagnostics – from the target to the substrate

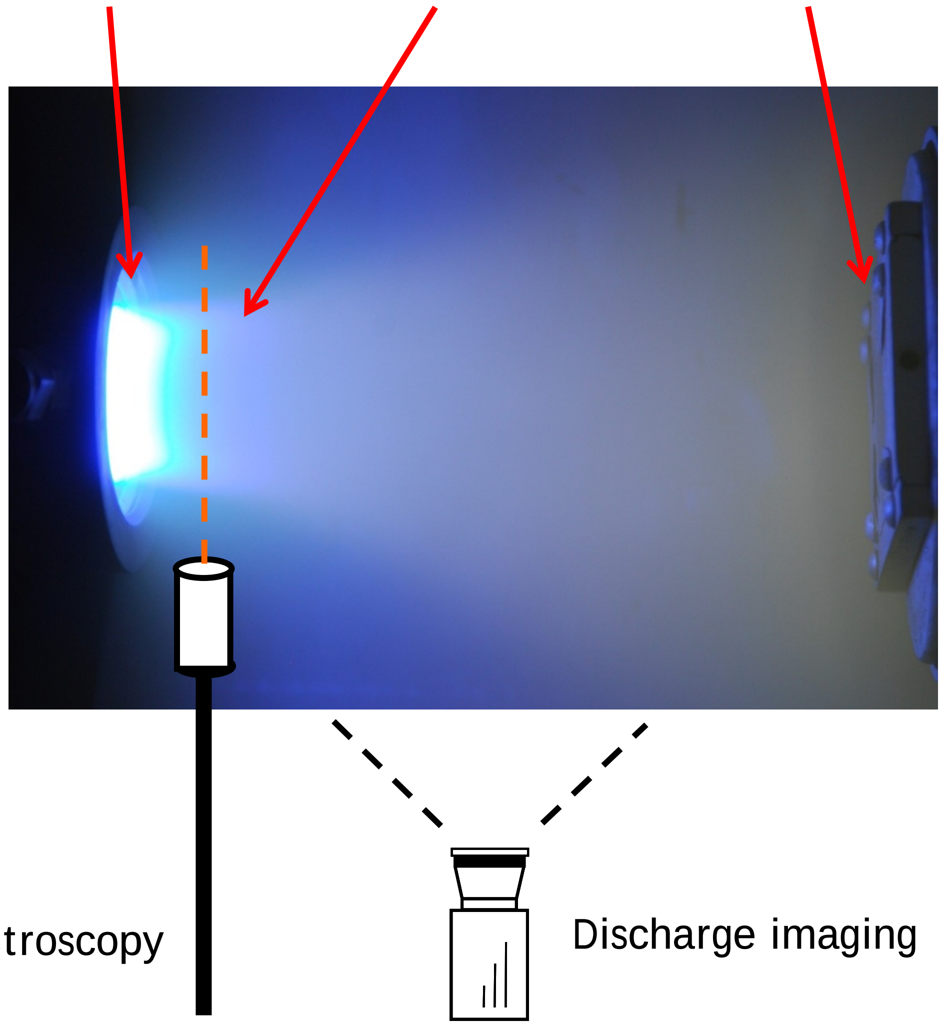

Magnetron

discharge emission

Sample holder

Spectroscopy

Discharge imaging

Reactive HiPIMS:

Pure O_2 typical in optical coatings

HIPIMS: Optical filters for species-resolved imaging
Filter performance and application

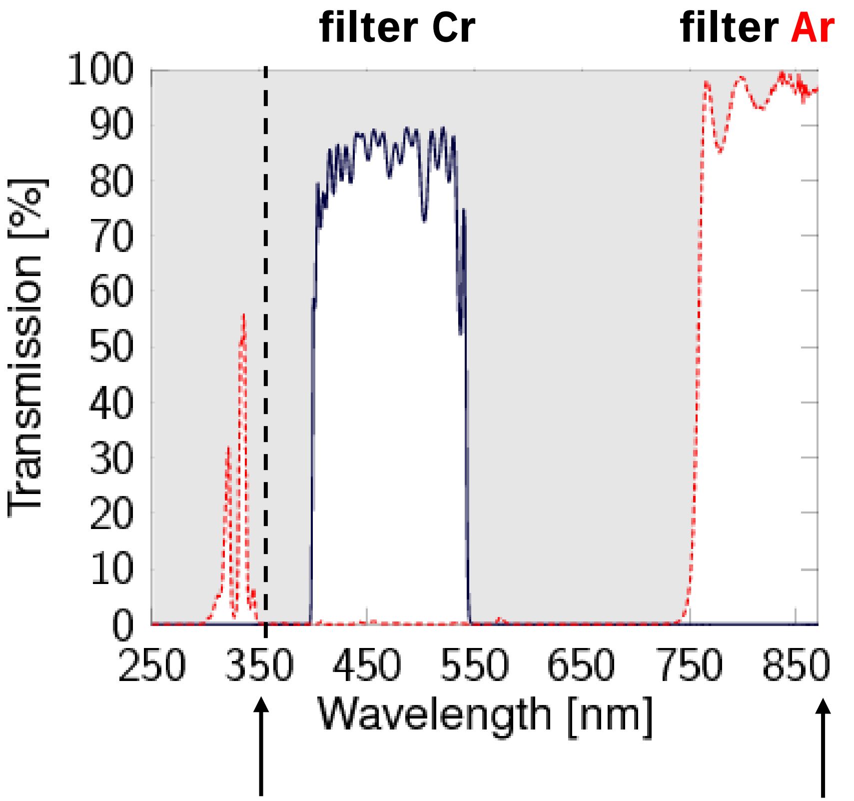

cut-off of the camera objective | CCD

Introduction of custom-made band-pass interference filters

- **high-transmission regions:**
- **400 to 540 nm - filter Cr**
- **above 750 nm - filter Ar**

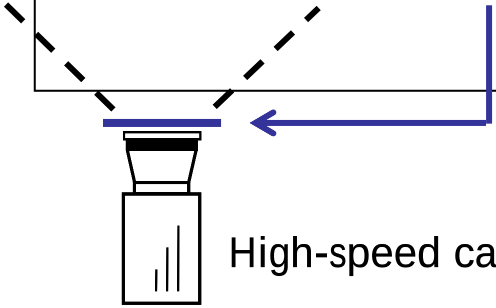

High-speed camera

M. Hala et al., IEEE Trans. plasm. sci. (2010)

HIPIMS with a Cr target:
Discharges in Ar, N_2, and in Ar/N_2 mixtures

5-cm magnetron p = **4** Pa (30 mTorr)
U_c = **-2000** V OES at ***d* = 3 cm**

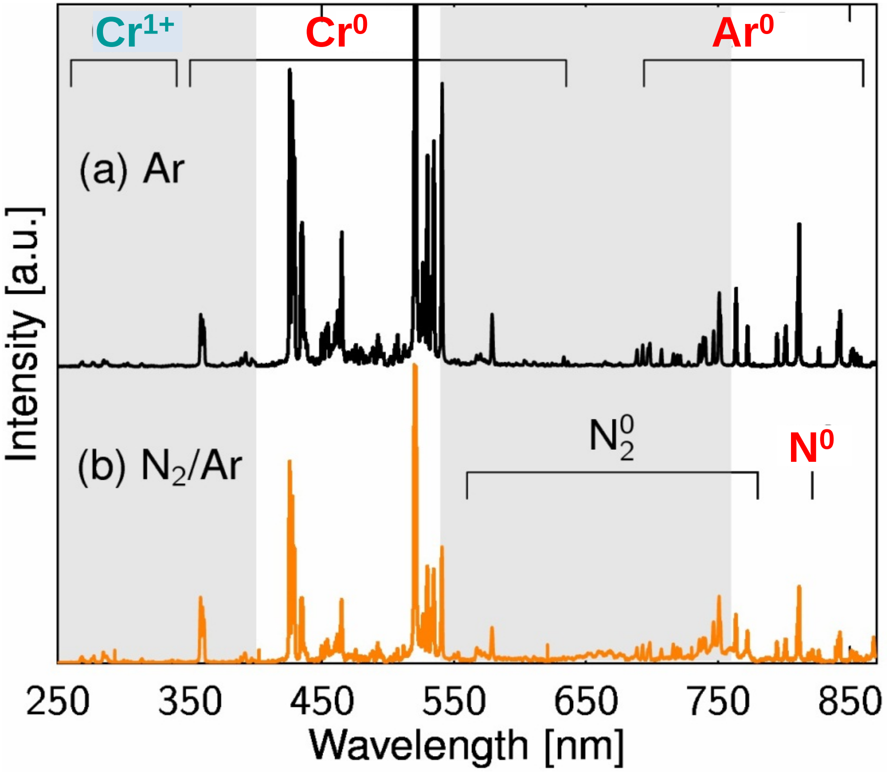

Sputtering of Cr

Two spectral regions of interest selected

- neutral chromium emission lines
- neutral gas emission lines and bands

M. Hala et al., IEEE Trans. Pl. Sci., 38 (2010) 3035

Dynamics of the HiPIMS discharge in Ar

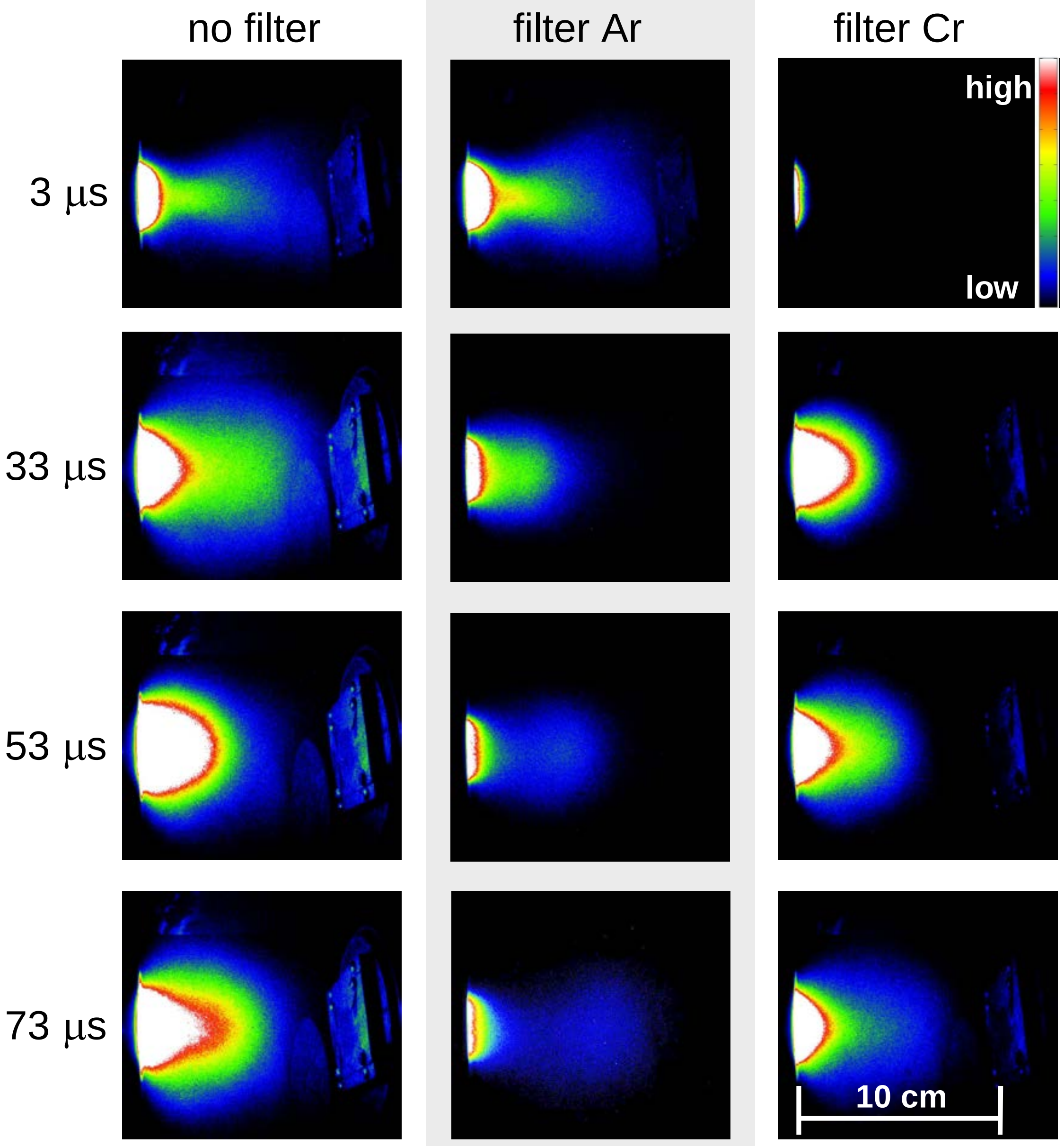

Ignition phase

Electron avalanches and

working-gas ion generation

Metal-dominated phase

Self-sputtering process

Plasma rich in sputtered Cr
expands outwards the target

Current and voltage waveforms

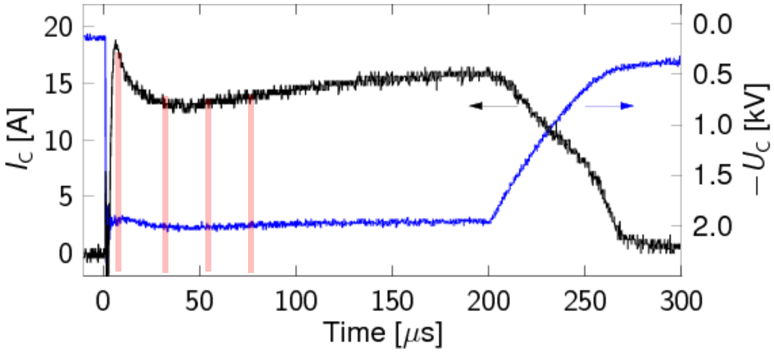

M. Hala et al., IEEE Trans. Pl. Sci. 38 (2010)

Bibliography

- F. F. Chen, J.P. Chang, *“Lecture notes on principles of plasma processing”* , Kluwer Academic, New York (2003)
- R. Hippler, S. Pfau, M. Schmidt, K.H. Shouenbach (Eds) “*Low temperature plasma physics : fundamental aspects and applications”,* Wiley-VCH, Berlin , 2001.
- M. A. Lieberman and A. J. Lichtenberg, "Principles of Plasma Discharges and Materials Processing", Wiley, New York, 1994.
- Donald M. Mattox, Handbook of Physical Vapor Deposition (PVD) Processing, Elsevier Science & Technology Books, 2010.
- A. Grill, “Cold Plasma in Materials Fabrication”, IEEE Press, New York, 1994.
- A. Fridman, “Plasma Chemistry”, Cambridge University Press, New York, 2008.
- R.F. Bunshah, ed., *“Handbook of Deposition Technologies for Films and Coatings",* Noyes publications, Park Ridge, NJ, 1994. http://www.knovel.com/knovel2/Toc.jsp?BookID=57
- H.O. Pierson, “Handbook of Chemical Vapor Deposition - Principles, Technology and Applications” William Andrew Publishing/Noyes, 1999 http://www.knovel.com/knovel2/Toc.jsp?BookID=60
- K. Seshan, ed., *“Handbook of Thin-Film Deposition Processes and Techniques - Principles, Methods, Equipment and Applications”* (2nd Edition), William Andrew Publishing/Noyes, 2002. http://www.knovel.com/knovel2/Toc.jsp?BookID=459
- S. M. Rossnagel, J. J. Cuomo, and W. D. Westwood, eds., "Handbook of Plasma Processing Technology", Noyes Publications, Park Ridge, NJ, 1990. http://www.knovel.com/knovel2/Toc.jsp?BookID=522

PHS 6317 Nanoengineering of thin films

Course schedule – Winter 2024

12 January	Introduction – Scientific and technological challenges
19	Fabrication methods – Vacuum physics and vapor-phase techniques
26*	Fabrication methods – Plasma processes and process optimization
2 February	Fabrication methods - Plasma-surface interactions and diagnostics
9**	Fabrication methods – Thermal/Plasma spray technologies
16*	Optics of thin films 1, optical characterization, *Miniquiz1 (5%)*
23*	Optics of thin films 2, design of optical filters
1*** March	*Presentations – Emerging fabrication techniques (30%)*

March 4-8 - Winter/Spring break

15**	Tribomechanical properties of films and coatings
22**	Electrochemical properties – corrosion and tribo-corrosion*(filter-20%)*
5 April	Passive functional films and coatings, *Miniquiz 2 (5%)*
12	Active functional films and coatings
16	Life cycle analysis and environmental impact
19***	*Presentations – Emerging applications of nanostructured films (40%)*

Deadlines:

Project #1 – Fabrication technique:

Choice of the subject: **26 January**

Abstract and references: **9 February**

Report and presentation: **1st March**

Projet #2 – Design of an optical filter:

Choice of the subject: **23 February**

Report: **22 March**

Projet #3 – Application of nanostructured thin films:

Choice of the subject: **16 February**

Abstract and references: **15 March**

Report and presentation: **19 April**